



**HAL**  
open science

# Mathematical methods in signal processing for spectral estimation

Rami Kanhouche

► **To cite this version:**

Rami Kanhouche. Mathematical methods in signal processing for spectral estimation. Mathematics [math]. École normale supérieure de Cachan - ENS Cachan, 2006. English. NNT: . tel-00136093

**HAL Id: tel-00136093**

**<https://theses.hal.science/tel-00136093>**

Submitted on 12 Mar 2007

**HAL** is a multi-disciplinary open access archive for the deposit and dissemination of scientific research documents, whether they are published or not. The documents may come from teaching and research institutions in France or abroad, or from public or private research centers.

L'archive ouverte pluridisciplinaire **HAL**, est destinée au dépôt et à la diffusion de documents scientifiques de niveau recherche, publiés ou non, émanant des établissements d'enseignement et de recherche français ou étrangers, des laboratoires publics ou privés.

**THÈSE DE DOCTORAT  
DE L'ÉCOLE NORMALE SUPÉRIEURE DE CACHAN**

Présentée par  
**Rami KANHOUCHE**

pour obtenir le grade de

DOCTEUR DE L'ÉCOLE NORMALE SUPÉRIEURE DE CACHAN  
Domaine: **Mathématiques Appliquées**

Sujet de la thèse:

**Méthodes Mathématiques En Traitement Du Signal Pour  
L'Estimation Spectrale**

Thèse présentée et soutenue à Cachan le 21-12-2006 devant le jury composé de :

M. Yves MEYER *Professeur*  
Mme. Christine FERNANDEZ-MALOIGNE *Professeur*  
M. Thierry CHONVAEL *Professeur*  
M. Abdellatif SEGHIER *Maître de conférences*  
M. Olivier ALATA *Maître de conférences*  
M. Hassane ESSAFI *PhD*

Centre de Mathématiques et de Leurs Applications  
ENS CACHAN / CNRS / UMR 8536  
61, avenue du Président Wilson, 94235 CACHAN CEDEX (France)



## **Remerciements**

*Je remercie profondément le professeur Yves Meyer pour m'avoir fait l'honneur de présider le jury de cette thèse.*

*Tous mes remerciements aux rapporteurs et membres de jury : Professeur Thierry Chonavel, Professeur Christine Fernandez-Maloigne, Maître Olivier Alata, Monsieur Hassane ESSAFI, pour avoir accepté de participer à l'évaluation de cette thèse. Leurs conseils et commentaires m'ont apporté les améliorations importantes sur la version finale de cette thèse.*

*Je remercie L'Ecole normale supérieure pour m'avoir donné la chance de poursuivre mes études au sein de son laboratoire CMLA, et pendant ma première année de DEA MVA.*

*Pendant la période de rédaction de ma thèse, j'ai bénéficié des conditions de travail optimales du Centre de Mathématiques et de Langages Appliqués de l'ENS de Cachan. Je remercie chaleureusement les membres du CMLA et le personnel technique et administratif, en particulier Véronique Almadoar et Pascal Bringas. Je tiens à les remercier pour leur contribution au bon fonctionnement du laboratoire.*

*Je veux témoigner mon immense reconnaissance à Maître Abdellatif Seghier, le directeur de cette thèse, pour toute l'attention qu'il m'a offerte et l'expérience qu'il m'a transmise avec patience, sympathie, et obstination. Je n'arriverai jamais à exprimer totalement ma gratitude envers lui. Sans son encouragement constant et son enthousiasme, je ne serais pas arrivé au bout de ce travail.*

*Un grand merci à mes amis, Saleh goumha, Firas Atfe, Ricardo Martinez, Lucero Lopez et Julien Jouanneau, qui m'ont toujours témoigné leur appui et leur sincérité.*

*Je remercie du fond du cœur ma mère, mon père et mes sœurs. Je ne pourrai jamais leur rétribuer tout ce que je leur dois. Ce n'est que par leur soutien pendant la période de mes études, que ce travail a pu voir la lumière.*





## Contents

Présentation des thèmes de la thèse.....	9
I Estimation de la densité spectrale .....	9
♦ Les coefficients de réflexion de type ND.....	11
♦ Conclusion.....	13
♦ Application au traitement du signal Radar (SAR) .....	16
II L'organisation de cette thèse.....	17
Introduction .....	19
I Multidimensional Spectral Power Estimation.....	19
♦ Spectral Power Estimation, Moments point of view.....	20
♦ Spectral Power Estimation, numerical considerations .....	21
♦ Spectral Power Estimation, the multidimensional case .....	22
II Overview of this thesis.....	23
♦ Chapter 3 .....	23
♦ Chapter 4 .....	24
♦ Chapter 5 .....	24
♦ Chapter 6 .....	24
♦ Chapter 7 .....	24
♦ Chapter 8 .....	24
♦ Chapter 9 .....	24
A Modified Burg Algorithm Equivalent In Results to Levinson Algorithm .....	27
I Introduction .....	27
II 1D Case .....	28
♦ The model.....	28
♦ The 1D Levinson Algorithm .....	29
♦ 1D Burg Algorithm .....	29
♦ Equivalency proof .....	29
III 2D Case .....	30
♦ The Model .....	30
♦ The 2D Levinson Algorithm (WWR) .....	32
♦ The 2D Burg Algorithm .....	32
♦ Equivalency proof .....	33
IV The Modified Burg Algorithm .....	35
♦ 1D Case .....	35
♦ 2D Case .....	36
V Numerical examples.....	37
VI Conclusion.....	40
Generalized Reflection Coefficients and The Inverse Factorization of Hermitian Block Toeplitz Matrix.....	41
I Introduction .....	41
II Notations .....	42
III Generalized Reflection Coefficients and Hermitian Strongly Regular matrices .....	42
IV Generalized Reflection Coefficients in the Hermitian Block Toeplitz Case.....	43
V Generalized reflection coefficients in the block Toeplitz case algorithm (GRCBT).....	46

♦	Algorithm's details.....	46
♦	Algorithm's developement.....	47
♦	Algorithm's complexity.....	48
VI	A Bezoutian Inversion Formula.....	48
VII	Conclusion.....	50
VIII	Acknowledgment.....	50
	Generalized Reflection Coefficients in Toeplitz-Block-Toeplitz Matrix Case and Fast Inverse 2D Levinson Algorithm.....	51
I	Introduction.....	51
II	Notations.....	52
III	Generalized Reflection Coefficients and Hermitian Strongly Regular Matrices.....	52
IV	Generalized Reflection Coefficients in the Hermitian Toeplitz Block Toeplitz case.....	53
V	Generalized reflection coefficients in the Toeplitz block Toeplitz case algorithm (GRCTBT).....	59
♦	Algorithm's details.....	59
♦	Algorithm's developement.....	60
♦	Algorithm's complexity.....	61
VI	A comparison with the WWR Algorithm in the TBT Case.....	62
VII	Conclusion.....	64
	Sequential Multidimensional Spectral Estimation.....	65
I	Introduction.....	65
I	Multidimensional Toeplitz Characters and Spectral Block Structure.....	66
II	Multidimensional Extension Approximation.....	69
III	Sequential Multidimensional Spectral Estimation Algorithm.....	71
IV	Numerical calculation cost.....	72
V	Numerical simulations and discussion.....	73
	Multidimensional Correlation Extension using Generalized Reflection Coefficients with application to Spectral Power Estimation.....	77
I	Introduction.....	77
II	Generalized Reflection Coefficients, and Positiveness Condition for Hermitian Strongly Regular matrices.....	78
III	Multidimensional Toeplitz Matrices.....	81
IV	Multidimensional Correlation Matrix Extension.....	83
V	Sequential Multidimensional Correlation Extension Algorithm.....	86
♦	SMCE.....	86
VI	Numerical simulations and application to Spectral Power Estimation.....	89
VII	Time domain extension characteristic.....	94
VIII	Conclusion.....	95
	Numerical Comparative Study of 2D Spectral Power Estimation Techniques.....	99
I	Introduction.....	99
II	Controlled Performance measure.....	101
III	Application to Synthetic Aperture Radar (SAR).....	103
♦	Naval Research Laboratory Database.....	104
♦	Application to MSTAR Database.....	106
♦	Sandia National Laboratory SAR Complex Data.....	107
IV	Conclusion.....	116
	Conclusion And Future Work.....	117

I	Main contribution of this thesis.....	117
II	Theoretical horizon and future work.....	117
	Bibliography.....	119
	Table Of Figures.....	127



**PRESENTATION DES THEMES DE LA THESE**

**I Estimation de la densité spectrale**

On se donne un processus stochastique, stationnaire,  $(X_t), t \in \mathbb{Z}^d$  (appelé aussi champ). On a :

$$E(X_t) = 0 \text{ et } E(X_t X_{t+s}) = r(s) \text{ pour tout } s;$$

Soit  $M$  une partie finie de  $\mathbb{Z}^d$ , la matrice de covariance associée à une partie  $M$  est donnée par

$$T_M = (E(X_t X_{t+s}) = r(s))_{s \in M}$$

( $M$  est définie aussi comme une fenêtre).

Les matrices de covariance  $T_M$  jouent un rôle capital en ce sens qu'elles contiennent toutes les informations concernant le processus  $(X_t)$  ( $M$  variant dans  $\mathbb{Z}^d$ ).

La densité spectrale du processus est définie par

$$\begin{aligned} F_X(e^{i\theta}) &= F_X(e^{i\theta_1}, \dots, e^{i\theta_d}) \\ &= \sum_{s \in \mathbb{Z}^d} r(s) e^{-i\langle \theta, s \rangle} \end{aligned} \quad (1.1)$$

où  $\theta = (\theta_1, \dots, \theta_d)$ ,  $s = (s_1, \dots, s_d)$  et  $\sum_{s \in \mathbb{Z}^d} |r(s)| < \infty$ .

**Un problème fondamental pour les applications : l'estimation spectrale**

Supposons que le processus  $X_t$  s'est réalisé au travers d'un échantillonnage des données réelles  $(X_k), k \in \Lambda \subset \mathbb{Z}^d$ , où  $\Lambda$  est un ensemble que l'on suppose de grand cardinal : par exemple la donnée d'une image.

Il s'agit alors d'estimer au mieux la densité spectrale théorique  $F_X$  définie en (1.1). Ce qui est équivalent à l'estimation des coefficients  $(r(s))_{s \in \mathbb{Z}^d}$  qui ont les coefficients de Fourier de  $F_X$ . Deux écueils se présentent :

**a.** Comment estimer au mieux la covariance théorique  $r(s)$  à partir des données qui sont limitées par nature. Soit  $T_{M_x}$  la matrice de covariance :

$T_{M_x} = (r_x(s))_{s \in M}$ . On sait que la matrice de covariance théorique est définie positive. Une méthode d'estimation devra conduire à des matrices  $T_{M_e}$  ayant la même propriété. D'autres questions de nature stochastique, peuvent être considérées portant sur la qualité de l'estimateur en fonction des données (comportement asymptotique des estimateurs, etc...).

**b.** Un deuxième aspect important consiste à reconstruire au mieux la densité spectrale  $F_x$  à partir d'un ensemble fini de coefficients de Fourier. C'est ainsi que l'insuffisance de données peut conduire à une perte de résolution : les hautes fréquences correspondant aux entiers éloignés de l'origine ne vont plus intervenir dans la finesse des détails de l'image. Aussi pour compenser ce manque de données fréquentielles on procède à ce qu'on appelle l'extension de covariances. Cette extension doit satisfaire trois contraintes :

**b.1-** Le caractère défini positif (toutes les valeurs propres de la matrice de covariance sont positives).

**b.2-** La structure ND-Toeplitz, qui traduira la stationarité du processus indexé par  $\mathbb{Z}^d$ .

**b.3-** Enfin, le choix de l'image après l'extension selon un critère d'entropie.

C'est un problème qui a son équivalent en analyse harmonique. Il est connu sous le nom d'extension de fonctions de type positif (voir A. Caldéron et W. Rudin [74], [75]). C'est un problème très difficile en plusieurs dimensions.

Un certain nombre de résultats partiels ont été obtenus. (voir A. Seghier[73]).

Revenons à la notion d'entropie. Les extensions vérifiant (b.1) et (b.2) peuvent exister en grand nombre, le choix qui sera retenu devra satisfaire à un principe de maximum d'entropie ou une notion proche. Soyons plus précis, soit  $T_{M_x}$  une covariance candidate, alors celle qui sera retenue devra vérifier

$$\det T_{M_{x,0}} = \max \det(T_{M_x}), T_{M_x} \in \mathcal{E}$$

$\mathcal{E}$  : ensemble de covariances vérifiant (b.1) et (b.2).

On prouve que si  $T_{M_{x,0}}$  est construite à l'aide de coefficients de Fourier de  $F_x$

$$\lim \det T_{M_{x,0}} = \exp \left( - \int_{\pi^d} \log F_x(\theta) d\theta \right), \text{ l'ensemble } M \text{ tend vers } \mathbb{Z}^d.$$

Ce critère a une signification très satisfaisante, dans le cadre de l'estimation spectrale, en effet : étendre la covariance selon le principe du maximum d'entropie, consiste à augmenter la résolution de l'image à partir uniquement des informations contenues dans les basses fréquences, (coefficients de Fourier indexés par des entiers, non éloignés de l'origine). Ainsi, aucune information supplémentaire n'est introduite, dans le cadre de l'image on dit que l'on introduit aucun artéfact.

Le moment est venu de définir l'outil principal de nos investigations.

◆ *Les coefficients de réflexion de type ND.*

Nous montrerons en effet que cet outil nous permet de répondre aux trois contraintes imposées pour atteindre l'extension de la corrélation d'un signal et éventuellement le débruitage de son spectre (qui dépend d'une construction pertinente de la matrice de covariance)

**A. Coefficients de réflexion généralisés.**

Nous nous plaçons ici dans un cadre plus général : les covariances  $R$  sont définies positives et symétriques sans structure particulière (introduite par exemple par l'hypothèse de stationnarité).

Notons, avant d'entrer dans les détails, que ces coefficients de réflexion généralisés jouent un rôle presque identique aux valeurs propres. Ils ne diffèrent que par leur nombre.

En effet pour une matrice de covariance  $R$ , de taille  $N$ ,  $N$  valeurs propres lui sont associées, alors que  $N(N-1)$  coefficients de réflexion généralisés lui sont associés.

Voici les propriétés de ces coefficients :

- Caractérisation de la propriété définie positive pour  $R$ .
- Calcul des déterminants.
- Ils traduisent la structure stationnaire de la matrice  $R$ , si elle en a une (structure ND-Toeplitz, Bloc Toeplitz, Toeplitz Bloc Toeplitz).

Une matrice de covariance ND-Toeplitz s'obtient comme la matrice de covariance d'un processus stationnaire relativement à l'ensemble d'indexation  $\mathbb{Z}^d$ .

Dans le cas de structure ND-Toeplitz un sous-ensemble de coefficients de réflexion  $2N_1, (N_1 > N)$ , permet de retrouver les  $N(N-1) - 2N_1$  restants.

Voici les étapes qui correspondent à la mise au point de ces coefficients.

Rappelons le cas classique pour les matrices de Toeplitz

$$T_N = (c_{k-l})_{0 \leq l, k \leq N-1}$$

Soit  $(e_0, e_1, \dots, e_{N-1})$  une base d'une espace vectorielle muni d'un produit scalaire

$$\langle U, V \rangle_{T_N} = U^T T_N V$$

On définit le système récursif suivant



$$\left\{ e_i = q_{i,i} = p_{i,i} \right\}_{i=0,\dots,N-1}$$

$$\begin{cases} p_k = p_{k-1} - \rho_k \tau q_{k-1} \\ q_k = \tau q_{k-1} - \bar{\rho}_k p_{k-1} \end{cases}$$

où  $\tau$  est définie pour  $U = (u_0, u_1, \dots, u_{N-1}) \rightarrow \tau U = (0, u_0, u_1, \dots, u_{N-1})$ .

$$\rho_k = \frac{\langle p_{k-1}, e_k \rangle_{T_N}}{\langle \tau q_{k-1}, e_k \rangle_{T_N}}$$

Nous en déduisons un certain nombre de propriétés de composition de Cholesky. Deux propriétés fondamentales sont à préciser :

- $|\rho_k| \leq 1$
- $\det T_N = \prod_{k=1}^{N-1} (1 - |\rho_k|^2)^{N-k}$

Nous allons étendre cette récurrence aux cas de matrices  $R$  symétriques définies positives.

La récurrence par diagonale :

Pour  $p_{i,i} = e_i$ ,  $q_{i,i} = e_i$  et  $0 \leq k, l \leq N-1$ , on a

$$p_{k,l} = p_{k,l-1} - \rho_{k,l} q_{k+1,l}$$

$$q_{k,l} = q_{k+1,l} - \rho'_{k,l} p_{k,l-1}$$

$$\rho_{k,l} = \frac{\langle p_{k,l-1}, e_l \rangle_R}{\langle q_{k+1,l}, e_l \rangle_R}$$

$$\rho'_{k,l} = \frac{\langle q_{k+1,l}, e_k \rangle_R}{\langle p_{k,l-1}, e_k \rangle_R}$$

On démontre que

- $R$  est définie non-négative  $\Leftrightarrow 0 \leq \rho_{k,l} \rho'_{k,l} \leq 1$ .
- $R$  est définie positive  $\Leftrightarrow 0 \leq \rho_{k,l} \rho'_{k,l} < 1$ .

Nous pouvons déduire un certain nombre de propriétés algébriques (voir A.Seghier, G. Castro [34]).

$$\det R = \prod_{0 \leq k < l \leq N-1} (1 - \rho_{k,l} \rho'_{k,l}).$$

## B. Coefficients de réflexion ND-Toeplitz.

Dans le cadre des coefficients de réflexion ND-Toeplitz, les coefficients de réflexion généralisés prennent une structure spéciale qui reflète cette structure.

D'où la définition d'une notion fondamentale des coefficients de réflexion ND. On découvre que les coefficients de réflexion ND ont un support minimal de même taille que celui qui permet de définir la matrice ND-Toeplitz, et participent d'une manière essentielle dans la reconstruction spectrale du signal.

Soit  $R$  une matrice de covariance ND-Toeplitz de taille  $N$ , alors les coefficients de réflexion ND-Toeplitz expriment totalement son inverse et leur extension est synonyme d'une estimation spectrale de maximum d'entropie.

Le théorème suivant est le point d'appui principal pour l'extension des matrices définies positives, et représente le résultat fondamental de notre travail.

Nous avons le résultat suivant que nous préciserons par la suite

*Chaque groupe des coefficients de réflexion  $\{\rho_{k,l}, \rho'_{k,l}\}_{0 \leq k < l \leq n-1}$  correspondant à une matrice ND-Toeplitz hermitienne, contient un groupe de coefficients de réflexion minimal permettant de déterminer pour la totalité des coefficients de réflexion. Le groupe minimal est composé des coefficients de réflexion localisés dans la position minimale dans la matrice  $R$ .*

◆ *Conclusion*

Notre contribution s'inscrit dans la démarche engagée par un grand nombre d'auteurs consistant à étendre au cas multidimensionnel, les propriétés remarquables des algorithmes de Levinson et de Burg. Nous pensons que la récursion par diagonale paraît être l'approche la plus naturelle pour réaliser une telle généralisation.

En effet dans un premier temps la récursion par diagonale concerne les matrices symétriques générales. Les algorithmes de Levinson et de Burg apparaissent alors comme spécifiques à la structure Toeplitz (unidimensionnelle).

Cette récursion par diagonale se simplifie dès que les matrices (de covariances) générales présentent des structures Toeplitz généralisées (ND Toeplitz, Bloc Toeplitz, Toeplitz Bloc Toeplitz). Nos résultats indiquent précisément la prise en compte de telles structures particulières. C'est en ce sens que notre démarche est optimale relativement aux approches classiques que nous rappelons brièvement.

Les méthodes basées sur le concept QP AR : il y a effectivement une grande famille des méthodes qui expriment le spectre d'un signal 2D  $x(t_1, t_2)$  sous la forme

$$\begin{aligned} |X(jw_1, jw_2)|^2 &\approx P_{QP2D}(jw_1, jw_2) \\ P_{QP2D}(jw_1, jw_2) &:= \frac{v_0}{\left| \sum_{k_1=0}^{N_1-1} \sum_{k_2=0}^{N_2-1} a_{k_1, k_2} e^{-jw_1 k_1} e^{-jw_2 k_2} \right|^2} \cdot (1.2) \end{aligned}$$

où les coefficients de filtre –connu aussi sous le nom du filtre autoregressif- sont exactement une normalisation de la première colonne de l'inverse de la matrice de corrélation  $T_{N_1 N_2}$  selon

$$T_{N_1 N_2} \mathbf{a}_{2D} v_0 = e_0, \quad \mathbf{a}_{2D} := \begin{bmatrix} 1 & a_{1,0} & \dots & a_{N_1-1,0} & a_{0,1} & \dots & a_{N_1-2, N_2-1} & a_{N_1-1, N_2-1} \end{bmatrix}^T \quad (1.3)$$

Ceci est toujours dans l'esprit de généralisation du cas 1D où le filtre  $\mathbf{a}_{1D}$  est défini de la même manière selon

$$T_N \mathbf{a}_{1D} v_0 = e_0, \quad \mathbf{a}_{1D} := \begin{bmatrix} 1 & a_1 & \dots & a_{N-2} & a_{N-1} \end{bmatrix}$$

$$\text{avec } P_{1D}(jw) := \frac{v_0}{\left| \sum_{k=0}^{N-1} a_k e^{-jwk} \right|^2}$$

Voici quelques points fondamentaux qui différencient le cas 1D de la manière selon laquelle le filtre  $P_{QP2D}$  est défini :

- Entropie : Contrairement au cas 1D où le filtre  $P_{1D}, \{a_k\}$  maximise l'entropie d'une manière optimale selon le critère  $\max_w \int \log(P(jw)) .dw$ , le filtre  $P_{QP2D}, \{a_{k_1, k_2}\}$  donné par (1.3), ne correspond pas à un maximum d'entropie.

- Stabilité : Contrairement au cas 1D où le filtre  $A(z) := \sum_{k=0}^N a_k z^{-k}$  a toujours les

racines dans le cercle  $|z| \leq 1$ , le filtre  $A(z_1, z_2) := \sum_{k_1, k_2} a_{k_1, k_2} z_1^{-k_1} z_2^{-k_2}$ ,

$\{a_{k_1, k_2}\}$  donné par (1.3), n'a pas nécessairement ces racines dans le cercle de l'unité.

- Relation Spectrale : Contrairement au cas 1D où le filtre reproduit les mêmes coefficients de corrélation de départ -ce qui est connu comme la propriété « matching »- le filtre  $P_{QP2D}, \{a_{k_1, k_2}\}$  donné par (1.3) ne les reproduit pas.

Alors, il reste seulement un point en commun entre le modèle AR 1D et le modèle AR 2D et c'est celui de la minimisation de l'erreur de prédiction dans l'espace temps au sens quadratique. Si on veut résumer le travail dans cette thèse, en ce qui concerne l'estimation spectrale avec une seule phrase elle sera la suivante

*« ce qui minimise l'erreur de la prédiction au sens quadratique dans le temps ne définit pas nécessairement une relation spectrale correcte »*

Pour répondre aux contraintes précédentes des méthodes basées sur le modèle (1.2) ont été proposées. Ces méthodes aident à avoir un meilleur contrôle sur la contrainte de stabilité [71], ou à remédier la relation spectrale [59]. Avec la méthode [71] des conditions pour la stabilité du filtre autoregressive 2D ont été présentées, mais ces conditions permettent seulement de savoir si le filtre produit selon (1.3) est stable, et ne proposent pas une manière uniforme selon laquelle le filtre est toujours stable. Avec la méthode [59], des améliorations sont apportées à la stabilité mais la question de la relation spectrale n'est pas toujours définie (voir chapitre 8).

Par rapport à ces points, nous avons dirigé notre contribution dans une direction qui leur donnera une réponse appropriée. Nous avons ainsi pu proposer deux méthodes pour l'estimation spectrale:

- *La méthode ASMSE, L'estimation spectrale multidimensionnelle (approximation séquentielle)* : avec cette méthode le point concernant la stabilité est résolu ; dans le cadre multidimensionnel, avec une relation spectrale de « matching » approximatif, et un support spectral de taille infinie, pour toute matrice de corrélation définie positive.
- *la méthode SMCE, l'estimation spectrale par l'extension séquentielle de la matrice de corrélation multidimensionnelle* : Avec cette méthode, et en utilisant la structure ND-Toeplitz des coefficients de réflexion généralisés, on remplit les trois points qu'on vient de relever. Par contre, cette méthode qui dépend sur une extension directe de la matrice de corrélation ND-Toeplitz n'offre pas un support spectral infini, ce qui représente une contrainte qu'on espère contourner dans un travail à venir, en utilisant la même technique.

Un axe général a été suivi pour arriver à notre fin, et c'est celui d'aller examiner la structure algébrique définissant les fondations de la théorie spectrale, et expliquant la

relation spectrale entre une matrice de corrélation de taille limitée et les matrices de taille infinie.

Les méthodes de type MUSIC ou ESPRIT : dans ce genre de méthodes d'estimation spectrale, on sépare l'espace linéaire défini par la matrice de corrélation en deux parties : la première est celui produit par le signal et le deuxième est celui produit par le bruit. En acceptant cette séparation, on arrive à capturer des fréquences quasi-instantanées. Cette approche est d'une grande utilité quand le signal a une configuration spectrale présentant des pics accentués— un nombre limité des pics spectraux. Par contre pour les applications réelles le signal est rarement de telle configuration. D'autre part, la séparation en « signal + bruit » demande la factorisation en SVD -ou en valeurs propres- qui est très coûteuse en temps de calculs. En plus, cette séparation dépend sur un seuil arbitraire qui peut conduire à une perte d'information. Aussi, une autre contrainte se présente avec cette approche, cette contrainte se présente par le fait que le nombre de points du support spectral est limité par la taille du signal, ce qui n'est pas approprié aux situations où l'on veut avoir un support plus étendu.

Les méthodes analytiques : dans ce cadre, on produit une estimation spectrale de Maximum d'entropie, selon le modèle (1.2) sans le passage par l'inverse de la matrice de corrélation, mais en se basant sur la propriété « matching » seulement. A notre connaissance il y a eu deux tentatives, la première [55] utilise une itération convergente, qui est très coûteuse dans le temps de calculs car il n'y a pas de prise en compte de la structure spéciale ND-Toeplitz. La deuxième méthode [54] est un peu hybride et artisanale, dans le sens où elle utilise la récursivité WWR [8]-[9] et modifie à chaque étape les coefficients du filtre multichannel bloc par rapport à l'entropie produite par (1.3). La manière dans laquelle les coefficients blocs sont modifiés contredit clairement l'intégrité de la structure initiale de l'algorithme WWR. Plus précisément cette méthode multiplie le coefficient de réflexion bloc à chaque étape par un coefficient qui est extérieur à la structure originale de l'algorithme WWR, ce qui peut conduire à rendre le système récursif singulier, à chaque instant.

Par ailleurs, signalons un travail récent de Clarisse RAMANANJARASOA [72] où ces approches ont été utilisées pour une étude approfondie des champs stochastiques et les différentes estimations des filtres prédictifs. L'une des applications concerne la texture dans les images.

Bien que le cadre semble identique, notre objectif concerne l'estimation spectrale :

La construction pertinente de la matrice de corrélation (à partir du spectre de l'image que l'on veut reconstituer) est à la base du débruitage et l'extension de la corrélation permet d'améliorer la résolution (super-résolution).

On indiquera brièvement que l'extension de la corrélation se fait par des procédés séquentiels grâce aux coefficients de réflexion (généralisés), ce qui permet à tout instant de contrôler la positivité et la structure Toeplitz généralisées, le procédé n'est cependant maîtrisé que de manière approximative.

Cette approche nous permet d'éviter l'emploi du filtre prédictif conduisant à une estimation spectrale à l'aide de l'inverse d'un polynôme positif de plusieurs variables, lequel, (dans le cas de plusieurs dimensions) pose un redoutable problème de stabilité du aux zéros éventuels de ce polynôme, qui en limite l'intérêt, (voir cependant les récents progrès réalisés par l'équipe du Professeur Mohamed Najim [71]).

◆ *Application au traitement du signal Radar (SAR)*

L'estimation spectrale multidimensionnelle est une partie importante de chaque système de Radar SAR. Plus précisément, la transformée de Fourier du signal reçu doit être réalisé de telle manière qu'on enlève le bruit et l'on préserve les informations.

Les systèmes SAR sont répartis dans plusieurs domaines de télédétection spatiale et aérienne. Après le développement du Radar SLR (Side looking Radar), le système SAR a été développé pour fournir de multiples avantages.

Dans notre étude de l'estimation spectrale pour l'application SAR nous avons testé plusieurs méthodes que nous avons ensuite comparées avec les méthodes de Maximum d'entropie (que nous avons développées).

On voit dans la Figure 1.1, Figure 1.2, Figure 1.3, et la Figure 1.4 les résultats de l'application des méthodes de Corrélograme, SMCE (Chapitre 7), ASMSE (Chapitre 6), et la méthode Capon, respectivement.



Figure 1.1

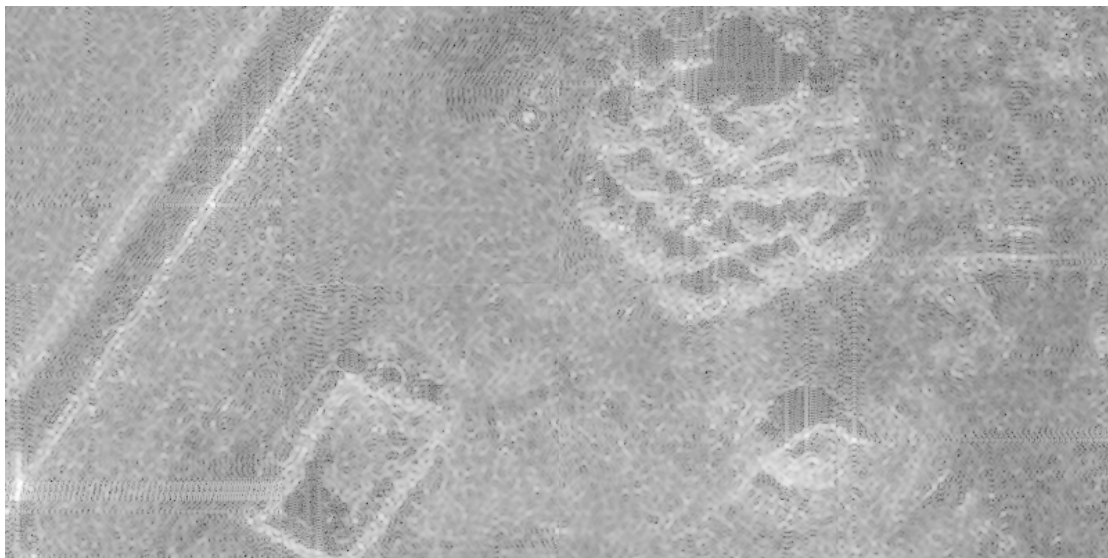


Figure 1.2



Figure 1.3

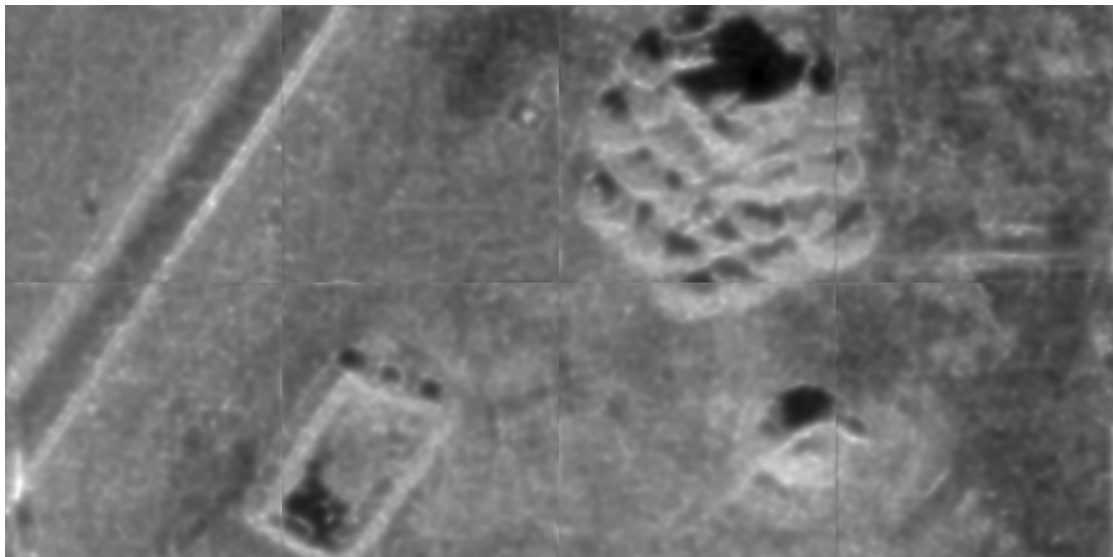


Figure 1.4

## II L'organisation de cette thèse

Cette thèse est organisée selon ce qui suit

*Chapitre 2, Introduction.*

*Chapitre 3, un nouvel Algorithme de Burg équivalent à l'algorithme de Levinson, dans les résultats: on étudie la relation entre l'algorithme de Burg et l'algorithme de Levinson, et on montre que cette relation qu'on lui donne la preuve théorique ne devra que produire les mêmes résultats numériques.*

*Chapitre 4, Les Coefficients de réflexion généralisés dans le cas de matrices Bloc Toeplitz*: nous étudierons la structure spéciale des coefficients de réflexion généralisés dans le cas de matrices Bloc Toeplitz ‘Strongly Regular’.

*Chapitre 5, Les Coefficients de réflexion généralisés dans le cas de matrices Toeplitz-Bloc-Toeplitz*: nous étudierons la structure spéciale des coefficients de réflexion généralisés dans le cas de matrices Toeplitz-Bloc-Toeplitz ‘Strongly Regular’.

*Chapitre 6, la méthode ASMSE, L’estimation spectrale multidimensionnelle (approximation séquentielle)*: on présente une nouvelle méthode pour l’estimation spectrale multidimensionnelle qui a la propriété de ‘matching’ approximative, et correspond à une estimation de quasi-Maximum d’Entropie, - La propriété de ‘matching’ (adéquation) signifie que pour une matrice de corrélation, l’estimation spectrale reproduit les mêmes coefficients de corrélation du départ.

*Chapitre 7, la méthode SMCE, l’estimation spectrale par l’extension séquentielle de la matrice de corrélation multidimensionnelle*: on présente une nouvelle méthode pour l’estimation spectrale multidimensionnelle qui a la propriété de ‘matching’ exact, avec un spectre de maximum d’entropie, et correspond à une estimation de Maximum d’Entropie.

*Chapitre 8, une étude comparative de plusieurs méthodes d’estimation spectrale*: on effectue une étude comparative de plusieurs méthodes de l’estimation spectrale. De plus, on présente l’application des ces méthodes dans le cadre de l’estimation spectrale pour le SAR (Synthetic Aperture Radar).

## INTRODUCTION

The area of this dissertation falls within the science of signal processing. It is concentrated around the subject of **Spectral Power Estimation**, and with it, the corresponding different mathematical theories concerning Toeplitz Systems and the Generalized Reflection Coefficients.

### I Multidimensional Spectral Power Estimation

Spectral Power Estimation is a principal component in many practical systems. Whenever there is indecision in spectral power localization and (or) amplitude, Spectral Power Estimation theory helps to counter this indecision, and produces a reasonable estimation or an image of better quality. This indecision has its sources at the following situations:

- a) **Discrete signal problem:** in contemporary times, discrete representation of the signal is a common practice. Of course, by the Shannon theory, there is a theoretical connection between the discrete form and the continuous form of the signal, but in many situations we have to decide the spectral power starting from a finite number of signal samples. This can be interpreted as an incomplete information situation. Spectral Power Estimation aims to compensate this lack of information by finding a “best guess” of the actual Spectral Power, for the entire signal and not only a finite part of it.
- b) **Low SNR:** for different reasons, the signal after acquisition may contain a high degree of additive noise. In situations where we are looking to correctly estimate the Spectral Power of the signal, Spectral Power Estimation is an ideal solution to the problem.
- c) **Practical constraints:** in many practical systems, as in SAR (Synthetic Aperture Radar) Radar Systems and MRI Systems, due to practical constraints we have to limit the number of signal sensors, which results in a 2D signal with a very limited number of signal samples in the direction of the sensors. For this, Multidimensional Spectral Power Estimation is also necessary.



For the above reasons, the domain(s) in which Spectral Power Estimation is in use include many practical applications. Among these applications we may mention: Radar Systems, Magnetic Resonance Systems (MRI), Astrophysics and Geophysics.

◆ *Spectral Power Estimation, Moments point of view*

The investigation of Spectral Power Estimation through signal moments-or correlation, was first established by Kolmogoroff [26]. By his famous relation the Spectral Power of the signal  $x[n]$ , expressed as  $|X(j\omega)|^2$ , is equivalent to  $R(j\omega)$ ,

where  $r$ , is the auto-correlation signal defined as  $r[n] := \frac{1}{c} \sum_k x[k+n]x^*[k]$ , and

$c$ , a constant. In other words, the Spectral Power of the signal is equal to the Fourier transformation of the correlation signal. For an example, in Figure 2.1, the time representation of a sampled audio signal is displayed.

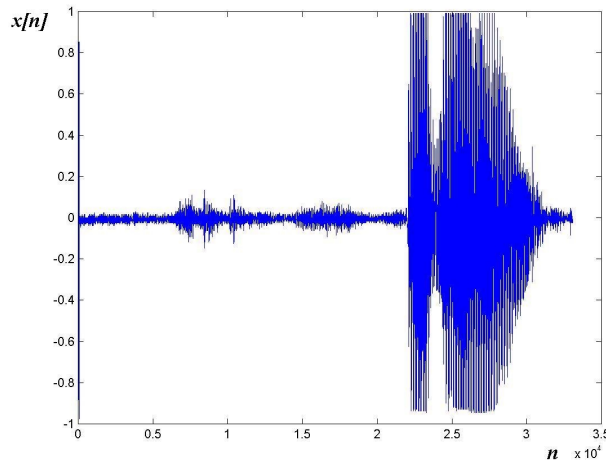


Figure 2.1

For the same signal, we present in Figure 2.2, the corresponding auto-correlation signal. Note that the correlation signal is almost descendent in its values. In other words, correlation values can be considered as a base for the signal, where the most important values for signal definition are near the zero region. Of course, the transformation between the signal and its auto-correlation is not reversible but it is sufficient so that a few correlation measures help to establish a starting point toward a more accurate picture of the spectral power of the signal.

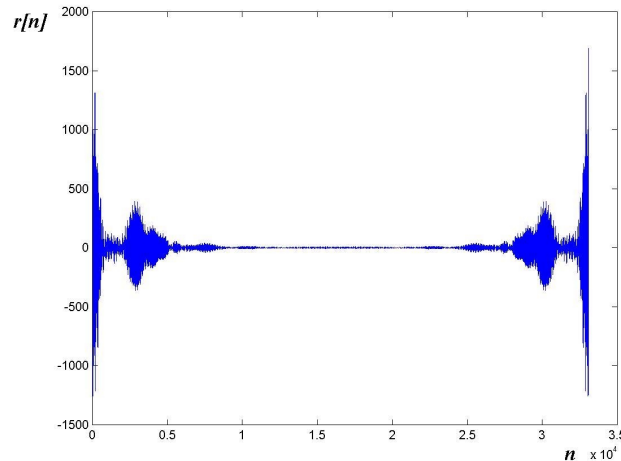


Figure 2.2

Almost all the algorithms of Spectral Power Estimation are based on the concept of providing Spectral Power Estimation that matches the presented time signal in its auto-correlation values. This is known as the “matching property”. In [6], the matching property was subject to a maximum of entropy ionoptimisat problem, whereas in [30], another property is used, which is the minimum of variance.

◆ *Spectral Power Estimation, numerical considerations*

Numerical stability of any algorithm for Spectral Power Estimation is important. This is because, mathematically, there is a great degree of ambiguity in the spectral power determination problem. While many presented algorithms follow a given optimization criteria, few have a solid implementation resistant to some parameter change. Instability does usually manifest itself in a broken inversion in the recursive linear systems. Moreover it usually produces a distorted Spectral Power Estimation, which can be sometimes worse than a direct Fast Fourier Transformation (FFT). In general, the parameters of the algorithm are selected as a compromise between *stability* and *precision- or output quality*. For example, for a given signal, augmenting the system order- correlations measure number should provide a better resolution in the Spectral Power Estimation. Unfortunately however, if the algorithm is not stable, it can cause the inverse. The above discussion suggests the following criteria for the appreciation of any Spectral Power Estimation method:

- a) **Stability:** as noted above, stability is considered as a counter weight to precision. This is known to be true in the general case, but we argue that this is true only in a very few cases. In this thesis we have the opportunity to shed light on this key point. What we have concluded from analyzing previous work, and from practical experience is that the contradictory relation between stability and precision is due to improper construction of the algorithm(s), which leaves the door open for singularity. On the other hand, when care is taken the contradictory relation happens only in the rare case of near zero signals, and thus it should not be considered as a general constraint. To explain this claim, we will give two examples, for algorithms for Spectral Power Estimation. In each, inconsistency in

the recursive linear system is the cause of great instability at application:

- In the normal Burg's Algorithm, the square root minimum of forward and backward prediction error signals is calculated. And a recursive relation for updating the error signals at each step of the algorithm is used. The latter relation, however, is generated from Levinson's Algorithm, and is applied in a manner that is inconsistent with the original Levinson's Algorithm. For that, as we will explain in Chapter 3, a modification in the Burg's Algorithm that keeps this linear system invertible gives the Burg's Algorithm the missing stability.
  - In the case of 2D Spectral Power Estimation using quarter plan and (or) half plan filters; filter coefficients are defined to minimize prediction error. Unlike the 1D case, where the prediction polynomial is known to have its roots inside the unit circle, the produced filter could be unstable. Hence, quarter plan, and half plan filters are well known to suffer from great instability, and erroneous results.
- b) **Precision:** for a given system order, and a measured input signal's SNR, two algorithms for Spectral Power Estimation can be compared for their precision in a controlled experiment. In general, output quality is lesser for low input SNR values. At the same time, if one algorithm produces a better quality for a given SNR value, it is more probable that it will continue to do so for higher values.
- c) **Calculations volume and time:** the number of calculations, required by a Spectral Power Estimation method is an important factor. Also, the ability of the algorithm to be performed through Parallel Processing is of a great value in minimizing execution time. The volume of calculations is also of great importance in particular when we are dealing with multidimensional signals, since the size of the correlation matrix grows exponentially for each dimension.

◆ *Spectral Power Estimation, the multidimensional case*

For applications concerning multidimensional signal, i.e. SAR Radar and 3D Magnetic Resonance Imaging MRI, multidimensional Spectral Power Estimation is necessary. The multidimensional Spectral Power Estimation problem is different than the 1D case and different difficulties arise due to its non-linear nature. In the generalization efforts, many of the 1D Spectral Power Estimation techniques were easily extended to the ND case for example, the Periodogram, the Correlogram, and the Capon Filter. On the other hand the Maximum of Entropy method, which is known for its optimal performance, remains an active domain of research. In Figure 2.3, we present a general diagram representing the state of the art in multidimensional Spectral Power Estimation.

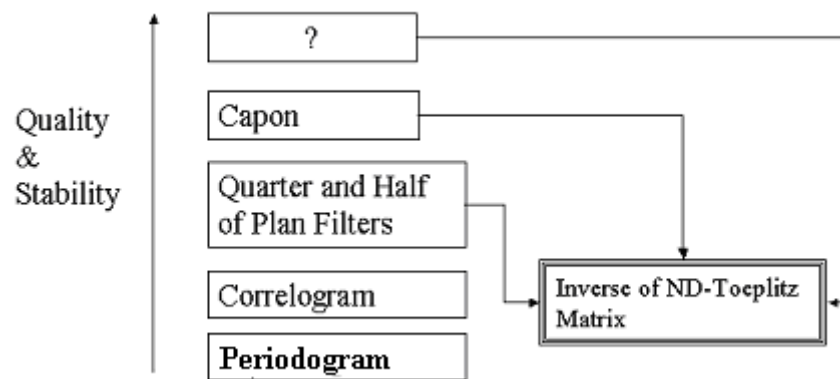


Figure 2.3

The efforts in this area were especially concentrated over the generalization of the maximum of entropy Spectral Power Estimation (MEM), for its well-known estimation precision. In [54] and [55], analytical methods were proposed for the multidimensional problem. Usually analytical methods are used, as contrary to the 1D case, there is no known direct algebraic solution to the MEM problem. Analytical methods suffer sometimes from initialization and convergence stability problems, and have the disadvantage of indeterminate execution time, and arbitrary parameters values. In this thesis, we are proposing two new Algebraic methods for multidimensional Spectral Power Estimation with a deterministic nature. In both methods, a new class of operator, which we have called the ‘Walking Operator’, permits the production of the estimation in a sequential manner. The first method, presented in Chapter 6, has an approximative matching property, and the second, presented in Chapter 7, gives an exact correlation matching and does not require polynomial approximation of the inverse of the Spectral Power Estimation.

## II Overview of this thesis

This dissertation is organized in two parts. The first part is on the subject of Spectral Estimation, and the second part is on the subjects of Vector Quantization of Colored Images and the Combinatorial Approach to Object Analysis.

### Spectral Power Estimation

Chapter 3 to Chapter 8 treat the main mathematical theory for the Multidimensional Spectral Power Estimation.

#### ◆ Chapter 3

This Chapter proposes a new Burg Algorithm equivalent in results to the Levinson Algorithm for the 1D case and the 2D case. From the presented numerical simulations we see the advantage of applying the Burg Algorithm in the way that we are proposing. Also, in the 2D case, the original WWR Algorithm [8]-[9] is optimized in the calculations cost aspect, through a proposition that proves a skew symmetry in the cross-correlation matrix between the forward and backward error vectors.

◆ *Chapter 4*

This Chapter studies the structure of the Generalized Reflection Coefficients in the case of Hermitian Block Toeplitz matrix. An optimized adapted algorithm is proposed.

◆ *Chapter 5*

This Chapter studies the structure of the generalized reflection coefficients in the case of Hermitian Toeplitz Block Toeplitz matrix. An optimized adapted algorithm is proposed.

◆ *Chapter 6*

This Chapter presents an approximative approach for the Multidimensional Spectral Power Estimation problem. The presented algorithm performs in a sequential manner, across each dimension. Numerical simulations are also presented for a three-dimensional test signal.

◆ *Chapter 7*

Building on the results of Chapter 4 and Chapter 5, Chapter 7 presents a novel maximum of entropy method for Multidimensional Spectral Power Estimation. The presented estimation has an exact matching property, and asymptotically is a Maximum of Entropy Estimation.

◆ *Chapter 8*

To be able to construct an equitable idea about the capabilities and the performance of each of the presented Spectral Power Estimation methods, we run a numerical comparative study over different methods for spectral estimation.

◆ *Chapter 9*

This Chapter presents the main conclusions of our work, and proposes new directions for future development.

# **Spectral Power Estimation**



---

## A MODIFIED BURG ALGORITHM EQUIVALENT IN RESULTS TO LEVINSON ALGORITHM

*Abstract*-We present a new modified Burg-Like algorithm for spectral estimation and adaptive signal processing that yields the same prediction coefficients as given by the Levinson algorithm for the solution of the normal equations. An equivalency proof is given for both the 1D signal and the 2D signal cases. Numerical simulations illustrate the improved accuracy and stability in spectral power amplitude and localization; especially in the cases of low signal to noise ratio, and (or) augmenting the used prediction coefficients number for relatively short data records. Our simulations also illustrate that for relatively short data records the unmodified version of the Burg Algorithm fails to minimize the mean square residual error beyond a certain order, while the new algorithm continues the minimization with higher orders.

*Résumé*- On présente un nouvel algorithme proche de celui de Burg pour l'estimation spectrale et le traitement adaptatif du signal. L'algorithme présenté produit les mêmes coefficients que ceux donnés par l'algorithme de Levinson, pour la solution des équations normales. La preuve d'équivalence est présentée pour les signaux 1D et 2D. La modification apportée permet de garantir la stabilité de l'algorithme de Burg. Cette modification est justifiée théoriquement. Par ailleurs les simulations numériques confirment une amélioration de cette stabilité, (ainsi que la précision), dans la détermination de l'amplitude et la localisation de la puissance spectrale. L'amélioration apparaît davantage dans le cas d'un faible rapport signal/bruit, et (ou) dans celui d'une taille minimale des données. Aussi, les simulations numériques montrent que pour certaines conditions de taille minimale des données et d'un ordre de système élevé, la version non-modifiée de l'algorithme de Burg ne minimise pas l'erreur résiduelle. En l'occurrence, l'algorithme de Levinson continue la minimisation avec l'augmentation de l'ordre.

### I Introduction

Linear Autoregressive Modeling has many contemporary fields of application [1]-[3]. At the same time, much work has been devoted to studying this model and its applications in the one-dimensional signal case, and more recently, for the two-dimensional signal. A common factor in most of the previous work is the solution of the normal equations –known also as the Yule-Walker equations. This is by using different techniques to find an estimation of the prediction coefficients, which are scalars in 1D case, and matrices in the Multichannel (multivariate) case. Starting from a given 1D signal, two main methods of estimating the prediction coefficients are the Levinson Algorithm [7] and the Burg Algorithm [6]. The counterparts of these two algorithms in the 2D case are, respectively, a modified version of the Whittle-Wiggins-Robinson Algorithm (WWR)[8][9], and a group of slightly in-between different algorithms given in [10], [11], [15], which will be referred-to in this chapter–excluding [10], as 2D Burg Algorithms. Historically, the 2D approach depended on the Multichannel Levinson (WWR) and the Multichannel Burg approach [12]. First, the Coefficients matrices are obtained, and next, an extra step is applied, to recover



the 2D quarter-plan causal Filter scalar coefficients from the calculated coefficients Matrices. The connection between the Coefficients Matrices and the prediction 2D Filter was first established by [14]. This was further invested by [11], through the application of the Multichannel Burg Algorithm [12] directly on the two dimensional data, which represented the first 2D-Burg algorithm. The same type of algorithm was presented in [15], but with an additional simplification that takes advantage of the 2D Correlation Matrix being Toeplitz-Block-Toeplitz, while it is just Block Toeplitz in the Multichannel case. In the alternate case, in [10], another Burg-like algorithm was presented, that calculates the 2D Prediction Filter directly without passing by the calculus of the corresponding Multichannel Coefficients Matrices.

In this chapter, we present a new 1D and 2D Burg Algorithm, that yields the same prediction coefficients as the Levinson Algorithm in the 1D case, and the WWR in the 2D case. Also we enhance WWR computational efficiency in the 2D case, through

**Proposition 3.3.** In practice, the motivation of using the Burg Algorithm is its computational efficiency over the Levinson Algorithm, since the latter demands the calculation of the correlation matrix in advance, which is a very time consuming task. For the same reason, the 2D Burg Algorithms are preferred over WWR. Still, for the reasons that we will explain in this chapter, the 1D and 2D Burg Algorithms suffer from a major numerical deficiency, and this was the motive behind our development of the new Burg Algorithm. While the computational efficiency of The New Modified Burg Algorithm needs to be further investigated, it gives a stable Levinson and WWR solution. We also believe that the new presented Burg Algorithm, in 1D and 2D cases, represent the natural Burg Algorithms, since it is now consistent, in theory and in application, to the original Levinson approach.

In [4]-[5], fast, and practical formulas are presented, that calculate the inverse of the Correlation Matrix in function of the prediction coefficients.

This chapter is organized as follows. In Section II, we establish the proof of asymptotic equivalency, for the 1D case, between, Levinson Algorithm's output, and that of the Burg Algorithm's. In Section III, we also establish the proof of asymptotic equivalency, between the output of the WWR, and that of the 2D Burg Algorithm. In Section IV, we present the practical modifications necessary for the current Burg Algorithms, in both 1D and 2D cases, to realize the equivalency in giving the same results. Finally, Section V contains the numerical examples that illustrate the gain in numerical stability of the new Burg Algorithm, in comparison with the original Burg Algorithm.

## II 1D Case

### ◆ *The model*

The autoregressive model

$$x(k) + \sum_{l=1}^n a_l^n x(k-l) = w(k) \quad (3.1)$$

where  $w$  represents the prediction error of the signal  $x$ , yields the Normal Equations

$$R_n \mathbf{a}_n = -\mathbf{r}_n \quad (3.2)$$

where  $R_n$  is a Toeplitz Hermitian matrix of size  $(n \times n)$ , defined as

$$R_n := \left[ r_{ij} \right]_{i,j=0,1,\dots,n-1}, r_{ij} = r_{ji}^* = r_{i-j} \quad (3.3)$$

$$r_t := E_k \left( x(k+t)x(k)^* \right), t = 0, \pm 1, \dots, \pm n, E_k(f(k)) := \frac{1}{|\{k\}|} \sum_k f(k) \quad (3.4)$$

$$\mathbf{a}_n := [a_1^n, a_2^n, \dots, a_n^n]^T, \mathbf{r}_n := [r_1, r_2, \dots, r_n]^T \quad (3.5)$$

◆ *The 1D Levinson Algorithm*

The Levinson Algorithm [7] proceeds to the solution of (3.2) in a recursive manner, for  $n > 1$

$$a_n^n = -\frac{r_n + \hat{\mathbf{r}}_{n-1}^T \mathbf{a}_{n-1}}{r_0 + \mathbf{r}_{n-1}^T \mathbf{a}_{n-1}^*} \quad (3.6)$$

$$\mathbf{a}_n = \begin{bmatrix} \mathbf{a}_{n-1} \\ 0 \end{bmatrix} + a_n \begin{bmatrix} \hat{\mathbf{a}}_{n-1}^* \\ 1 \end{bmatrix} \quad (3.7)$$

starting from

$$a_1^1 = -\frac{r_1}{r_0} \quad (3.8)$$

where the notation  $\hat{\mathbf{x}}$  defines a vector with the same elements of  $\mathbf{x}$  taken in the reverse order.

◆ *1D Burg Algorithm*

The Burg Algorithm [6] defines an estimate of the prediction errors

$$e_n^f(k) := \sum_{l=1}^n a_l^n x(k-l) + x(k) \quad (3.9)$$

$$e_n^b(k) := \sum_{l=1}^n a_l^{n*} x(k+l-n) + x(k-n)$$

The prediction coefficient is also calculated in a recursive manner, according to the relation

$$a_n^n = \frac{-E_k(e_{n-1}^f(k)e_{n-1}^{b*}(k-1))}{\frac{1}{2}E_k(|e_{n-1}^f(k)|^2 + |e_{n-1}^b(k-1)|^2)} \quad (3.10)$$

Using the Levinson relation (3.7), a recursive relation between the errors signals is obtained and used in the calculus, to update the error signals to the next order

$$e_{n+1}^f(k) = e_n^f(k) + a_{n+1}^{n+1} e_n^b(k-1) \quad (3.11)$$

$$e_{n+1}^b(k) = e_n^b(k-1) + (a_{n+1}^{n+1})^* e_n^f(k). \quad (3.12)$$

◆ *Equivalency proof*

To proceed in our construction, we need the following proposition, which is easy to verify.

**Proposition 3.1.** *Asymptotically, the forward and backward prediction errors square means are asymptotically equal,*

$$\lim_{k \rightarrow +\infty} \frac{1}{|\{k\}|} \sum_k |e_n^f(k)|^2 = \lim_{k \rightarrow +\infty} \frac{1}{|\{k\}|} \sum_k |e_n^b(k-1)|^2. \quad (3.13)$$

**Theorem 3.1.** *Asymptotically, the prediction coefficients calculated using Levinson Algorithm and Burg Algorithm are Equals.*

**PROOF.** Using the relation (3.13) we can now write the Burg relation (3.10) in the form

$$a_n^n = \frac{-E_k (e_{n-1}^f(k) e_{n-1}^{b*}(k-1))}{E_k (|e_{n-1}^b(k)|^2)}. \quad (3.14)$$

Replacing (3.9) into (3.14), we proceed according to the following

$$a_{n+1}^{n+1} = E_k \left( \begin{array}{l} x(k)x(k-n-1) + \\ \sum_{l=1}^n x(k)x^*(k-1-n+l)a_l + \\ \sum_{l=1}^n a_l^n x(k-l)x^*(k-n-1) + \\ \sum_{l=1}^n a_l^n \sum_{l'=1}^n x(k-l)x^*(k-1-n+l')a_{l'} \end{array} \right) / \left( \begin{array}{l} x(k-n)x(k-n) + \sum_{l=1}^n x(k-n)x^*(k-n+l)a_l^n \\ + \sum_{l=1}^n a_l^{n*} x(k-n+l)x^*(k-n) \\ + \sum_{l=1}^n a_l^{n*} \sum_{l'=1}^n x(k-n+l)x^*(k-n+l')a_{l'} \end{array} \right) \quad (3.15)$$

$$a_{n+1}^{n+1} = - \left( \begin{array}{l} r_{n+1} + \sum_{l=1}^n r_{n+1-l} a_l^n \\ + \sum_{l=1}^n a_l^n r_{n+1-l} + \sum_{l=1}^n a_l^n \sum_{l'=1}^n r_{n+1-l-l'} a_{l'} \end{array} \right) / \left( \begin{array}{l} r_0 + \sum_{l=1}^n r_{-l} a_l^n \\ + \sum_{l=1}^n a_l^{n*} r_l + \sum_{l=1}^n a_l^{n*} \sum_{l'=1}^n r_{l-l'} a_{l'} \end{array} \right) \quad (3.16)$$

Using the equality

$$\sum_{l=1}^n a_l r_{d-l} = -r_d \quad d = 1, 2, \dots, n \quad (3.17)$$

which is just another form for the relation (3.2), the second and fourth terms, in both the numerator and denominator of (3.16) are eliminated

$$a_{n+1}^{n+1} = - \left( r_{n+1} + \sum_{l=1}^n r_{n+1-l} a_l \right) / \left( r_0 + \sum_{l=1}^n a_l^* r_l \right). \quad (3.18)$$

This completes the proof.

### III 2D Case

#### ◆ The Model

The multichannel signal linear autoregressive model is defined as [16]

$$X(k) = -\sum_{l=1}^{n_1} A_l^{n_1} X(k-l) + W(k) \quad (3.19)$$

where  $X$ ,  $W$  are vectors of size  $n_2 + 1$ , changing according to the time  $k$ ,  $A_l^{n_1}$  is the  $l$  prediction coefficient matrix of degree  $n_1$  of size  $((n_2 + 1) \times (n_2 + 1))$ .

This model yields also the Multichannel Normal Equations, known as Multichannel Yule-Walker Equations

$$\mathbf{A}_{n_1, n_2} \cdot R_{n_1, n_2} = \mathbf{r}_{n_1, n_2} \quad (3.20)$$

$$\mathbf{A}_{n_1, n_2} := [A_1^{n_1}, A_2^{n_1}, \dots, A_{n_1}^{n_1}] \quad (3.21)$$

$$R_{n_1, n_2} := \begin{bmatrix} R_0 & R_1 & \cdots & R_{n_1-1} \\ R_{-1} & R_0 & \ddots & \vdots \\ \vdots & \ddots & \ddots & R_1 \\ R_{1-n_1} & \cdots & R_{-1} & R_0 \end{bmatrix} \quad (3.22)$$

$$R_k := E_n (X(n+k)X^H(n)), k = 0, \pm 1, \dots, \pm n_1 \quad (3.23)$$

$$\mathbf{r}_{n_1, n_2} := [R_1, R_2, \dots, R_{n_1}] \quad (3.24)$$

The correlation matrix  $R_{n_1, n_2}$  is Hermitian and Block Toeplitz. In the Case of 2D signal the same multichannel model can be used, by redefining the multichannel vector, using the 2D signal [14][15]

$$X(k) := \begin{bmatrix} x(k, t_2' + n_2) & x(k, t_2' + n_2 + 1) & \cdots & x(k, t_2'') \\ x(k, t_2' + n_2 - 1) & x(k, t_2' + n_2) & \cdots & x(k, t_2'' - 1) \\ \vdots & \vdots & \ddots & \vdots \\ x(k, t_2') & x(k, t_2' + 1) & \cdots & x(k, t_2'' - n_2) \end{bmatrix}$$

$$x(t_1, t_2) \in \mathbb{C}, t_1 \in \mathbb{N}, t_2' \in \mathbb{N}, t_2'' \in \mathbb{N}, t_2' \leq t_2 \leq t_2'' \quad (3.25)$$

In this case, the definitions and relations (3.19)-(3.23) still hold for the expression of the Normal Equations and the correlation matrix in the case of the 2D signal, with the Hermitian correlation matrix having a Toeplitz Block Toeplitz (TBT) structure.

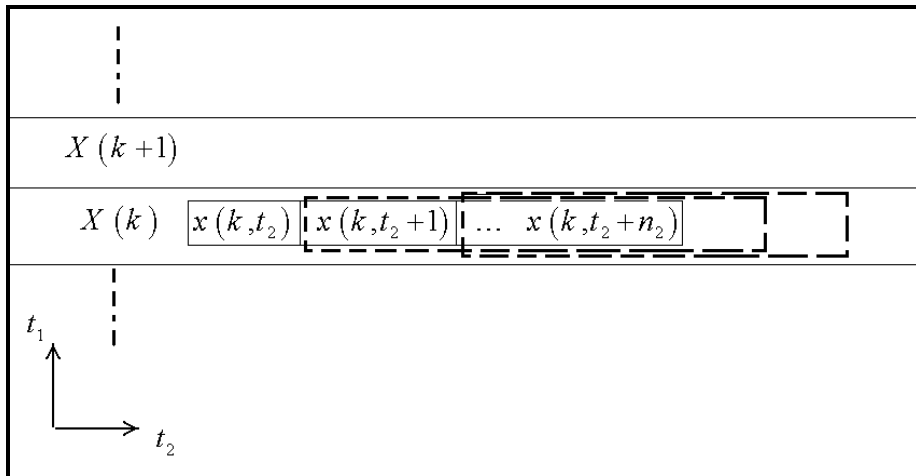


Figure 3.1, the columns of  $X(k)$  are generated by a sliding vector of size  $n_2 + 1$  in the signal line  $k$ .

◆ *The 2D Levinson Algorithm (WWR)*

The coefficients matrices are calculated in a recursive manner, starting from  $n > 0$ , according to [8][9][16]:

$$A_n^n = -\Delta_n (P_{n-1})^{-1} \quad (3.26)$$

$$\Delta_n := R_n + \sum_{l=1}^{n-1} A_l^{n-1} R_{n-l} \quad (3.27)$$

$$P_{n-1} := R_0 + \sum_{l=1}^{n-1} J A_l^{n-1*} J R_l \quad (3.28)$$

with,

$$\mathbf{A}_{n,n_2} = [\mathbf{A}_{n-1,n_2}, \mathbf{0}] + A_n^n \begin{bmatrix} J A_{n-1}^{n-1*} J, J A_{n-2}^{n-1*} J, \dots, J A_1^{n-1*} J, \mathbf{1} \end{bmatrix} \quad (3.29)$$

where  $J$  is the Exchange Matrix defined as:

$$J := \begin{bmatrix} 0 & \dots & 0 & 1 \\ \vdots & \ddots & 1 & 0 \\ 0 & \ddots & \ddots & \vdots \\ 1 & 0 & \dots & 0 \end{bmatrix} \quad (3.30)$$

starting From

$$P_0 = R_0 \quad (3.31)$$

◆ *The 2D Burg Algorithm*

As in the 1D case, two Prediction Error signals are defined as [11][12][15]

$$\mathbf{e}_n^f(k) := \sum_{l=1}^n A_l^n X(k-l) + X(k) \quad (3.32)$$

$$\mathbf{e}_n^b(k) := \sum_{l=1}^n J (A_l^n)^* J X(k-n+l) + X(k-n) \quad (3.33)$$

$n \geq 0$

with the following recursive relation

$$\mathbf{e}_{n+1}^f(k) = \mathbf{e}_n^f(k) + A_{n+1}^{n+1} \mathbf{e}_n^b(k-1) \quad (3.34)$$

$$\mathbf{e}_{n+1}^b(k) = \mathbf{e}_n^b(k-1) + J (A_{n+1}^{n+1})^* J \mathbf{e}_n^f(k) \quad (3.35)$$

The Prediction Coefficient Matrix of order  $n$ , is calculated according to [15]

$$A_{n+1}^{n+1} = -[P_n^{fb} + J(P_n^{fb})^T J][P_n^b + J(P_n^f)^* J]^{-1} \quad (3.36)$$

where

$$P_n^{fb} := E_k \left( \mathbf{e}_n^f(k) (\mathbf{e}_n^b(k-1))^H \right) \quad (3.37)$$

$$P_n^f := E_k \left( \mathbf{e}_n^f(k) (\mathbf{e}_n^f(k))^H \right) \quad (3.38)$$

$$P_n^b := E_k \left( \mathbf{e}_n^b(k) (\mathbf{e}_n^b(k))^H \right). \quad (3.39)$$

The relation (36) results from minimizing the value

$$\text{tr} \left( P_n^f + J (P_n^b)^* J \right). \quad (3.40)$$

◆ *Equivalency proof*

**Proposition 3.2.**

$$P_n^b = J(P_n^f)^* J \quad (3.41)$$

**Proposition 3.3.**

$$P_n^{fb} = J(P_n^{fb})^T J \quad (3.42)$$

**PROOF.** Using the notation  $A_0^n \equiv 1$ , and replacing (3.34), (3.35) into (3.37) we get

$$P_n^{fb} = E_k \left( \sum_{l=0}^n \sum_{l'=0}^n A_l^n X(k-l) (X(k-1-n+l'))^H J (A_{l'}^n)^T J \right) \quad (3.43)$$

By taking the Expectation inside, and by definition (3.23) we get

$$P_n^{fb} = \sum_{l=0}^n \sum_{l'=0}^n A_l^n R_{n+1-l-l'} J (A_{l'}^n)^T J. \quad (3.44)$$

This can be written in the form

$$P_n^{fb} = R_{n+1} + \sum_{l=1}^n \sum_{l'=1}^n A_l^n R_{n+1-l-l'} J (A_{l'}^n)^T J + \sum_{l'=1}^n R_{n+1-l'} J (A_{l'}^n)^T J + \sum_{l=1}^n A_l^n R_{n+1-l} \quad (3.45)$$

By applying the equality

$$\sum_{l=1}^n A_l^n R_{d-l} = -R_d \quad d = 1, 2, \dots, n \quad (3.46)$$

the second term of (3.45), can be written as

$$\sum_{l'=1}^n \left( \sum_{l=1}^n A_l^n R_{(n+1-l')-l} \right) J (A_{l'}^n)^T J = - \sum_{l'=1}^n R_{n+1-l'} J (A_{l'}^n)^T J \quad (3.47)$$

which yields

$$P_n^{fb} = R_{n+1} + \sum_{l=1}^n A_l^n R_{n+1-l} \quad (3.48)$$

Again by rewriting the second term of (3.45) as

$$\begin{aligned} \sum_{l=1}^n \sum_{l'=1}^n A_l^n R_{n+1-l-l'} J (A_{l'}^n)^T J &= \sum_{l=1}^n A_l^n \sum_{l'=1}^n \left( J (A_{l'}^n)^* J R_{n+1-l-l'}^H \right)^H \\ &= \sum_{l=1}^n A_l^n \left( \sum_{l'=1}^n J (A_{l'}^n)^* J R_{l'-(n+1-l)} \right)^H \end{aligned} \quad (3.49)$$

and using the equality

$$\sum_{l=1}^n J (A_l^n)^* J R_{l-d} = -R_{-d}, \quad d = 1, \dots, n \quad (3.50)$$

we find

$$\sum_{l=1}^n \sum_{l'=1}^n A_l^n R_{n+1-l-l'} J (A_{l'}^n)^T J = - \sum_{l=1}^n A_l^n (R_{-(n+1-l)})^H = - \sum_{l=1}^n A_l^n R_{n+1-l} \quad (3.51)$$

which yields

$$P_n^{fb} = R_{n+1} + \sum_{l'=1}^n R_{n+1-l'} J(A_{l'}^n)^T J. \quad (3.52)$$

By considering the fact that for any Toeplitz matrix  $T$  the following is always true:

$$J(T)^T J = T, \quad (3.53)$$

we apply the transformation  $J(\cdot)^T J$  to the expression (3.52), from which we get

$$J(P_n^{fb})^T J = R_{n+1} + J\left(\sum_{l'=1}^n R_{n+1-l'} J(A_{l'}^n)^T J\right)^T J. \quad (3.54)$$

And by noticing that for any matrix  $M$  we have:

$$J(M)^T J = (JMJ)^T \quad (3.55)$$

we get

$$J(P_n^{fb})^T J = R_{n+1} + \sum_{l'=1}^n \left( J R_{n+1-l'} J (A_{l'}^n)^T J J \right)^T = R_{n+1} + \sum_{l'=1}^n A_{l'}^n J (R_{n+1-l'})^T J \quad (3.56)$$

By this the proof is complete.

**Theorem 3.2.** *Asymptotically, the prediction coefficients calculated using WWR Algorithm and 2D Burg Algorithms are Equals.*

**PROOF.** According to (3.41) and (3.42), (3.36) can be expressed as

$$A_{n+1}^{n+1} = -[P_n^{fb}] [P_n^b]^{-1}. \quad (3.57)$$

Replacing according to (3.34), (3.35), we get

$$P_n^{fb} = E_k \left( \begin{array}{c} \left( X(k) + \sum_{l=1}^n A_l^n X(k-l) \right) \\ \left( X(k-n-1) \right)^H + \\ \left( \sum_{l=1}^n (X(k-n-1+l))^H (J(A_l^n)^* J)^H \right) \end{array} \right) \quad (3.58)$$

$$P_n^{fb} = E_k \left( \begin{array}{c} X(k)(X(k-n-1))^H + \sum_{l=1}^n X(k)(X(k-n-1+l))^H (J(A_l^n)^* J)^H + \\ \sum_{l=1}^n A_l^n X(k-l)(X(k-n-1))^H + \sum_{l=1}^n A_l^n \sum_{l'=1}^n X(k-l)(X(k-n-1+l'))^H (J(A_{l'}^n)^* J)^H \end{array} \right) \quad (3.59)$$

By taking the expectation over each term and by definition (3.23) we get

$$P_n^{fb} = \left( \begin{array}{c} R_{n+1} + \sum_{l=1}^n R_{n+1-l} (J(A_l^n)^* J)^H + \\ \sum_{l=1}^n A_l^n R_{n-l+1} + \\ \sum_{l=1}^n A_l^n \sum_{l'=1}^n R_{n-l-l'+1} (J(A_{l'}^n)^* J)^H \end{array} \right) \quad (3.60)$$

Using the equality

$$\sum_{l=1}^n A_l^n R_{d-l} = -R_d \quad d = 1, 2, \dots, n \quad (3.61)$$

which is just another form of (3.20), we obtain

$$P_n^{fb} = R_{n+1} + \sum_{l=1}^n A_l^n R_{n-l+1}. \quad (3.62)$$

Also in the same way we obtain

$$P_n^b = E_k \left( \begin{array}{l} X(k-n)(X(k-n))^H + \\ \sum_{l=1}^n X(k-n)(X(k-n+l))^H \left( J(A_l^n)^* J \right)^H + \\ \sum_{l=1}^n J(A_l^n)^* J X(k-n+l)(X(k-n))^H + \\ \sum_{l=1}^n J(A_l^n)^* J \left( \sum_{l'=1}^n X(k-n+l)(X(k-n+l'))^H \left( J(A_{l'}^n)^* J \right)^H \right) \end{array} \right) \quad (3.63)$$

$$P_n^b = \left( \begin{array}{l} R_0 + \sum_{l=1}^n R_{-l} \left( J(A_l^n)^* J \right)^H + \sum_{l=1}^n J(A_l^n)^* J R_l + \\ \sum_{l=1}^n J(A_l^n)^* J \sum_{l'=1}^n R_{l-l'} \left( J(A_{l'}^n)^* J \right)^H \end{array} \right) \quad (3.64)$$

Also by using the equality

$$\sum_{l=1}^n J(A_l^n)^* J R_{l-d} = -R_{-d}, \quad d = 1, \dots, n \quad (3.65)$$

our proof is completed.

#### IV The Modified Burg Algorithm

Before going into the details of the New Burg Algorithm, it is necessary to state precisely an important fact about the calculation of the prediction error auto-correlation. In the case of 2D signal a recursive relation exists in a way that enhances calculation cost for both of Levinson and Burg Algorithms. More precisely, according to [15][16]

$$P_n^b = P_{n-1}^b + A_n^n \Delta_n^H \quad (3.66)$$

By that, and according to the previous sections, numerically, we can consider the equivalent steps in each iteration of both Levinson Algorithm and Burg Algorithm, as the steps concerning the calculations of relations (3.26), (3.29), (3.66). The difference between the two algorithms resides in the way in which the error cross correlation matrix is calculated; using (3.27) in Levinson Algorithm, and (3.34), (3.35), (3.37) in Burg Algorithm, the same type of discussion also apply to the 1D case.

After demonstrating the Asymptotic In-Results Equivalency between Levinson Algorithms and Burg Algorithms, in both 1D and 2D case, it is now simple to see the modifications needed in order to realize this equivalency in the case of size-limited signal. The principal modification to the existing Burg Algorithms would be in the way in which relations (3.11) and (3.12) in the 1D case, (3.34) and (3.35) in the 2D case, are applied.

##### ◆ 1D Case

For a size-limited signal  $x(k), k \in [0, N-1]$ , the current version of Burg Algorithm, expresses the relation (3.11) and (3.12) in the form:

$$e_{n+1}^f(k) = e_n^f(k) + a_{n+1}^{n+1} e_{n+1}^b(k-1) \quad (3.67)$$



$$e_{n+1}^b(k) = e_n^b(k-1) + (a_{n+1}^{n+1})^* e_{n+1}^f(k)$$

$$k \in [n+1, N-1].$$

As a result of this, the size of the new calculated error signals diminishes with each new order. And as result of this also, the relation (3.10) is expressed in the form [6]

$$a_n^n = \frac{-\sum_{k=n}^{N-1} e_{n-1}^f(k) e_{n-1}^{b*}(k-1)}{\frac{1}{2} \sum_{k=n}^{N-1} \left( |e_{n-1}^f(k)|^2 + |e_{n-1}^b(k-1)|^2 \right)}. \quad (3.68)$$

The correction to this is to proceed with the calculation until the last non-zero value, so instead of the error signal size being diminishing, we should produce an augmentation in the size of both of the forward and backward error signals, according to

$$e_n^b(-1) := 0, e_n^f(N+n) := 0 \quad (3.69)$$

$$e_{n+1}^f(k) = e_n^f(k) + a_{n+1}^{n+1} e_{n+1}^b(k-1)$$

$$e_{n+1}^b(k) = e_n^b(k-1) + (a_{n+1}^{n+1})^* e_{n+1}^f(k)$$

$$k \in [0, N+n] \quad (3.70)$$

and the corrected form of the relation (3.10) becomes

$$a_n^n = \frac{-\sum_{k=1}^{N+n-1} e_{n-1}^f(k) e_{n-1}^{b*}(k-1)}{\sum_{k=0}^{N+n-1} \left( |e_{n-1}^f(k)|^2 \right)}. \quad (3.71)$$

#### ◆ 2D Case

The same discussion for the 1D case is applied to the 2D case also. In the case of size-limited signal

$$x(k, t), k = 0 \dots N_1 - 1, t = 0 \dots N_2 - 1, \quad (3.72)$$

by the new modified algorithm, the relations (3.34) and (3.35) are applied according to

$$\mathbf{e}_n^b(-1) := 0, \mathbf{e}_n^f(N_1+n) := 0 \quad (3.73)$$

$$\mathbf{e}_{n+1}^f(k) = \mathbf{e}_n^f(k) + A_{n+1}^{n+1} \mathbf{e}_n^b(k-1)$$

$$\mathbf{e}_{n+1}^b(k) = \mathbf{e}_n^b(k-1) + J(A_{n+1}^{n+1})^* J \mathbf{e}_n^f(k)$$

$$k \in [0, N_1+n] \quad (3.74)$$

and the relation (3.36) is expressed in the form

$$A_{n+1}^{n+1} = - \left[ \sum_{k=1}^{N_1+n} \mathbf{e}_n^f(k) (\mathbf{e}_n^b(k-1))^H \right] \cdot \left[ \sum_{k=0}^{N_1+n} \mathbf{e}_n^b(k) (\mathbf{e}_n^f(k))^H \right]^{-1} \quad (3.75)$$

Also to achieve the equivalency in the calculus results with the 2D Levinson Algorithm, the 2D Signal needs to be distributed into the multiple-vectors X Matrix in a way that guarantees the Toeplitz block Toeplitz structure of the correlation matrix. Therefore, for a size-limited 2D signal defined in (3.72), the definition (3.25) is applied to the signal according to:

$$X(k) := \begin{bmatrix} x(k,0) & \cdots & x(k,N_2-1) \\ & \ddots & \ddots \\ & & \\ & x(k,0) & \cdots & x(k,N_2-1) \end{bmatrix},$$

so that each row of the signal is repeated and shifted into the next line of the matrix, with zero filled elsewhere.

## V Numerical examples

It is important to note that numerically the modified algorithm is totally equivalent in result to the Levinson Algorithm, in both the 1D and the 2D case. Our objective in this section is to compare Levinson Algorithm application to the Original Burg Algorithm toward spectral estimation, and prediction efficiency. We applied both of algorithms on 20 samples of a noised one-sinusoid signals with a relative frequency positioned at  $f = 0.25$ . The noise signals were generated artificially and added to the spectrum, and the signal samples were obtained using IFFT. Also care was taken to ensure that all generated signals had precisely a signal to noise ratio equal to 30db.

Figure 3.2 and Figure 3.3 represent the spectral estimation versus phase change, resulting from applying Original Burg algorithm, and Levinson Algorithm respectively. The sinusoid phase was changed over 100 equal intervals from zero to  $360^\circ$ . For each phase change the same signal was submitted to each of the two algorithms, with the used prediction order equal to 10. The same results are displayed on a logarithmic scale in Figure 3.4 for Original Burg Algorithm and in Figure 3.5 for Levinsons Algorithm. We notice in this case the inaccuracy of the Burg Algorithm toward phase change, and toward different noise realizations. On the other hand the Levinson Algorithm manifested much more stable results toward noise change, and a stable pattern toward phase change. In fact the results, displayed in Figure 3.2, necessitated the use of the log function so that they could be compared.

Figure 3.6 and Figure 3.7 represent the spectral estimation versus order change, resulting from applying the Original Burg Algorithm, and the Levinson Algorithm respectively. The same signal was submitted to both algorithms with consecutive orders, going from 1 up until 19. We notice that with the order changing the frequency identification is stable for both algorithms applied to the same signal. On the other hand the Burg Algorithm, in this case, suffers from inconsistency in the frequency power value across different order values.

Finally, Figure 3.8 and Figure 3.9 display the Mean square residual error in function of the used order, resulting from applying the Original Burg Algorithm, and the Levinson Algorithm respectively. These results are obtained for the same simulations corresponding to Figure 3.6 and Figure 3.7. The error signal was calculated according to relation (3.1) using the prediction coefficients given by each algorithm, with zero values given for samples outside the provided support. We notice that the original Burg Algorithm fails to minimize the Mean Square Error for order values above 2, while the Levinson Algorithm continues the minimization with order elevation. This comes to illustrate the Original Burg Algorithm handicap when applied to short data records, or what we can call the *border effect*. This effect is due to the application of the recursive relation (3.7) without applying the needed modifications stated above. Failing to apply the modifications (3.68), (3.69) will results in a mistaken cross

correlation value, and it is easy to see that the effect of this will diminish by augmenting the samples number  $N$ , relatively to a given order value  $n$ .

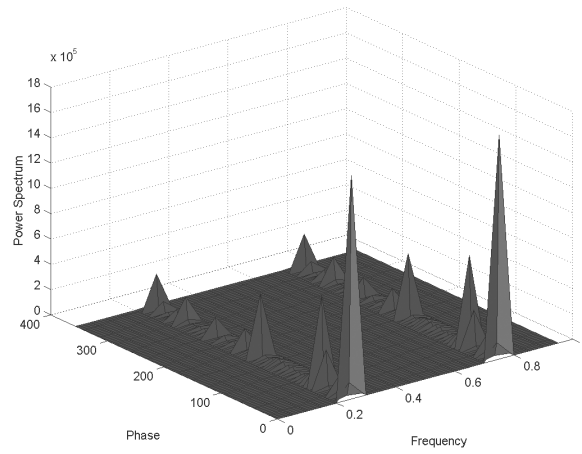


Figure 3.2

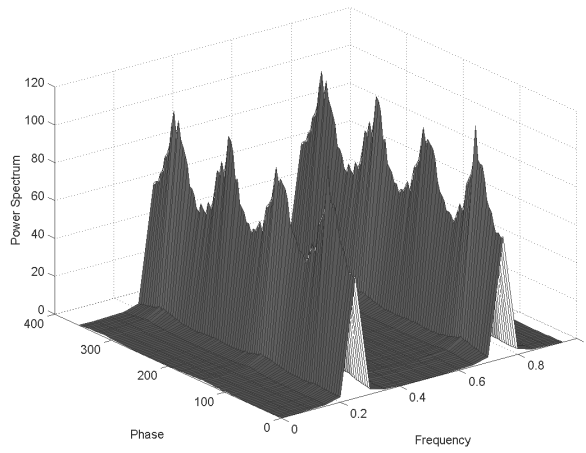


Figure 3.3

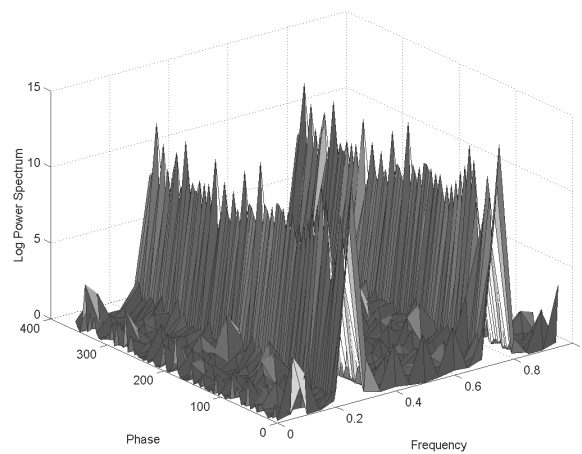


Figure 3.4

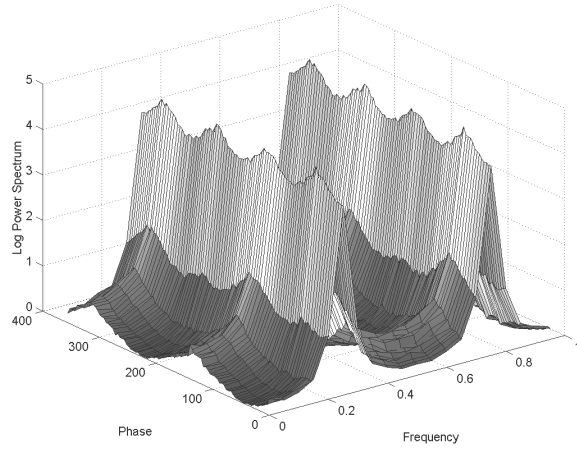


Figure 3.5

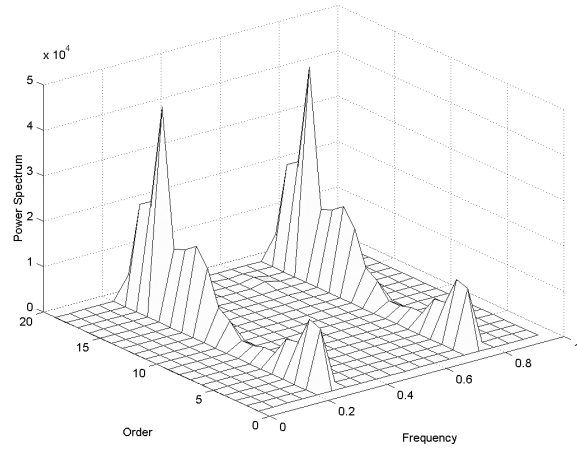


Figure 3.6

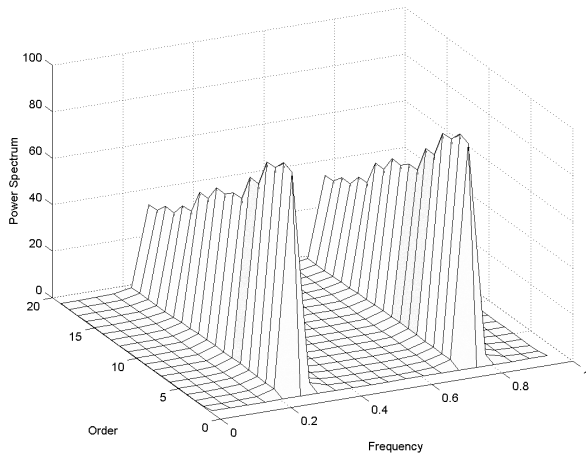


Figure 3.7

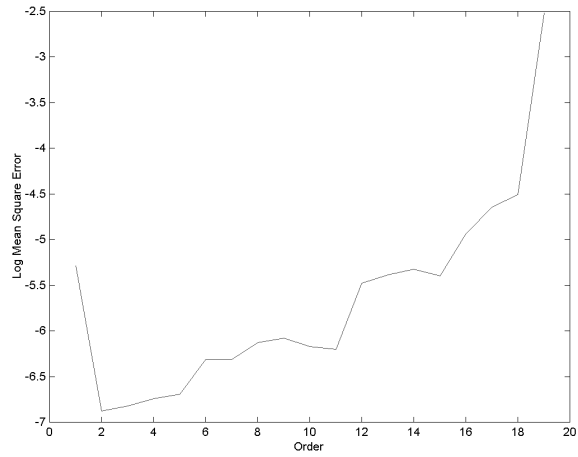


Figure 3.8

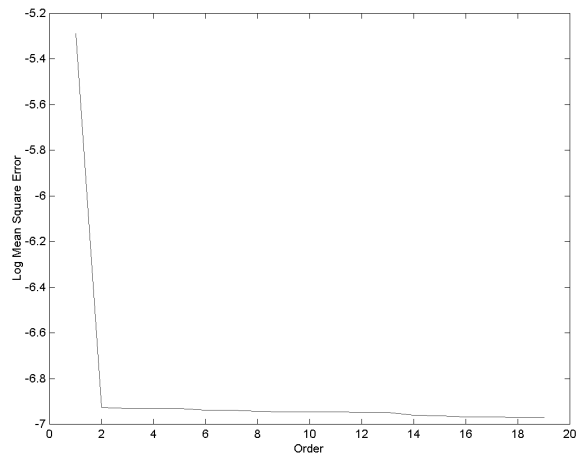


Figure 3.9

## VI Conclusion

The presented results, establish a theoretical and practical connection between the Levinson Algorithm and the Burg Algorithm, in the 1D and 2D cases. The fact that the Unmodified Burg Algorithm fails to minimize the residual error, for a certain order, is of a great importance to multiple applications. Especially for Spectral Power Estimation, precision and solution stability are required, and in Signal Compression error minimization is a priority.

## GENERALIZED REFLECTION COEFFICIENTS AND THE INVERSE FACTORIZATION OF HERMITIAN BLOCK TOEPLITZ MATRIX.

*Abstract*-A factorization of the inverse of a Hermitian strongly regular matrix based on a diagonal by diagonal recursive formula permits the inversion of Block Toeplitz matrices using only matrix-vector products, and with a complexity of  $O(n_1^3 n_2^2)$ , where  $n_1$  is the block size, and  $n_2$  is the block matrix block-size.

*Résumé*-Une diagonalisation de l'inverse basée sur des formules de récurrence par diagonales ( basées sur les coefficients de réflexion généralisés ) permet l'inversion des matrices Blocs Toeplitz en utilisant seulement des produits vectoriels. La complexité de calcul est de l'ordre  $O(n_1^3 n_2^2)$  où  $n_1$  est la taille de bloc et  $n_2$  est le nombre de bloc(s) de la matrice.

### I Introduction

The techniques developed here are based on a generalization of the reflection coefficients or partial autocorrelation presented in [18]. They appear when the well known Levinson recursion for inverting Toeplitz matrix [21][22] is extended to two families of bi-orthogonal polynomials.

These generalized coefficients turn out to be two triangular arrays of numbers, which completely describe the structure of the related matrix. In the Toeplitz case, the coefficients along each diagonal are identical, so they are determined by two sequences of pairs of numbers. In the Toeplitz Hermitian case, the coefficients collapse to the classical reflection coefficients.

In the case of Hermitian positive definite matrices, the reflection coefficients are a triangular array of pairs of numbers whose product is a positive number less than one. The families of related orthogonal polynomials determine two Cholesky factorizations of the inverse of the matrix.

These generated coefficients are computed recursively diagonal by diagonal. Setting some initial conditions on the principal diagonal, at each step of the recursion a whole diagonal is computed from the previous results.

In the Block Toeplitz case, the related two triangular arrays of the generalized coefficients keep the block structure. The Levinson Algorithm has been generalized to this case.

When applying the algorithm obtained in the general Strongly Regular matrix case to the Block Toeplitz case, at each step of the recursion, instead of computing a whole diagonal, only  $n_1$  coefficients are computed from the previous results. From which we obtain a factorization of the inverse with a complexity  $O(n_1^3 n_2^2)$ , where  $n_2$  is the number of blocks in the matrix.

## II Notations

We consider the Hermitian Strongly Regular matrix,

$$R := \{r_{i,j}\}_{i,j=0,1,\dots,n-1}, \quad (4.1)$$

$$r_{i,j} \in \mathbb{C},$$

$$n \in \mathbb{N}.$$

For each matrix  $R$  we consider the sub matrices family:

$$R^{k,l} := \{b_{i,j}\}_{i,j=0,\dots,l-k}, b_{i,j} := r_{i+k,j+k}, k < l, k, l := 0 \dots n-1,$$

for each  $R^{k,l}$  matrix we define the following block diagonal matrix :

$${}^0R^{k,l} := \begin{bmatrix} 0_{k \times k} & & & \\ & R^{k,l} & & \\ & & & \\ & & & 0_{(n-l) \times (n-l)} \end{bmatrix},$$

which contains  $R^{k,l}$ , diagonally positioned, with zero filled elsewhere.

The transport square matrix  $J$  defined as:

$$J := \begin{bmatrix} 0 & \cdots & 0 & 1 \\ \vdots & \ddots & 1 & 0 \\ 0 & \ddots & \ddots & \vdots \\ 1 & 0 & \cdots & 0 \end{bmatrix}.$$

## III Generalized Reflection Coefficients and Hermitian Strongly Regular matrices

For any Hermitian Strongly Regular matrix the inverse can be factorized into the form [18]

$$R^{-1} = (R^P)^* (D^P)^{-1} (R^P)^T = (R^Q)^* (D^Q)^{-1} (R^Q)^T, \quad (4.2)$$

where both of

$$D^P = (R^P)^T (R) (R^P)^*, \text{ and } D^Q = (R^Q)^T (R) (R^Q)^*, \quad (4.3)$$

are diagonal, and  $R^P$ ,  $R^Q$  are lower triangular and upper triangular respectively. Both are formed from Vectors  $\mathbf{p}_{k,l}, \mathbf{q}_{k,l}$ ,  $k, l = 0, 1, \dots, n-1$ ,  $k \leq l$  according to

$$R^P = [\mathbf{p}_{0,n-1}, \mathbf{p}_{1,n-1}, \dots, \mathbf{p}_{n-1,n-1}], \quad (4.4)$$

$$R^Q = [\mathbf{q}_{0,1}, \mathbf{q}_{0,2}, \dots, \mathbf{q}_{0,n-1}].$$

These vectors (or polynomials) are mutually orthogonal relatively to the matrix-defined product:

$$\langle v_1, v_2 \rangle := v_1^T R (v_2)^*,$$

this can be expressed in the conditions:

$$\forall 0 \leq k, 0 \leq k', k < l, k' < l, l \leq n-1,$$

$$\langle p_{k,l}, p_{k',l} \rangle = 0 \text{ if } k \neq k',$$

$$\langle p_{k,l}, p_{k',l} \rangle > 0 \text{ if } k = k'.$$

and

$$\forall 0 \leq k, k < l, k < l', l' \leq n-1, l \leq n-1,$$

$$\langle q_{k,l}, q_{k,l'} \rangle = 0 \text{ if } l \neq l',$$

$$\langle q_{k,l}, q_{k,l'} \rangle > 0 \text{ if } l = l'.$$

The orthogonal polynomials  $p_{k,l}, q_{k,l}$  are obtained for  $R$  in a recursive manner. The matrix  $R$ , being strongly regular, permits us to establish a recursive system in which the famous reflection coefficients are designated. The Generalized Reflection Coefficients define the relation between a group of vectors  $p_{k,k+d}, q_{k,k+d}$  and the next step group of vectors  $p_{k,k+d+1}, q_{k,k+d+1}$ ,  $d := 0, 1, \dots, n-2$ , according to

$$p_{k,l} = p_{k,l-1} - a_{k,l} q_{k+1,l}, \quad (4.5)$$

$$q_{k,l} = q_{k+1,l} - a'_{k,l} p_{k,l-1}, \quad (4.6)$$

and that is starting from the canonical basis vectors  $p_{k,k} := e_k, q_{k,k} := e_k$ ,  $k = 0, 1, \dots, n-1$ .

The Generalized Reflection Coefficients are complex numbers, obtained at each step according to:

$$a_{k,l} = \frac{p_{k,l-1}^T R e_l}{q_{k+1,l}^T R e_l}, \quad (4.7)$$

$$a'_{k,l} = \frac{q_{k+1,l}^T R e_k}{p_{k,l-1}^T R e_k}. \quad (4.8)$$

The definition of  $v_{k,l} := q_{k,l}^T R e_l$ ,  $v'_{k,l} := p_{k,l}^T R e_k$  installs the following recursive system:

$$v_{k,l} = v_{k+1,l} (1 - a_{k,l} a'_{k,l}) \in \mathbf{R}^+, \quad (4.9)$$

$$v'_{k,l} = v'_{k,l-1} (1 - a_{k,l} a'_{k,l}) \in \mathbf{R}^+. \quad (4.10)$$

This permits us to avoid applying the product in the denominator in (4.7) and (4.8) at each step, while for the numerators, the following holds

$$p_{k,l-1}^T R e_l = (q_{k+1,l}^T R e_k)^*. \quad (4.11)$$

#### IV Generalized Reflection Coefficients in the Hermitian Block Toeplitz Case

In this section we will consider the more limiting case of Block Toeplitz matrix, in which, each block is not necessarily Toeplitz. Each matrix block is of size  $n_1 \times n_1$ , while the total block matrix is of size  $n_1 n_2 \times n_1 n_2$ . To assist our approach, we notice that the matrix elements  $r_{i,j}$ , in this context, admit the following property.



**Proposition 4.1.**

$$r_{i,j} = r_{i \bmod n_1, j - i \operatorname{sec} n_1} \quad \text{if } i \leq j,$$

$$r_{i,j} = (r_{j,i})^* \quad \text{if } i > j.$$

where  $a \operatorname{sec} b := b \operatorname{int}(a/b)$ ,  $\operatorname{int}(x)$  is the integer part of  $x$ , and  $a \bmod b$  is equal to the remainder of division of  $a$  by  $b$ .

**PROOF.** From the T-B-T structure we have for  $k := 0, 1, \dots, n_1 - 1, l := 0, 1, \dots, n_1 n_2 - 1$ :

$$r_{k+tn_1, l+tn_1} = r_{k,l}, \quad t = 0, 1, \dots, n_2 - 1 - \operatorname{int}(l/n_1),$$

Setting  $i := k + tn_1, j := l + tn_1$ , we notice that  $(i, j) \in [0, n_1 n_2 - 1] \times [0, n_1 n_2 - 1]$ ,

and:

$$r_{i,j} = r_{i-tn_1, j-tn_1}.$$

By the definition of  $i$ ,  $i - tn_1 = i \bmod n_1$  and  $tn_1 = i \operatorname{sec} n_1$ .

The previous proposition is to simplify the direct mathematical representation of the Hermitian Block Toeplitz Matrix case. The following propositions, **Proposition 4.2** and **Proposition 4.3** will help us to consider the main recursive system in the Block Toeplitz case, segmented into recurrent sub matrices.

**Proposition 4.2.**

$$\left( \mathbf{p}_{k,l}^{0R^s d}, \mathbf{q}_{k,l}^{0R^s d}, \mathbf{a}_{k,l}^{0R^s d}, \mathbf{a}'_{k,l}{}^{0R^s d}, \mathbf{v}_{k,l}^{0R^s d}, \mathbf{v}'_{k,l}{}^{0R^s d} \right) = \left( \mathbf{p}_{k,l}^R, \mathbf{q}_{k,l}^R, \mathbf{a}_{k,l}^R, \mathbf{a}'_{k,l}{}^R, \mathbf{v}_{k,l}^R, \mathbf{v}'_{k,l}{}^R \right),$$

with condition that  $s \leq k < l \leq d$ , where the entities  $\mathbf{p}_{k,l}, \mathbf{q}_{k,l}, \mathbf{a}_{k,l}, \mathbf{a}'_{k,l}, \mathbf{v}_{k,l}, \mathbf{v}'_{k,l}$  that corresponds to a given covariance matrix  $M$ , are noted respectively as

$$\mathbf{p}_{k,l}^M, \mathbf{q}_{k,l}^M, \mathbf{a}_{k,l}^M, \mathbf{a}'_{k,l}{}^M, \mathbf{v}_{k,l}^M, \mathbf{v}'_{k,l}{}^M.$$

**Proposition 4.3.**  $R^{k,l} = R^{k \bmod n_1, l - k \operatorname{sec} n_1}$

**PROOF.** for each of both matrices elements we apply **Proposition 4.1** :

$$r_{i,j}^{R^{k,l}} = r_{k+i, k+j} = r_{(k+i) \bmod n_1, (k+j) - (k+i) \operatorname{sec} n_1}, \quad i, j = 0, 1, \dots, l - k,$$

$$r_{i,j}^{R^{k \bmod n_1, l - k \operatorname{sec} n_1}} = r_{k \bmod n_1 + i, k \bmod n_1 + j} = r_{(k \bmod n_1 + i) \bmod n_1, k \bmod n_1 + j - (k \bmod n_1 + i) \operatorname{sec} n_1},$$

from which our proof is completed.

Now we are ready to state the main result of this chapter.

**Theorem 4.1.** In the case of Hermitian Block Toeplitz Matrix we have:

$$\mathbf{a}_{k,l} = \mathbf{a}_{k \bmod n_1, l - k \operatorname{sec} n_1},$$

$$\mathbf{a}'_{k,l} = \mathbf{a}'_{k \bmod n_1, l - k \operatorname{sec} n_1},$$

$$\mathbf{p}_{k,l} = U^{k \operatorname{sec} n_1} \mathbf{p}_{k \bmod n_1, l - k \operatorname{sec} n_1},$$

$$\mathbf{q}_{k,l} = U^{k \operatorname{sec} n_1} \mathbf{q}_{k \bmod n_1, l - k \operatorname{sec} n_1},$$

$$\mathbf{v}_{k,l} = \mathbf{v}_{k \bmod n_1, l - k \operatorname{sec} n_1},$$

$$\mathbf{v}'_{k,l} = \mathbf{v}'_{k \bmod n_1, l-k \sec n_1},$$

where  $U$  is the  $(n_1 n_2 \times n_1 n_2)$  shift matrix defined as ,

$$U := \begin{bmatrix} 0 & 0 & \cdots & 0 & 0 \\ 1 & 0 & \ddots & & 0 \\ 0 & \ddots & \ddots & 0 & \vdots \\ \vdots & \ddots & 1 & 0 & 0 \\ 0 & \cdots & 0 & 1 & 0 \end{bmatrix},$$

with  $U^0 := \mathbf{1}$ .

**PROOF.** We start by noticing that

$\forall 0 \leq k < l \leq n_1 n_2 - 1 \exists s, d : s \leq k < l \leq d$  , so that we can write

$$\begin{aligned} & \left( \mathbf{p}_{k,l}^{0R^{s,d}}, \mathbf{q}_{k,l}^{0R^{s,d}}, \mathbf{a}_{k,l}^{0R^{s,d}}, \mathbf{a}'_{k,l}^{0R^{s,d}}, \mathbf{v}_{k,l}^{0R^{s,d}}, \mathbf{v}'_{k,l}^{0R^{s,d}} \right) = \\ & \left( U_{d-s}^s \mathbf{p}_{k-s,l-s}^{R^{s,d}}, U_{d-s}^s \mathbf{q}_{k-s,l-s}^{R^{s,d}}, \mathbf{a}_{k-s,l-s}^{R^{s,d}}, \mathbf{a}'_{k-s,l-s}^{R^{s,d}}, \mathbf{v}_{k-s,l-s}^{R^{s,d}}, \mathbf{v}'_{k-s,l-s}^{R^{s,d}} \right), \end{aligned}$$

where  $U_x$  is a Matrix of size  $(n_1 n_2) \times (x+1)$ , defined as:

$$U_x := \begin{bmatrix} 0 & 0 & \cdots & 0 \\ 1 & 0 & \ddots & \vdots \\ 0 & 1 & \ddots & 0 \\ 0 & 0 & \ddots & 0 \\ \vdots & \vdots & \ddots & 1 \\ 0 & 0 & \cdots & 0 \end{bmatrix}, \quad U_x^0 := \begin{bmatrix} \mathbf{1}_{(x+1) \times (x+1)} \\ \mathbf{0} \end{bmatrix},$$

coupling this with **Proposition 4.2**, we obtain:

$$\begin{aligned} & \left( U_{d-s}^s \mathbf{p}_{k-s,l-s}^{R^{s,d}}, U_{d-s}^s \mathbf{q}_{k-s,l-s}^{R^{s,d}}, \mathbf{a}_{k-s,l-s}^{R^{s,d}}, \mathbf{a}'_{k-s,l-s}^{R^{s,d}}, \mathbf{v}_{k-s,l-s}^{R^{s,d}}, \mathbf{v}'_{k-s,l-s}^{R^{s,d}} \right) = \\ & \left( \mathbf{p}_{k,l}^R, \mathbf{q}_{k,l}^R, \mathbf{a}_{k,l}^R, \mathbf{a}'_{k,l}^R, \mathbf{v}_{k,l}^R, \mathbf{v}'_{k,l}^R \right). \end{aligned}$$

By setting  $s = k \sec n_1$ , admitting that  $k - k \sec n_1 = k \bmod n_1$ , and using

**Proposition 4.3**, we obtain:

$$\begin{aligned} & \left( U_{d-s}^s \mathbf{p}_{k \bmod n_1, l-k \sec n_1}^{R^{0,d-s}}, U_{d-s}^s \mathbf{q}_{k \bmod n_1, l-k \sec n_1}^{R^{0,d-s}}, \right. \\ & \left. \mathbf{a}_{k \bmod n_1, l-k \sec n_1}^{R^{0,d-s}}, \mathbf{a}'_{k \bmod n_1, l-k \sec n_1}^{R^{0,d-s}}, \mathbf{v}_{k \bmod n_1, l-k \sec n_1}^{R^{0,d-s}}, \mathbf{v}'_{k \bmod n_1, l-k \sec n_1}^{R^{0,d-s}} \right) = \\ & \left( \mathbf{p}_{k,l}^R, \mathbf{q}_{k,l}^R, \mathbf{a}_{k,l}^R, \mathbf{a}'_{k,l}^R, \mathbf{v}_{k,l}^R, \mathbf{v}'_{k,l}^R \right). \end{aligned}$$

Finally our proof is completed by the following:

$$\begin{aligned} & \left( U_{d-s}^s \mathbf{p}_{k \bmod n_1, l-k \sec n_1}^{R^{0,d-s}}, U_{d-s}^s \mathbf{q}_{k \bmod n_1, l-k \sec n_1}^{R^{0,d-s}}, \right. \\ & \left. \mathbf{a}_{k \bmod n_1, l-k \sec n_1}^{R^{0,d-s}}, \mathbf{a}'_{k \bmod n_1, l-k \sec n_1}^{R^{0,d-s}}, \mathbf{v}_{k \bmod n_1, l-k \sec n_1}^{R^{0,d-s}}, \mathbf{v}'_{k \bmod n_1, l-k \sec n_1}^{R^{0,d-s}} \right) = \\ & \left( U^s \mathbf{p}_{k \bmod n_1, l-k \sec n_1}^{R^{0,d-s}}, U^s \mathbf{q}_{k \bmod n_1, l-k \sec n_1}^{R^{0,d-s}}, \right. \\ & \left. \mathbf{a}_{k \bmod n_1, l-k \sec n_1}^{R^{0,d-s}}, \mathbf{a}'_{k \bmod n_1, l-k \sec n_1}^{R^{0,d-s}}, \mathbf{v}_{k \bmod n_1, l-k \sec n_1}^{R^{0,d-s}}, \mathbf{v}'_{k \bmod n_1, l-k \sec n_1}^{R^{0,d-s}} \right) = \\ & \left( U^s \mathbf{p}_{k \bmod n_1, l-k \sec n_1}^R, U^s \mathbf{q}_{k \bmod n_1, l-k \sec n_1}^R, \right. \\ & \left. \mathbf{a}_{k \bmod n_1, l-k \sec n_1}^R, \mathbf{a}'_{k \bmod n_1, l-k \sec n_1}^R, \mathbf{v}_{k \bmod n_1, l-k \sec n_1}^R, \mathbf{v}'_{k \bmod n_1, l-k \sec n_1}^R \right). \end{aligned}$$

We are also interested in the algorithmic aspect of **Theorem 4.1**; more precisely the following theorem explains the resulting algorithmic details and calculus cost.

## V Generalized reflection coefficients in the block Toeplitz case algorithm (GRCBT)

### ◆ Algorithm's details

In the Hermitian Block Toeplitz case, the application of the recursive relations (4.5)-(4.10) resumes in the following:

First we rewrite Equations (4.5)-(4.10) as the subroutine,

#### Subroutine 1:

$$a_{k,l} = \frac{\mathbf{p}_{k^0,l^-}^T R \mathbf{e}_l}{v} \quad a'_{k,l} = \frac{\hat{\mathbf{q}}^T R \mathbf{e}_k}{v'_{k^0,l^-}} \quad (\text{t2.1})$$

$$\mathbf{p}_{k,l} = \mathbf{p}_{k^0,l^-} - a_{k,l} \hat{\mathbf{q}} \quad \mathbf{q}_{k,l} = \hat{\mathbf{q}} - a'_{k,l} \mathbf{p}_{k^0,l^-} \quad (\text{t2.2})$$

$$v_{k,l} = v (1 - a_{k,l} a'_{k,l}) \quad v'_{k,l} = v'_{k^0,l^-} (1 - a_{k,l} a'_{k,l}) \quad (\text{t2.3})$$

Next we proceed as the following,

#### Initialization:

For  $k = 0$  to  $n_1 - 1$ : {  
 $\mathbf{p}_{k,k} = \mathbf{q}_{k,k} = \mathbf{e}_k$ ,  $v_{k,k} = v'_{k,k} = r_{0,0}$   
 }

#### Main routine:

For  $d_2 = 0$  to  $n_2 - 1$  do : (loop 1)

{

If  $d_2$  not equal to zero:

{

For  $d_1 = n_1 - 1$  to 0 do : (Lower triangle loop)

{

For  $u = 0$  to  $n_1 - d_1 - 1$  do :

{

$k = u + d_1$   $l = d_2 n_1 + u$

$(k^0, l^-) = (k, l - 1)$

if  $u$  equal to  $n_1 - d_1 - 1$ : {

$(k^+, l^0) = ((k + 1) \bmod n_1, l - (k + 1) \text{sec } n_1)$

$\hat{\mathbf{q}} = U^{n_1} \mathbf{q}_{k^+, l^0}$ ,  $v = v_{k^+, l^0}$  (t2.4)

}

else {

$(k^+, l^0) = (k + 1, l)$

$\hat{\mathbf{q}} = \mathbf{q}_{k^+, l^0}$ ,  $v = v_{k^+, l^0}$

}

*Apply Subroutine 1*

$$\begin{array}{l}
 \} \\
 \} \\
 \} \\
 \text{For } d_1 = 1 \text{ to } n_1 - 1 \text{ do : (Upper triangle loop)} \\
 \{ \\
 \quad \text{For } u = 0 \text{ to } n_1 - d_1 - 1 \text{ do :} \\
 \quad \{ \\
 \quad \quad k = u \quad l = d_2 n_1 + u + d_1 \\
 \quad \quad (k^0, l^-) = (k, l - 1) \\
 \quad \quad (k^+, l^0) = (k + 1, l) \\
 \quad \quad \hat{q} = q_{k^+, l^0}, v = v_{k^+, l^0} \\
 \quad \quad \text{Apply Subroutine 1} \\
 \quad \quad \} \\
 \quad \} \\
 \} \\
 \}
 \end{array}$$

◆ *Algorithm's development*

For any element  $(i, j) \in T_d$ ,

$$T_d := \{(k, l) : k < l, (k, l) \in [0, n_1 d - 1] \times [0, n_1 d - 1]\}, d = 1, 2, \dots, n_2;$$

$$(i \bmod d, j - i \operatorname{secd}) \in P_d,$$

$$P_d := \{(k, l) : k < l, (k, l) \in [0, n_1 - 1] \times [0, n_1 d - 1]\}$$

From **Theorem 4.1**, by obtaining  $p_{k,l}, q_{k,l}, a_{k,l}, a'_{k,l}, v_{k,l}, v'_{k,l}$  for all subscripts

$(k, l) \in P_d$  we obtain directly these values for  $(k, l) \in T_d$ .

The algorithm proceeds in calculating values for all subscripts contained in the following groups, with respective order:

$$\Lambda_1, \Lambda_2, \dots, \Lambda_{n_2}, \text{ where } \Lambda_d := P_d \setminus P_{d-1}, \text{ and } P_0 := \emptyset.$$

In *Lower triangle loop* we obtain values for

$$\forall (k, l) \in \Lambda_d^-, \text{ where } \Lambda_d^- := \{(k, l) \in \Lambda_d : k \geq l \bmod n_1\}.$$

To demonstrate this, first we notice that for any group defined as

$$\Lambda_d^{-, d_1} := \{(k, l) : (k, l) \in \Lambda_d^-, k - l \bmod n_1 = d_1\},$$

$$\Lambda_d^- = \bigcup_{d_1=0}^{n_1-1} \Lambda_d^{-, d_1},$$

we have, for  $d_1 \in [0, n_1 - 1]$ :

$$\Lambda_d^{-, d_1} = \{(k, l) : l \bmod n_1 \in [0, n_1 - 1 - d_1], k = l \bmod n_1 + d_1\}.$$

By defining  $u := l \bmod n_2$  we conclude that we did consider all  $(k, l) \in \Lambda_d^-$ .

Using the same logic we conclude that in the *Upper triangle loop* we obtain values for

$\forall (k, l) \in \Lambda_d^+$ , where  $\Lambda_d^+ := \{(k, l) \in \Lambda_d : k < l \bmod n_1\}$ . It is clear that

$$\Lambda_d = \Lambda_d^- \cup \Lambda_d^+$$

In the *upper triangle loop* it is easy to verify that:

$$\forall (k, l) \in \Lambda_d^+, \{(k, l-1), (k+1, l)\} \subset \Lambda_d,$$

while in the *Lower triangle loop* this is not always true, more precisely for  $k = n_1 - 1$ , or/and  $l \bmod n_1 = 0$ . So we can write:

$$\forall (k, l) \in \Lambda_d^-, k \neq n_1 - 1 \Rightarrow \{(k, l-1), (k+1, l)\} \subset P_d.$$

Finally for the case of  $k = n_1 - 1$ , we apply **Theorem 4.1** to obtain the needed values, since:  $\forall (k, l) \in \Lambda_d^-, \{(k, l-1), ((k+1) \bmod n_1, l \bmod n_1)\} \subset P_d$ .

◆ *Algorithm's complexity*

For computing the complexity, we proceed as the following:

Each Entry in the routine will require operations of  $O(l - k)$ , by noting  $c_1$  as the step constant,  $opc$  as the total number of operation, the calculus cost take the form of:

$$\begin{aligned} opc &= \sum_{d_2=0}^{n_2-1} \sum_{d_1=1}^{n_1-1} \sum_{u=0}^{n_1-d_1-1} c_1(n_1 d_2 + d_1) + \sum_{d_2=1}^{n_2-1} \sum_{d_1=0}^{n_1-1} \sum_{u=0}^{n_1-d_1-1} c_1(n_1 d_2 - d_1), \\ &= \sum_{d_1=1}^{n_1-1} (n_1 - d_1 - 1) c_1(d_1) + \sum_{d_2=1}^{n_2-1} \sum_{d_1=1}^{n_1-1} (n_1 - d_1 - 1) c_1(n_1 d_2 + d_1) + \sum_{d_2=1}^{n_2-1} \sum_{d_1=0}^{n_1-1} (n_1 - d_1 - 1) c_1(n_1 d_2 - d_1), \end{aligned}$$

This can be further simplified into

$$\begin{aligned} &= (n_1 - 1) c_1 \frac{1}{2} (n_1 - 1) n_1 - c_1 \frac{1}{6} (n_1 - 1) (n_1) (2n_1 - 1) + \\ &2c_1 n_1 \frac{1}{2} (n_2 - 1) n_2 (n_1 - 1)^2 - 2c_1 n_1 \frac{1}{2} (n_2 - 1) n_2 \frac{1}{2} (n_1 - 1) n_1 + \quad (12) \\ &(n_1 - 1) c_1 n_1 \frac{1}{2} (n_2 - 1) n_2. \end{aligned}$$

From which we conclude the complexity order of  $n_1^3 n_2^2$ .

## VI A Bezoutian Inversion Formula

One can directly develop a bezoutian factorization of the inverse, depending on (4.2). Instead of that, and for the benefit of the reader, we will express our new formula depending on the already existing work of [4].

In [4], the inverse of a Hermitian Block Toeplitz matrix can be expressed in the form of:

$$R^{-1} = (L_A)^H D (P_f^{-1}) L_A - (L_B)^H D (P_b^{-1}) L_B, \quad (4.12)$$

where both of  $L_A$ , and  $L_B$  are Block Toeplitz having the form :

$$L_A = \begin{bmatrix} I & A_1 & \cdots & A_{n_2-1} \\ 0 & I & \ddots & \vdots \\ \vdots & \ddots & \ddots & A_1 \\ 0 & \cdots & 0 & I \end{bmatrix}, L_B = \begin{bmatrix} 0 & B_{n_2-1} & \cdots & B_1 \\ 0 & 0 & \ddots & \vdots \\ \vdots & \ddots & \ddots & B_{n_2-1} \\ 0 & \cdots & 0 & 0 \end{bmatrix}. \quad (4.13)$$

While the entities  $\{A_i\}, \{B_i\}, P_f, P_b$ , are defined as the unique solution to the equations [8],[9]:

$$\begin{bmatrix} I & A_1 & \cdots & A_{n_2-1} \end{bmatrix} R = \begin{bmatrix} P_f & 0 & \cdots & 0 \end{bmatrix}, \quad (4.14)$$

$$\begin{bmatrix} B_{n_2-1} & \cdots & B_1 & I \end{bmatrix} R = \begin{bmatrix} 0 & \cdots & 0 & P_b \end{bmatrix}, \quad (4.15)$$

$D(M)$  is a block diagonal matrix containing  $M$  on its main block diagonal with zeros elsewhere.

The next theorem will help establishing the correspondence between the WWR algorithm, and the Generalized Reflection Coefficients algorithm.

**Theorem 4.3.** *In the case of strongly regular Hermitian Block Toeplitz matrix, the inverse is equal to*

$$R^{-1} = (L_p)^H D(V'^{-1})L_p - (L_q)^H D(V^{-1})L_q, \quad (4.16)$$

where

$$L_p = \begin{bmatrix} P_0^T & P_1^T & \cdots & P_{n_2-1}^T \\ 0 & P_0^T & \ddots & \vdots \\ \vdots & \ddots & \ddots & P_1^T \\ 0 & \cdots & 0 & P_0^T \end{bmatrix}, L_q = \begin{bmatrix} 0 & Q_{n_2-1}^T & \cdots & Q_1^T \\ 0 & 0 & \ddots & \vdots \\ \vdots & \ddots & \ddots & Q_{n_2-1}^T \\ 0 & \cdots & 0 & 0 \end{bmatrix}, \quad (4.17)$$

While the entities  $\{P_i\}, \{Q_i\}, V', V$  are defined as:

$$\begin{bmatrix} P_0 \\ P_1 \\ \vdots \\ P_{n_2-1} \end{bmatrix} := \begin{bmatrix} p_{0,n_1n_2-1} & p_{1,n_1n_2-1} & \cdots & p_{n_1-1,n_1n_2-1} \end{bmatrix}, \begin{bmatrix} Q_{n_2-1} \\ \vdots \\ Q_1 \\ Q_0 \end{bmatrix} := \begin{bmatrix} q_{0,n_1n_2-n_1} & \cdots & q_{0,n_1n_2-2} & q_{0,n_1n_2-1} \end{bmatrix},$$

$$\text{and } V' := \begin{bmatrix} v'_{0,n_1n_2-1} & 0 & \cdots & 0 \\ 0 & v'_{1,n_1n_2-1} & \ddots & \vdots \\ \vdots & \ddots & \ddots & 0 \\ 0 & \cdots & 0 & v'_{n_1-1,n_1n_2-1} \end{bmatrix}, V := \begin{bmatrix} v_{0,n_1n_2-n_1} & 0 & \cdots & 0 \\ 0 & \ddots & \ddots & \vdots \\ \vdots & \ddots & v_{0,n_1n_2-2} & 0 \\ 0 & \cdots & 0 & v_{0,n_1n_2-1} \end{bmatrix}.$$

**PROOF.** It is clear that both of  $P_0$  and  $Q_0$ , are lower and upper triangular, respectively. From (4.2), and (4.3) we can write that:

$$R \cdot \begin{bmatrix} P_0 \\ P_1 \\ \vdots \\ P_{n_2-1} \end{bmatrix}^* V'^{-1} (P_0)^T = \begin{bmatrix} I \\ 0 \\ \vdots \\ 0 \end{bmatrix}, R \cdot \begin{bmatrix} Q_{n_2-1} \\ \vdots \\ Q_1 \\ Q_0 \end{bmatrix}^* V^{-1} (Q_0)^T = \begin{bmatrix} 0 \\ \vdots \\ 0 \\ I \end{bmatrix}.$$

From which, and since R is Hermitian, we can write:

$$(P_0)^* V'^{-1} [P_0^T \ P_1^T \ \dots \ P_{n_2-1}^T] R = [I \ 0 \ \dots \ 0], (Q_0)^* V^{-1} [Q_{n_2-1}^T \ \dots \ Q_1^T \ Q_0^T] R = [0 \ \dots \ 0 \ I].$$

This leads us to the equalities of

$$(P_0)^* V'^{-1} P_0^T = (P_f)^{-1}, \quad (4.18)$$

$$(Q_0)^* V^{-1} Q_0^T = (P_b)^{-1}, \quad (4.19)$$

and eventually to

$$A_i = (P_0^T)^{-1} P_i^T, \quad (4.20)$$

$$B_i = (Q_0^T)^{-1} Q_i^T, \quad (4.21)$$

since that  $P_f = (P_0^T)^{-1} V' (P_0^*)^{-1}$ , and  $P_b = (Q_0^T)^{-1} V (Q_0^*)^{-1}$ .

By replacing (4.18)-(4.21) into (4.12), (4.13) the proof is completed.

## VII Conclusion

The previously presented results, explain clearly the structure of the Generalized Reflection Coefficients, and their relevant orthogonal polynomials in the Hermitian Block Toeplitz Case. While the reflection coefficients admit the same Block Toeplitz status, the polynomials  $p_{k,l}$ ,  $q_{k,l}$ , show a block Toeplitz recurrence with an added shift between Blocks polynomials counterparts.

## VIII Acknowledgment

I would like to thank Dr. G. Castro<sup>1</sup>, for providing, so gracefully, advice, and valuable information, for this chapter.

---

<sup>1</sup> Universidad Central de Venezuela, Laboratorio de Probabilidades, CEPE, Escuela de Matemáticas UCV, Caracas Venezuela. tel: 58-2126051512, fax: 52-2126051190

## GENERALIZED REFLECTION COEFFICIENTS IN TOEPLITZ-BLOCK-TOEPLITZ MATRIX CASE AND FAST INVERSE 2D LEVINSON ALGORITHM

*Abstract*-A factorization of the inverse of a Hermitian strongly regular matrix, based on a diagonal by diagonal recurrent formulae, permits the inversion of Toeplitz Block Toeplitz matrices using minimized matrix-vector products, with a complexity of  $O(n_1^3 n_2^2)$ , where  $n_1$  is the block size, and  $n_2$  is the block matrix size. A 2D Levinson Algorithm is introduced that outperforms the Wittle-Wiggins-Robinson Algorithm in calculation cost.

*Résumé*- La diagonalisation de l'inverse d'une matrice hermitienne « strongly regular », basée sur des formules de récurrence par diagonales permet l'inverse des matrices Toeplitz Bloc Toeplitz, en utilisant seulement des produits vectoriels optimisés, avec une complexité de l'ordre  $O(n_1^3 n_2^2)$  où  $n_1$  est la taille de bloc, et  $n_2$  est le nombre de bloc(s) de la matrice. L'Algorithme de Levinson présenté nécessite un nombre d'opérations inférieur à celui de l'algorithme de Whittle, Wiggins, and Robinson.

### I Introduction

**F**ast inversion algorithms for Toeplitz forms play an important role in modern applications; they represent also the mathematical solutions to many different problems arising in signal processing theory. In this work, we treat the case of linear systems with a Hermitian Toeplitz Block Toeplitz Matrix, which is directly connected to the 2D Autoregressive model. In the case of the Hermitian Toeplitz matrix the famous Levinson Algorithm [22] introduced the concept of reflection coefficients. This was further generalized in [18] into the generalized reflection coefficients, which are applied to any Strongly Regular Hermitian matrix. In [23] the special case of a Hermitian Block Toeplitz matrix was treated and an algorithm was established. In this chapter we treat the case of a strongly regular Hermitian TBT matrix. The algorithm that is introduced in [23] and the one that will be introduced in this chapter, provide a better counterparts in terms of calculation cost than the ones presented by Wittle, Wiggins and Robinson [8][9], and their 2D version, respectively. For a better overview of the latter algorithms with connection to 2D signal processing the reader is invited to examine [24]. Even if the inverse is factorized, the use of Gohberg-Semencul Formula [4][5] would be most appropriate to fully calculate the inverse, and take advantage of the current work.



## II Notations

We consider the Hermitian Strongly Regular matrix,

$$R := \{r_{i,j}\}_{i,j:=0,1,\dots,n-1} \quad (5.1)$$

$$r_{i,j} \in \mathbb{C}$$

$$n \in \mathbb{N}$$

For each matrix  $R$  we consider the sub matrices family:

$$R^{k,l} := \{b_{i,j}\}_{i,j:=0,\dots,l-k}, b_{i,j} := r_{i+k,j+k} \quad k < l, \\ k, l := 0 \dots n-1$$

For each  $R^{k,l}$  matrix we define the following block diagonal matrix:

$${}^0R^{k,l} := \begin{bmatrix} \mathbf{0}_{k \times k} & & \\ & R^{k,l} & \\ & & \mathbf{0}_{(n-l) \times (n-l)} \end{bmatrix}$$

which contains  $R^{k,l}$  diagonally positioned, with zero filled elsewhere.

The transport square matrix  $J$  will be defined as:

$$J := \begin{bmatrix} 0 & \cdots & 0 & 1 \\ \vdots & \ddots & 1 & 0 \\ 0 & \ddots & \ddots & \vdots \\ 1 & 0 & \cdots & 0 \end{bmatrix}$$

## III Generalized Reflection Coefficients and Hermitian Strongly Regular Matrices

For any Hermitian Strongly Regular matrix the inverse can be factorized into the form [18]

$$R^{-1} = (R^P)^* (D^P)^{-1} (R^P)^T \quad (5.2)$$

where

$$D^P = (R^P)^T (R) (R^P)^* \quad (5.3)$$

is diagonal, and  $R^P$  is a lower triangular matrix formed from vectors  $\mathbf{p}_{k,l}$ ,  $k, l = 0, 1, \dots, n-1$ ,  $k \leq l$  according to

$$R^P = [\mathbf{p}_{0,n-1}, \mathbf{p}_{1,n-1}, \dots, \mathbf{p}_{n-1,n-1}] \quad (5.4)$$

These vectors (or polynomials) are mutually orthogonal relatively to the matrix defined cross product:

$$\langle \mathbf{v}_1, \mathbf{v}_2 \rangle := \mathbf{v}_1^T R \mathbf{v}_2$$

$$\forall 0 \leq k, 0 \leq k', k < l, k' < l, l \leq n-1$$

$$\langle \mathbf{p}_{k,l}, \mathbf{p}_{k',l} \rangle = 0 \text{ if } k \neq k'$$

$$\langle \mathbf{p}_{k,l}, \mathbf{p}_{k',l} \rangle > 0 \text{ if } k = k'$$

This also do apply for a second family of polynomials  $q_{k,l}$ , which also realize the following orthogonality:

$$\forall 0 \leq k, k < l, k < l', l \leq n-1, l' \leq n-1$$

$$\langle \mathbf{q}_{k,l'}, \mathbf{q}_{k,l'} \rangle = 0 \text{ if } l \neq l'$$

$$\langle \mathbf{q}_{k,l'}, \mathbf{q}_{k,l'} \rangle > 0 \text{ if } l = l'$$

The two families  $\mathbf{p}_{k,l}, \mathbf{q}_{k,l}$  are produced from  $R$  in a recursive manner. The matrix  $R$ , being strongly regular, permits us to establish a recursive system in which the famous reflection coefficients are used. The Generalized Reflection Coefficients define the relation between a group of vectors  $\mathbf{p}_{k,k+d}, \mathbf{q}_{k,k+d}$  and the next step group of vectors  $\mathbf{p}_{k,k+d+1}, \mathbf{q}_{k,k+d+1}$ , according to

$$\mathbf{p}_{k,l} = \mathbf{p}_{k,l-1} - a_{k,l} \mathbf{q}_{k+1,l} \quad (5.5)$$

$$\mathbf{q}_{k,l} = \mathbf{q}_{k+1,l} - a'_{k,l} \mathbf{p}_{k,l-1} \quad (5.6)$$

and that is, starting from the canonical basis vectors  $\mathbf{p}_{k,k} := \mathbf{e}_k, \mathbf{q}_{k,k} := \mathbf{e}_k$   $k = 0, 1, \dots, n-1$ .

The Generalized Reflection Coefficients are complex numbers, obtained at each step according to:

$$a_{k,l} = \frac{\mathbf{p}_{k,l-1}^T R \mathbf{e}_l}{\mathbf{q}_{k+1,l}^T R \mathbf{e}_l} \quad (5.7)$$

$$a'_{k,l} = \frac{\mathbf{q}_{k+1,l}^T R \mathbf{e}_k}{\mathbf{p}_{k,l-1}^T R \mathbf{e}_k} \quad (5.8)$$

The definition of  $v_{k,l} := \mathbf{q}_{k,l}^T R \mathbf{e}_l, v'_{k,l} := \mathbf{p}_{k,l}^T R \mathbf{e}_k$  installs the following recursive system:

$$v_{k,l} = v_{k+1,l} (1 - a_{k,l} a'_{k,l}) \in \mathbf{R}^+ \quad (5.9)$$

$$v'_{k,l} = v'_{k,l-1} (1 - a_{k,l} a'_{k,l}) \in \mathbf{R}^+ \quad (5.10)$$

This permits us to avoid applying at each step the product in the denominator of (5.7) and (5.8). While for numerators, the following holds:

$$\mathbf{p}_{k,l-1}^T R \mathbf{e}_l = \left( \mathbf{q}_{k+1,l}^T R \mathbf{e}_k \right)^* \quad (5.11)$$

#### IV Generalized Reflection Coefficients in the Hermitian Toeplitz Block Toeplitz case

In the Toeplitz Block Toeplitz Case each Matrix Block is a Toeplitz matrix of size  $n_1$ , while the number of Block Matrices is of size  $n_2$ . We can formalize this structure through the following proposition.

##### **Proposition 5.1.**

For any  $i \leq j$

$$r_{i,j} = r_{i \bmod n_1 - j \bmod n_1, j \bmod n_1 - i \bmod n_1} \text{ if } j \bmod n_1 < i \bmod n_1$$

$$r_{i,j} = r_{0,j-i} \text{ if } j \bmod n_1 \geq i \bmod n_1$$

where  $a \bmod b := b \text{ int}(a/b)$ ,  $\text{int}(x)$  is the integer part of  $x$ .

**PROOF.** From [23], property 1 -**Proposition 4.1**, according to the Block-Toeplitz property we can write,

$$\text{for } i \leq j, r_{i,j} = r_{i \bmod n_1, j-i \sec n_1}$$

in the case of the Blocks being Toeplitz matrices, for each element inside the block we differentiate between two cases:

i)  $(j - i \sec n_1) \bmod n_1 < i \bmod n_1$ : Element exclusively in the lower triangular part of the block.

ii)  $(j - i \sec n_1) \bmod n_1 \geq i \bmod n_1$ : Element in the upper triangular part of the block.

From this, one can project back on the first line and first column elements of each block in the first block line:

For  $i \leq j$

$$r_{i,j} = r_{i \bmod n_1, (j-i \sec n_1) \bmod n_1, j-i \sec n_1 - (j-i \sec n_1) \bmod n_1} \quad \text{if } (j - i \sec n_1) \bmod n_1 < i \bmod n_1$$

$$r_{i,j} = r_{0, (j-i \sec n_1) - i \bmod n_1} \quad \text{if } (j - i \sec n_1) \bmod n_1 \geq i \bmod n_1$$

While for  $i > j$ ,  $r_{i,j} = (r_{j,i})^*$ .

From which the proof is completed.

**Theorem 5.1.** In the case of Toeplitz block Toeplitz Matrix the generalized reflection coefficients admit the following:

$$a_{k,l} = a_{k',l'}^*$$

$$a'_{k,l} = a_{k',l'}^*$$

$$p_{k,l} = U^{k-k'} (\tilde{q}_{k',l'})^*$$

$$q_{k,l} = U^{k-k'} (\tilde{p}_{k',l'})^*$$

$$v_{k,l} = v_{k',l'}^*$$

$$v'_{k,l} = v_{k',l'}^*$$

where,  $(k', l') := (k \sec n_1 + n_1 - 1 - l \bmod n_1, l \sec n_1 + n_1 - 1 - k \bmod n_1)$ , and for any

$$v_{k,l} := [x_i]_{i=0,\dots,w}, \quad k, l \leq w, \quad \tilde{v}_{k,l} := [\tilde{x}_i]_{i=0,\dots,w}, \quad \begin{cases} \tilde{x}_i := x_{l-i+k} & \text{if } k \leq i \leq l \\ \tilde{x}_i := x_i & \text{if } i < k, \text{ or } i > l \end{cases}$$

$U$  is the  $(n_1 n_2) \times (n_1 n_2)$  up-down shift matrix defined as

$$U := \begin{bmatrix} 0 & 0 & \cdots & 0 & 0 \\ 1 & 0 & \ddots & & 0 \\ 0 & \ddots & \ddots & 0 & \vdots \\ \vdots & \ddots & 1 & 0 & 0 \\ 0 & \cdots & 0 & 1 & 0 \end{bmatrix}, \quad U^{-1} := \begin{bmatrix} 0 & 1 & 0 & \cdots & 0 \\ 0 & 0 & \ddots & \ddots & \vdots \\ 0 & \ddots & \ddots & 1 & 0 \\ \vdots & \ddots & 0 & 0 & 1 \\ 0 & \cdots & 0 & 0 & 0 \end{bmatrix} \quad \text{and } U^0 := \mathbf{1} \text{ is the identity}$$

matrix.

Before going into the proof details we will note  $\mathbf{p}_{k,l}, \mathbf{q}_{k,l}, \mathbf{a}_{k,l}, \mathbf{a}'_{k,l}, \mathbf{v}_{k,l}, \mathbf{v}'_{k,l}$ ,  $0 \leq k < l \leq n-1$ , corresponding to a Hermitian matrix  $M$  of size  $(n \times n)$ , respectively as  $\mathbf{p}_{k,l}^M, \mathbf{q}_{k,l}^M, \mathbf{a}_{k,l}^M, \mathbf{a}'_{k,l}^M, \mathbf{v}_{k,l}^M, \mathbf{v}'_{k,l}^M$ .

**Lemma 5.1.**

$$\forall h < s, s : s \bmod r = 0$$

$$i) (s-h) \bmod r = r-1-(h-1) \bmod r$$

$$ii) (s-h) \operatorname{sec} r = s-r-(h-1) \operatorname{sec} r$$

**PROOF.** For any  $(s-h) \bmod r = k$ , it is clear that we can write  $h$  in the form:

$$h = tr + r - k, \quad t \in \mathbb{N}. \text{ Also it is clear that}$$

$$\forall x, r, w : x \bmod r = w$$

$$w > n \Rightarrow (x-n) \bmod r + n = w$$

Since for  $k = 1, 2, \dots, r-1$ :

$$h \bmod r = r - k, \text{ this also realize } (h-1) \bmod r + 1 = r - k, \text{ which can be}$$

reorganized to yield  $k = r - (h-1) \bmod r - 1$ . The equality also holds for the case of  $k = 0$ . Finally relation (ii) is a direct replacement of (i) result in the definition of  $\operatorname{sec}$  according to  $x \operatorname{sec} r = x - x \bmod r$ .

**Proposition 5.2.** In the case of Hermitian Toeplitz-block-Toeplitz matrix the sub matrices admit the following

$$R_{k,l} = J (R_{k \otimes l})^T J, \text{ where } (k \otimes l) := (k', l')$$

**PROOF.** We start by noting the elements of each sub matrix  $M$  as  $r_{i,j}^M$ , from

which we have  $r_{i,j}^{R_{k,l}} = r_{i+k,j+k}$ , where  $i, j = 0, 1, \dots, l-k$ . (p.1)

This can be put into the form  $r_{i,j}^{R_{k,l}} = r_{f_1(k,i), f_1(k,j)}$ , where  $f_1(k, t) = k + t$ .

Next we notice that for any two matrices  $M_1, M_2$  of size  $n$ :

$$M_1 = J M_2 \Leftrightarrow r_{i,j}^{M_1} = r_{n-1-i,j}^{M_2}$$

$$M_1 = M_2 J \Leftrightarrow r_{i,j}^{M_1} = r_{i,n-1-j}^{M_2}$$

from which we get :

$$M_1 = M_2^T J \Leftrightarrow r_{i,j}^{M_1} = r_{j,n-1-i}^{M_2}$$

$$\text{and } M_1 = J M_2^T J \Leftrightarrow r_{i,j}^{M_1} = r_{n-1-i,j}^{M_2^T J} \Leftrightarrow r_{i,j}^{M_1} = r_{n-1-i,n-1-j}^{M_2^T} \Leftrightarrow r_{i,j}^{M_1} = r_{n-1-j,n-1-i}^{M_2}.$$

$$\text{and eventually } M_1 = J M_2^T J \Leftrightarrow r_{i,j}^{M_1} = r_{n-1-j,n-1-i}^{M_2}.$$

Or  $r_{i,j}^{J(R_{k \otimes l})^T J} = r_{(l-k)-j, (l-k)-i}^{R_{k \otimes l}}$ , from the definition of  $k \otimes l$ , and (p.1),

$$r_{i,j}^{R_{k \otimes l}} = r_{(k \operatorname{sec} n_1 + n_1 - 1 - l \bmod n_1) + i, (k \operatorname{sec} n_1 + n_1 - 1 - l \bmod n_1) + j} \text{ which gives}$$

$$r_{i,j}^{J(R_{k \otimes l})^T J} = r_{(k \operatorname{sec} n_1 + n_1 - 1 - l \bmod n_1) + (l-k) - j, (k \operatorname{sec} n_1 + n_1 - 1 - l \bmod n_1) + (l-k) - i}$$

and simplified into

$$r_{i,j}^{J(R_{k \otimes l})^T J} = r_{f_2(k,l,j), f_2(k,l,i)}, \text{ where } f_2(k, l, t) = l \operatorname{sec} n_1 - k \bmod n_1 + n_1 - 1 - t.$$

According to Lemma 5.1, by replacing with  $r = n_1, s = l \sec n_1 + n_1$ , and  $h = k \bmod n_1 + 1 + t$ ,

$$\begin{aligned} (f_1(k, t)) \bmod n_1 &= n_1 - 1 - (f_2(k, l, t)) \bmod n_1 \\ (f_1(k, t)) \sec n_1 &= l \sec n_1 - (f_2(k, l, t)) \sec n_1. \end{aligned}$$

This will oblige the following

$$\begin{aligned} (f_1(k, i)) \bmod n_1 > (f_1(k, j)) \bmod n_1 &\Leftrightarrow (f_2(k, l, i)) \bmod n_1 < (f_2(k, l, j)) \bmod n_1 \\ (f_1(k, i)) \bmod n_1 - (f_1(k, j)) \bmod n_1 &= (f_2(k, l, j)) \bmod n_1 - (f_2(k, l, i)) \bmod n_1 \\ (f_1(k, j)) \sec n_1 - (f_1(k, i)) \sec n_1 &= (f_2(k, l, i)) \sec n_1 - (f_2(k, l, j)) \sec n_1 \end{aligned}$$

Since  $f_2(k, l, i) - f_2(k, l, j) = f_1(k, j) - f_1(k, i)$ , we did cover both conditions of Proposition 5.1, in the case of  $f_1(k, i) \leq f_1(k, j)$ , while for the case  $f_1(k, i) > f_1(k, j)$  the equality of matrices  $R_{k,l}, J(R_{k \otimes l})^T J$  follows from each being Hermitian, with which the proof is completed.

**Proposition 5.3.** For any Hermitian matrix  $M$  of size  $(n \times n)$ ,

$$\begin{aligned} (\mathbf{p}_{k,l}^{JM^T J}, \mathbf{q}_{k,l}^{JM^T J}, \mathbf{a}_{k,l}^{JM^T J}, \mathbf{a}'_{k,l}^{JM^T J}, \mathbf{v}_{k,l}^{JM^T J}, \mathbf{v}'_{k,l}^{JM^T J}) = \\ \left( (\tilde{\mathbf{q}}_{n-1-l, n-1-k}^M)^*, (\tilde{\mathbf{p}}_{n-1-l, n-1-k}^M)^*, (\mathbf{a}'_{n-1-l, n-1-k}^M)^*, (\mathbf{a}_{n-1-l, n-1-k}^M)^*, (\mathbf{v}'_{n-1-l, n-1-k}^M)^*, (\mathbf{v}_{n-1-l, n-1-k}^M)^* \right) \end{aligned}$$

**PROOF.** To prove this we will apply the main algorithm (5.5)-(5.10), on the matrix  $JM^T J$ .

We notice that by eliminating  $J$  at each step we would have:

$$\mathbf{a}_{k,l}^{JM^T J} = \frac{(\tilde{\mathbf{p}}_{k,l-1}^{JM^T J})^T M^T \mathbf{e}_{n-1-l}}{(\tilde{\mathbf{q}}_{k+1,l}^{JM^T J})^T M^T \mathbf{e}_{n-1-l}} \quad \mathbf{a}'_{k,l}^{JM^T J} = \frac{(\tilde{\mathbf{q}}_{k+1,l}^{JM^T J})^T M^T \mathbf{e}_{n-1-k}}{(\tilde{\mathbf{p}}_{k,l-1}^{JM^T J})^T M^T \mathbf{e}_{n-1-k}}$$

Taking the conjugate on both sides of each relation, since  $M^T = M^*$ , we get

$$\left( \mathbf{a}_{k,l}^{JM^T J} \right)^* = \frac{(\tilde{\mathbf{p}}_{k,l-1}^{JM^T J})^{*T} M \mathbf{e}_{n-1-l}}{(\tilde{\mathbf{q}}_{k+1,l}^{JM^T J})^{*T} M \mathbf{e}_{n-1-l}} \quad \left( \mathbf{a}'_{k,l}^{JM^T J} \right)^* = \frac{(\tilde{\mathbf{q}}_{k+1,l}^{JM^T J})^{*T} M \mathbf{e}_{n-1-k}}{(\tilde{\mathbf{p}}_{k,l-1}^{JM^T J})^{*T} M \mathbf{e}_{n-1-k}}$$

By defining  $s := n - 1 - k$   $h := n - 1 - l$ , we can write the above relations in the form:

$$\left( \mathbf{a}_{n-1-s, n-1-h}^{JM^T J} \right)^* = \frac{(\tilde{\mathbf{p}}_{n-1-s, n-1-(h+1)}^{JM^T J})^{*T} M \mathbf{e}_h}{(\tilde{\mathbf{q}}_{n-1-(s-1), n-1-h}^{JM^T J})^{*T} M \mathbf{e}_h} \quad \left( \mathbf{a}'_{n-1-s, n-1-h}^{JM^T J} \right)^* = \frac{(\tilde{\mathbf{q}}_{n-1-(s-1), n-1-h}^{JM^T J})^{*T} M \mathbf{e}_s}{(\tilde{\mathbf{p}}_{n-1-s, n-1-(h+1)}^{JM^T J})^{*T} M \mathbf{e}_s}$$

Next, we will take advantage of the definitions:

$$\begin{aligned} \tilde{\mathbf{p}}_{k,l} &:= (\tilde{\mathbf{p}}_{n-1-l, n-1-k}^{JM^T J})^* & \tilde{\mathbf{q}}_{k,l} &:= (\tilde{\mathbf{q}}_{n-1-l, n-1-k}^{JM^T J})^* \\ \tilde{\mathbf{a}}_{k,l} &:= (\mathbf{a}_{n-1-l, n-1-k}^{JM^T J})^* & \tilde{\mathbf{a}}'_{k,l} &:= (\mathbf{a}'_{n-1-l, n-1-k}^{JM^T J})^* \end{aligned}$$

Our definitions hold for all values  $k \leq l$ ,  $k, l = 0, \dots, n - 1$ . For that, we can write into the form:

$$\bar{a}_{h,s} = \frac{(\bar{p}_{h+1,s})^T M \mathbf{e}_h}{(\bar{q}_{h,s-1})^T M \mathbf{e}_h} \quad \bar{a}'_{h,s} = \frac{(\bar{q}_{h,s-1})^T M \mathbf{e}_s}{(\bar{p}_{h+1,s})^T M \mathbf{e}_s} \quad (\text{p3.1})$$

Also by taking the conjugate on both sides of (5-6), and multiplying by  $J$  we

$$\text{obtain: } \bar{p}_{h,s} = \bar{p}_{h+1,s} - \left( a_{n-1-s,n-1-h}^{JM^T J} \right)^* \bar{q}_{h,s-1} \quad \bar{q}_{h,s} = \bar{q}_{h,s-1} - \left( a'_{n-1-s,n-1-h} \right)^* \bar{p}_{h+1,s},$$

which yield

$$\bar{p}_{h,s} = \bar{p}_{h+1,s} - \bar{a}_{h,s} \bar{q}_{h,s-1} \quad \bar{q}_{h,s} = \bar{q}_{h,s-1} - \bar{a}'_{h,s} \bar{p}_{h+1,s} \quad (\text{p3.2})$$

By comparing the new relations (p3.1,p3.2) with the basic algorithm we conclude that

$$\bar{p}_{k,l} = q_{k,l}^M, \bar{q}_{k,l} = p_{k,l}^M \quad \text{and} \quad \bar{a}_{k,l} = a'_{k,l}{}^M, \quad \bar{a}'_{k,l} = a_{k,l}^M, \text{ from which our proof is completed.}$$

**Proposition 5.4.**

$$\left( p_{s,d}^{0R^k,l}, q_{s,d}^{0R^k,l}, a_{s,d}^{0R^k,l}, a'_{s,d}{}^{0R^k,l}, v_{s,d}^{0R^k,l}, v'_{s,d}{}^{0R^k,l} \right) = \left( p_{s,d}^R, q_{s,d}^R, a_{s,d}^R, a'_{s,d}{}^R, v_{s,d}^R, v'_{s,d}{}^R \right)$$

With the condition that  $k \leq s < d \leq l$ .

The previous proposition is obvious and therefore we will omit its proof.

**PROOF OF Theorem 5.1.** We start by noticing that

$\forall 0 \leq k < l \leq n_1 n_2 - 1 \exists s, d : k \leq s < d \leq l$ , so that we can write

$$\left( p_{s,d}^{0R^k,l}, q_{s,d}^{0R^k,l}, a_{s,d}^{0R^k,l}, a'_{s,d}{}^{0R^k,l}, v_{s,d}^{0R^k,l}, v'_{s,d}{}^{0R^k,l} \right) = \left( U_{l-k}^k p_{s-k,d-k}^{R^k,l}, U_{l-k}^k q_{s-k,d-k}^{R^k,l}, a_{s-k,d-k}^{R^k,l}, a'_{s-k,d-k}{}^{R^k,l}, v_{s-k,d-k}^{R^k,l}, v'_{s-k,d-k}{}^{R^k,l} \right)$$

where  $U_x$  is a Matrix of size  $(n_1 n_2) \times (x+1)$ , defined as:

$$U_x := \begin{bmatrix} 0 & 0 & \dots & 0 \\ 1 & 0 & \ddots & \vdots \\ 0 & 1 & \ddots & 0 \\ 0 & 0 & \ddots & 0 \\ \vdots & \vdots & \ddots & 1 \\ 0 & 0 & \dots & 0 \end{bmatrix}, \quad U_x^0 := \begin{bmatrix} \mathbf{1}_{(x+1) \times (x+1)} \\ \mathbf{0} \end{bmatrix}$$

Coupling this with **Proposition 5.4**, we obtain that

$$\left( p_{s,d}^R, q_{s,d}^R, a_{s,d}^R, a'_{s,d}{}^R, v_{s,d}^R, v'_{s,d}{}^R \right) = \left( U_{l-k}^k p_{s-k,d-k}^{R^k,l}, U_{l-k}^k q_{s-k,d-k}^{R^k,l}, a_{s-k,d-k}^{R^k,l}, a'_{s-k,d-k}{}^{R^k,l}, v_{s-k,d-k}^{R^k,l}, v'_{s-k,d-k}{}^{R^k,l} \right)$$

By selecting  $d = l, s = k$  we get

$$\left( p_{k,l}^R, q_{k,l}^R, a_{k,l}^R, a'_{k,l}{}^R, v_{k,l}^R, v'_{k,l}{}^R \right) = \left( U_{l-k}^k p_{0,l-k}^{R^k,l}, U_{l-k}^k q_{0,l-k}^{R^k,l}, a_{0,l-k}^{R^k,l}, a'_{0,l-k}{}^{R^k,l}, v_{0,l-k}^{R^k,l}, v'_{0,l-k}{}^{R^k,l} \right) \quad (\text{t1.1})$$

In the same way we obtain for  $(k', l') = k \otimes l$

$$\left( p_{k \otimes l}^R, q_{k \otimes l}^R, a_{k \otimes l}^R, a'_{k \otimes l}{}^R, v_{k \otimes l}^R, v'_{k \otimes l}{}^R \right) =$$

$$\left( U_{l'-k'}^{k'} p_{0,l'-k'}^{R^{k \otimes l}}, U_{l'-k'}^{k'} q_{0,l'-k'}^{R^{k \otimes l}}, a_{0,l'-k'}^{R^{k \otimes l}}, a'_{0,l'-k'}^{R^{k \otimes l}}, v_{0,l'-k'}^{R^{k \otimes l}}, v'_{0,l'-k'}^{R^{k \otimes l}} \right)$$

By combining the application of both **Proposition 5.2** and **Proposition 5.3** we obtain

$$\left( p_{k \otimes l}^R, q_{k \otimes l}^R, a_{k \otimes l}^R, a'_{k \otimes l}^R, v_{k \otimes l}^R, v'_{k \otimes l}^R \right) = \left( U_{l-k}^{k'} \left( \tilde{q}_{0,l-k}^{R^{k,l}} \right)^*, U_{l-k}^{k'} \left( \tilde{p}_{0,l-k}^{R^{k,l}} \right)^*, \left( a'_{0,l-k}^{R^{k,l}} \right)^*, \left( a_{0,l-k}^{R^{k,l}} \right)^*, \left( v'_{0,l-k}^{R^{k,l}} \right)^*, \left( v_{0,l-k}^{R^{k,l}} \right)^* \right) \quad (\text{t1.2})$$

By comparing the first sides of each of (t1.1), and (t1.2), with the second sides, we find that

$$a_{k,l} = a_{k',l'}^*$$

$$a'_{k,l} = a_{k',l'}^{*}$$

$$v_{k,l} = v_{k',l'}^{*}$$

$$v'_{k,l} = v_{k',l'}^*$$

To complete our proof we need only notice that

$$p_{k,l}^R = U_{l-k}^k p_{0,l-k}^{R^{k,l}} \quad (\text{t1.3})$$

$$q_{k \otimes l}^R = U_{l-k}^{k'} \left( \tilde{p}_{0,l-k}^{R^{k,l}} \right)^*$$

By multiplying both sides of the last relation with  $\left( U_{l-k}^{k'} \right)^T$ , we obtain,

$$\left( U_{l-k}^{k'} \right)^T q_{k \otimes l}^R = \left( \tilde{p}_{0,l-k}^{R^{k,l}} \right)^* \quad (\text{t1.4}), \text{ since}$$

$\left( U_{l-k}^{k'} \right)^T \left( U_{l-k}^{k'} \right) = \mathbf{1}$ . To prove the later relation; we observe that by definition

$k' < l' \leq n_1 n_2 - 1 \Rightarrow l' - k' \leq n_1 n_2 - 1 - k'$ , from which we have

$k' \leq n_1 n_2 - 1 - (l' - k')$ , also that the equality  $l - k = l' - k'$  is always realized.

From (t1.4) we can further write  $\left( U_{l-k}^{k'} \right)^T \left( \tilde{q}_{k \otimes l}^R \right)^* = p_{0,l-k}^{R^{k,l}}$ . By replacing

$p_{0,l-k}^{R^{k,l}}$  from the last relation in (t1.3) we conclude that:

$p_{k,l}^R = U_{l-k}^k \left( U_{l-k}^{k'} \right)^T \left( \tilde{q}_{k \otimes l}^R \right)^*$ . Since, for any vector  $v_{k',l'}$ , defined as

$$v_{b,g} := [x_i]_{i=0,\dots,n-1} : 0 \leq b < g \leq n-1, x_i = 0 \text{ if } i < b \text{ or } i > g$$

we have always  $\forall k \geq 0, U_{g-b}^k \left( U_{g-b}^b \right)^T v_{b,g} = U^{k-b} v_{b,g}$ ,

and we get  $p_{k,l}^R = U^{k-k'} \left( \tilde{q}_{k \otimes l}^R \right)^*$ . In the same way we obtain that

$$q_{k,l}^R = U^{k-k'} \left( \tilde{p}_{k \otimes l}^R \right)^*. \text{ This completes the proof.}$$

The next algorithm will help us obtaining our inverse factorization with a minimum of calculus effort. It follows the main steps of the one presented in [23]. The main difference is that it will be working only on the first skew symmetric part of each Toeplitz block.

## V Generalized reflection coefficients in the Toeplitz block Toeplitz case algorithm (GRCTBT)

### ◆ Algorithm's details

In the Hermitian Toeplitz Block Toeplitz case, the application of the recursive relations (5.5)-(5.10) happens according to the following:

First we rewrite Equations (5.5)-(5.10) as the subroutine

#### Subroutine 1

$$a_{k,l} = \frac{\hat{\mathbf{p}}^T R \mathbf{e}_l}{\hat{\mathbf{v}}} \quad a'_{k,l} = \frac{\hat{\mathbf{q}}^T R \mathbf{e}_k}{\hat{\mathbf{v}'}} \quad (\text{t2.1})$$

$$\mathbf{p}_{k,l} = \hat{\mathbf{p}} - a_{k,l} \hat{\mathbf{q}} \quad \mathbf{q}_{k,l} = \hat{\mathbf{q}} - a'_{k,l} \hat{\mathbf{p}} \quad (\text{t2.1})$$

$$\mathbf{v}_{k,l} = \hat{\mathbf{v}}(1 - a_{k,l} a'_{k,l}) \quad \mathbf{v}'_{k,l} = \hat{\mathbf{v}'}(1 - a_{k,l} a'_{k,l}) \quad (\text{t2.3})$$

Next proceed as the following

#### Initialization

For  $k = 0$  to  $n_1 - 1$ : {

$$\mathbf{p}_{k,k} = \mathbf{q}_{k,k} = \mathbf{e}_k, \mathbf{v}_{k,k} = \mathbf{v}'_{k,k} = r_{0,0}$$

}

#### Main routine

For  $d_2 = 0$  to  $n_2 - 1$  do :

{

  If  $d_2$  not equal to zero:

  {

    For  $d_1 = n_1 - 1$  to  $0$  do : (Lower triangle loop)

    {

      For  $u = 0$  to  $n_1 - d_1 - 1$  do :

      {

$$k = u + d_1 \quad l = d_2 n_1 + u$$

$$k' = k \operatorname{sec} n_1 + n_1 - 1 - l \operatorname{mod} n_1$$

      if  $k \leq k'$  {

$$(k^0, l^-) = (k, l - 1)$$

      if  $u$  equal to  $0$ : {

$$(k^{0'}, l'^-) = (k^0 \otimes l^-)$$

$$\hat{\mathbf{p}} = U^{n_1-1} (\tilde{\mathbf{q}}_{k^{0'}, l'^-})^*, \hat{\mathbf{v}'} = \mathbf{v}_{k^{0'}, l'^-} \quad (\text{t2.4})$$

      }

      else {

$$\hat{\mathbf{p}} = \mathbf{p}_{k^0, l^-}, \hat{\mathbf{v}'} = \mathbf{v}'_{k^0, l^-}$$

      }

      if  $k$  equal to  $k'$ : {

$$\hat{\mathbf{q}} = U (\tilde{\hat{\mathbf{p}}})^*, \hat{\mathbf{v}} = \hat{\mathbf{v}'} \quad (\text{t2.5})$$

      }

      else {





$\Lambda_1, \Lambda_2, \dots, \Lambda_{n_2}$ , where  $\Lambda_d := P_d \setminus P_{d-1}$ , and  $P_0 := \emptyset$

In the *Lower Triangle Loop* we obtain values for

$$\forall (k, l) \in \Lambda_d^-, \text{ where } \Lambda_d^- := \{(k, l) \in \Lambda_d : k \geq l \bmod n_1\}$$

To demonstrate this, first we notice that for

$$\Lambda_d^{-,d_1} := \{(k, l) : (k, l) \in \Lambda_d^-, k - l \bmod n_1 = d_1\}$$

$$\Lambda_d^- = \bigcup_{d_1=0}^{n_1-1} \Lambda_d^{-,d_1}$$

we have, for  $d_1 \in [0, n_1 - 1]$ :

$$\Lambda_d^{-,d_1} = \{(k, l) : l \bmod n_1 \in [0, n_1 - 1 - d_1], k = l \bmod n_1 + d_1\}$$

By defining  $u := l \bmod n_2$  we conclude that we did consider all  $(k, l) \in \Lambda_d^-$ .

Using the same logic we conclude that in the *Exclusively Upper Triangle Loop* we obtain values for

$$\forall (k, l) \in \Lambda_d^+, \text{ where } \Lambda_d^+ := \{(k, l) \in \Lambda_d : k < l \bmod n_1\}. \text{ It is clear that}$$

$$\Lambda_d = \Lambda_d^- \cup \Lambda_d^+$$

In the *EUTL* it is easy to verify that:

$$\forall (k, l) \in \Lambda_d^+, \{(k, l - 1), (k + 1, l)\} \subset \Lambda_d,$$

while in the *Lower Triangle Loop* this is not always true, more precisely for  $k = n_1 - 1$ , or/and  $l \bmod n_1 = 0$ . Each of  $\Lambda_d^+, \Lambda_d^-$  is divided into two skew symmetric parts relative to the antidiagonal, this division comes from the fact that  $(k, l)$  and  $(k \otimes l)$  mark two symmetric points relative to the antidiagonal of each Block. The condition  $k \leq k'$  let us treat only the first skew symmetric part, since by **Theorem 5.1** the other parts values need not to be calculated. A special case arise when  $k = k'$ , in which needed values from the second parts are reintroduced according to **Theorem 5.1**, (t2.5), (t2.6). In the case when  $(k, l) \in \Lambda_d^-$ , when  $l \bmod n_1 = 0$ ,  $(k, l - 1)$ , is in the second skew symmetric part of  $\Lambda_{d-1}$  for which again **Theorem 5.1** let us obtain its values by the means of  $(k \otimes l - 1)$ , (t2.4).

◆ *Algorithm's complexity*

For complexity estimation we proceed as the following:

Each Entry in the routine will require operations of  $O(l - k)$ , by noting  $c_1$  as the step constant,  $opc$  as the total number of operation, the calculus cost take the form of:

$$opc \approx \frac{1}{2} \left[ \sum_{d_2=0}^{n_2-1} \sum_{d_1=1}^{n_1-1} \sum_{u=0}^{n_1-d_1-1} c_1 (n_1 d_2 + d_1) + \sum_{d_2=1}^{n_2-1} \sum_{d_1=0}^{n_1-1} \sum_{u=0}^{n_1-d_1-1} c_1 (n_1 d_2 - d_1) \right],$$

which can be expanded into:

$$opc \approx \frac{1}{2} \left[ \begin{array}{l} (n_1 - 1)c_1 \frac{1}{2}(n_1 - 1)n_1 - c_1 \frac{1}{6}(n_1 - 1)(n_1)(2n_1 - 1) + \\ 2c_1 n_1 \frac{1}{2}(n_2 - 1)n_2 (n_1 - 1)^2 - 2c_1 n_1 \frac{1}{2}(n_2 - 1)n_2 \frac{1}{2}(n_1 - 1)n_1 + \\ (n_1 - 1)c_1 n_1 \frac{1}{2}(n_2 - 1)n_2 \end{array} \right] \quad (5.12)$$

From which we conclude the complexity order of  $n_1^3 n_2^2$ .

## VI A comparison with the WWR Algorithm in the TBT Case

WWR Algorithm in the TBT case gives a solution to the linear problem:

$$\mathbf{A}_{n_1, n_2} \cdot \mathbf{R}_{n_1, n_2} = \mathbf{r}_{n_1, n_2} \quad (5.13)$$

$\mathbf{A}_{n_1, n_2} := [A_1^{n_2-1}, A_2^{n_2-1}, \dots, A_{n_2-1}^{n_2-1}]$ , where  $A_k^l, k \leq l$  is the well know  $k$  matrix polynomial coefficient of order  $l$ .

And  $\mathbf{r}_{n_1, n_2} := [R_1, R_2, \dots, R_{n_2-1}]$ ,  $R_i := R^{in_1(i+1)n_1-1}$

$$R_{n_1, n_2} := \begin{bmatrix} R_0 & R_1 & \cdots & R_{n_2-2} \\ R_{-1} & R_0 & \ddots & \vdots \\ \vdots & \ddots & \ddots & R_1 \\ R_{2-n_2} & \cdots & R_{-1} & R_0 \end{bmatrix}$$

The Coefficients Matrix is calculated in a recursive manner, starting from  $n > 0$ , up until  $n = n_2 - 1$ , according to the order [8][9][16]:

$$\Delta_n := R_n + \sum_{l=1}^{n-1} A_l^{n-1} R_{n-l}$$

$$A_n^n := -\Delta_n (P_{n-1})^{-1}$$

$$P_n := P_{n-1} + A_n^n \Delta_n^H$$

With,

$$\mathbf{A}_{n_1, n+1} = [\mathbf{A}_{n_1, n-1}, \mathbf{0}] + A_n^n [JA_{n-1}^{n-1*} J, JA_{n-2}^{n-1*} J, \dots, JA_1^{n-1*} J, \mathbf{1}]$$

Starting From

$$P_0 = R_0$$

The total calculus cost of WWR in the TBT case can be written as:

$$\begin{aligned} opcwrr &= \sum_{n=1}^{n_2-1} \left[ 3(n_1)^3 \right] + \sum_{n=2}^{n_2-1} \left[ 2 \sum_{i=1}^{n-1} (n_1)^3 \right] \\ &= (n_2 - 1)3(n_1)^3 + 2(n_1)^3 \sum_{n=2}^{n_2-1} [(n-1)] \\ &= (n_2 - 1)3(n_1)^3 + 2(n_1)^3 \frac{(4 + (n_2 - 3))(n_2 - 2)}{2} \\ opcwrr &= (n_2 - 1)3(n_1)^3 + (n_1)^3 (n_2 + 1)(n_2 - 2) \end{aligned} \quad (5.14)$$

To be able to draw a precise comparison we need to state more precisely the expression in (5.12). To do this we will set the constant factor as  $c_1 = 3$ , which takes

into account the Matrix and Vector multiplication operations in (t2.1) and (t2.2). For the divisions in (t2.1) and (t2.2), and the multiplications in (t2.3) we will add a total value of  $\frac{5}{2}(n_1)^2 n_2$ , from which we can write the total number of operations according to GRCTBT as:

$$\begin{aligned}
 opc &= (n_1 - 1) \frac{3}{4} (n_1 - 1) n_1 - \frac{3}{12} (n_1 - 1) (n_1) (2n_1 - 1) + \\
 & n_1 \frac{3}{2} (n_2 - 1) n_2 (n_1 - 1)^2 - n_1 (n_2 - 1) n_2 \frac{3}{4} (n_1 - 1) n_1 + \\
 & (n_1 - 1) n_1 \frac{3}{4} (n_2 - 1) n_2 + \frac{5}{2} (n_1)^2 n_2
 \end{aligned} \tag{5.15}$$

Figure 5.1 shows the plot for both relation (5.14), and (5.15), for  $n_1 = n_2$ ; WWR Algorithm in dashed line, and GRCTBT algorithm in solid line. Figure 5.2 plots the ratio  $\frac{opcwwr}{opc}$  for the same  $n_1, n_2$  values of Figure 5.1.

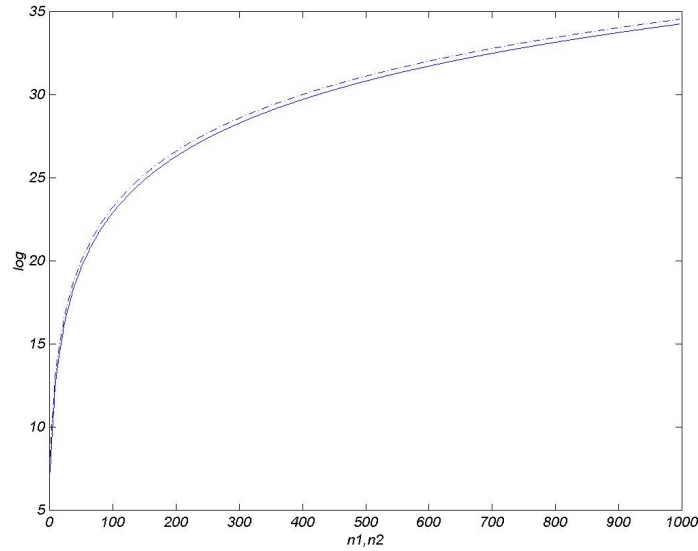


Figure 5.1

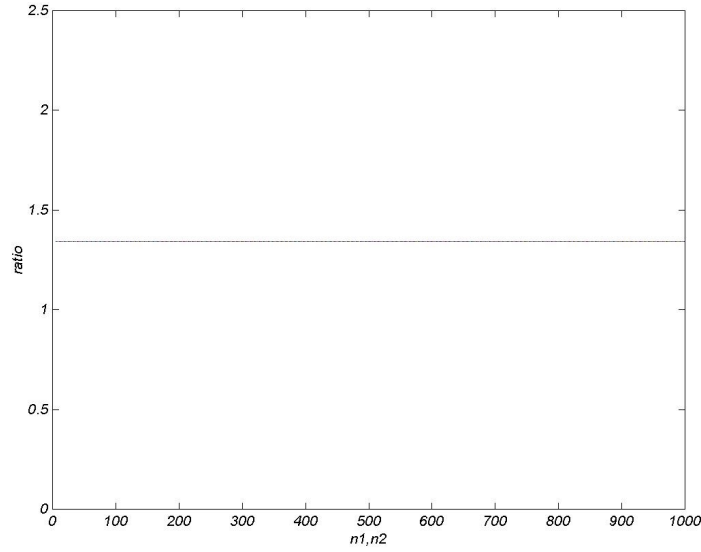


Figure 5.2

## VII Conclusion

The presented results, explain clearly the structure of the Generalized Reflection Coefficients, and their relevant orthogonal polynomials in the Hermitian Toeplitz Block Toeplitz Case. The reflection coefficients admit the same Block Toeplitz recurrence, and the polynomials  $p_{k,l}$ ,  $q_{k,l}$  show a block Toeplitz recurrence with an added shift between Blocks polynomials counterparts. Both of reflection coefficients and the polynomials  $a_{k,l}$ ,  $a'_{k,l}$ ,  $p_{k,l}$ ,  $q_{k,l}$  with indices  $k, l$ , show an exchange structure with values of indices  $k \otimes l$ , symmetric to the antidiagonal of each block. The later fact did establish a faster Levinson-like inversion algorithm. At this same time, the antidiagonal symmetry is a direct expression of **Proposition 3.3** in the Generalized Reflection Coefficients context. In other words, the gain in calculations cost using the Generalized Reflection Coefficients in the TBT case, is equivalent to the gain that we would have by taking advantage of **Proposition 3.3** while applying WWR Algorithm.

---

## SEQUENTIAL MULTIDIMENSIONAL SPECTRAL ESTIMATION

*Abstract*-By considering an empirical approximation, and a new class of operators that we will call ‘walking operators’, we construct, for any positive ND-Toeplitz matrix, an infinite in all dimensions matrix, for which the inverse approximates the original matrix in its finite part. A recursive hierarchical algorithm is presented for sequential dimension spectral representation. A positive comparison in calculus cost, and numerical simulation, for 2D and 3D signals, is also presented.

*Résumé*- En considérant une approximation empirique et une nouvelle classe d’opérateurs qu’on appelle les opérateurs « Walking », on arrive à construire, pour toute matrice positive ND-Toeplitz, une matrice infinie dans toutes les dimensions, et pour laquelle l’inverse est une approximation de la matrice originale dans sa partie finie. L’algorithme hiérarchique récursif que l’on présente produit une estimation séquentielle de la puissance spectrale multidimensionnelle. On montre aussi une comparaison positive dans le coût de calcul par rapport à la méthode de Capon, et des simulations numériques pour des signaux 2D et 3D.

### Introduction

A great deal of work has been done in the past in the domain of spectral analysis. As a basic mathematical problem giving solutions to many physical systems, it remains as still a not totally resolved problem in its multidimensional aspect. While the foundations of the theory were established by [25],[26], a series of very important advances in the field were achieved, especially the connection to information theory [27], by the introduction of the spectral maximum of entropy principle in [6]. Also the connection to an optimized Toeplitz linear system was made in [22] and [21]. In the two dimensional case, and more generally in the multidimensional case, actually, and contrary to the correlation matching, and maximum of entropy criteria achieved in the 1D case, two algebraic methods are used. Each has its advantages and disadvantages. The first method is what we can call the quarter-plan forced autoregressive filters [16], and the second is the Capon Minimum variance method [15],[30]. While the Capon estimation provides a good stable estimation it has the disadvantage of high calculus coast. On the other hand the quarter-plan method follows an unreal model<sup>2</sup>, and hence suffers from high instability with order elevation. In this chapter we propose a method that is less costly than the Capon method, and far more stable than the quarter-plan autoregressive estimation.

---

<sup>2</sup> Polynomial roots are not forcefully inside the unit circle.

## I Multidimensional Toeplitz Characters and Spectral Block Structure

For a multidimensional signal  $x(t), t \in \mathbb{Z}^d$ , we will define the  $\gamma$  order correlation matrix,  $\gamma \in (\mathbb{Z}^+)^d$  as

$$R := E \left( X(t) (X(t))^H \right)$$

where  $X$  is defined as

$$X(t) := \begin{bmatrix} x(t_0, t_1, \dots, t_{d-1}) \\ x(t_0+1, t_1, \dots, t_{d-1}) \\ \vdots \\ x(t_0+\gamma_0-1, t_1, \dots, t_{d-1}) \\ x(t_0, t_1+1, \dots, t_{d-1}) \\ \vdots \\ x(t_0, t_1+\gamma_1-1, \dots, t_{d-1}) \\ \vdots \\ x(t_0, t_1, \dots, t_{d-1}+\gamma_{d-1}-1) \end{bmatrix}.$$

As far as this chapter is concerned we will be only dealing with the case where the correlation matrix admits a toeplitz nature in all dimensions, in other words, it is  $d$  time toeplitz, so it is also adequate to represent it as an operator of a  $d$  dimension correlation signal  $c(t)$  so that

$$c(t) \in \mathbb{C}, t \in [-\gamma, \gamma], \gamma \in (\mathbb{Z}^+)^d,$$

$$c(t) \equiv \sum_{n \in \mathbb{Z}^d} x(n+t) x^*(n)$$

and we will write

$$R = R(c(\gamma)) \text{ which is of size } q = \prod_{i=0}^{d-1} \gamma_i.$$

It is also well known, and according to Kolmogoroff's relation [26] that

$$c(t) = \frac{1}{(2\pi)^d} \oint_{|\mathbb{C}^d|=1} \left| \sum_{n \in \mathbb{Z}^d} x[n] e^{jw \cdot (n^T)} \right|^2 e^{-jw \cdot (t^T)} dw.$$

By considering  $\Omega$ , a redistribution of the dimensions nesting, such that

$$\Omega \in \left\{ (\Omega_0, \Omega_1, \dots, \Omega_{d-1}) : k \neq l \Rightarrow \Omega_k \neq \Omega_l, \forall \Omega_l \in \mathbb{N}, 0 \leq \Omega_l \leq d-1 \right\}$$

we will define

$$q_l^\Omega := \begin{cases} \prod_{i=0}^{l-1} \gamma_{\Omega_i} & \text{if } l \neq 0 \\ 1 & \text{if } l = 0 \end{cases}$$

Of course  $\Omega$  is invertible in the sense that  $\Omega_k = l \Rightarrow \Omega^{-1}(l) = k$ .

**Definition 6.1.** We will define the walking operator as

$$\begin{aligned}
 W_{\Omega \rightarrow \Omega'}(M) : [M]_{i,j} &\rightarrow [M]_{X^{\Omega \rightarrow \Omega'}(i), X^{\Omega \rightarrow \Omega'}(j)} \\
 X^{\Omega \rightarrow \Omega'}(i_0 q_0^\Omega + i_1 q_1^\Omega + \dots + i_{d-1} q_{d-1}^\Omega) &= i_0 q_{\Omega^{-1}(\Omega_1(0))}^{\Omega'} + i_1 q_{\Omega^{-1}(\Omega_1(1))}^{\Omega'} + \dots + i_{d-1} q_{\Omega^{-1}(\Omega_1(d-1))}^{\Omega'} \\
 \text{where } [i_0, i_1, \dots, i_{d-1}] &\in (\mathbb{Z}^*)^d, 0 \leq i_k \leq \gamma_{\Omega(k)}.
 \end{aligned}$$

From a basic point of view, the walking operator corresponds to the convention used in the relation defining the vector  $X$ , but, as we will see later, it represents also a very important constraint on the degree of liberty of the correlation matrix, and eventually its inverse.

**Definition 6.2.** We call for any  $t \in (\mathbb{Z}^+)^d$ ,  $t$ -block matrix any matrix of size  $\prod_{i=0}^{d-1} t_i$ .

A  $d$ -block matrix  $M$  can be indexed by the virtue of some dimensions nesting  $\Omega$  according to

$$M \left[ i_0 q_0^\Omega + i_1 q_1^\Omega + \dots + i_{d-1} q_{d-1}^\Omega \right] \left[ j_0 q_0^\Omega + j_1 q_1^\Omega + \dots + j_{d-1} q_{d-1}^\Omega \right], \quad 0 \leq i_l \leq \gamma_{\Omega(l)}, 0 \leq j_l \leq \gamma_{\Omega(l)}.$$

**Definition 6.3.** A matrix admits  $(\gamma, u, \Omega)$ -toeplitz character when it is  $\gamma$ -block matrix and realize the following

$$\begin{aligned}
 M \left[ i_0 q_0^\Omega + i_1 q_1^\Omega + \dots + i_{d-1} q_{d-1}^\Omega \right] \left[ j_0 q_0^\Omega + j_1 q_1^\Omega + \dots + j_{d-1} q_{d-1}^\Omega \right] &= \\
 M \left[ i_0 q_0^\Omega + i_1 q_1^\Omega + (i_u - j_u) q_u^\Omega \dots + i_{d-1} q_{d-1}^\Omega \right] \left[ j_0 q_0^\Omega + j_1 q_1^\Omega + 0 \cdot q_u^\Omega + \dots + j_{d-1} q_{d-1}^\Omega \right] &\text{ if } i_u - j_u \geq 0 \\
 M \left[ i_0 q_0^\Omega + i_1 q_1^\Omega + (0) q_u^\Omega \dots + i_{d-1} q_{d-1}^\Omega \right] \left[ j_0 q_0^\Omega + j_1 q_1^\Omega + (j_u - i_u) q_u^\Omega + \dots + j_{d-1} q_{d-1}^\Omega \right] &\text{ if } i_u - j_u < 0
 \end{aligned}$$

**Definition 6.4.** In the case that an  $\gamma$ -block matrix contains more than one toeplitz character, such that it is  $(\gamma, u_0, \Omega), (\gamma, u_1, \Omega) \dots (\gamma, u_{s-1}, \Omega)$ , toeplitz character, we will call it an  $(\gamma, u, \Omega)$ - $s$ -toeplitz character matrix, with  $u$  equal in that case to  $[u_0, u_1, \dots, u_{s-1}]$ .

According to **Definition 6.3** we can index the matrix elements using the notation

$$M \left[ i_0 q_0^\Omega + i_1 q_1^\Omega + \dots + i_{u-1} q_{u-1}^\Omega \right] \left[ j_0 q_0^\Omega + j_1 q_1^\Omega + \dots + j_{u-1} q_{u-1}^\Omega \right] (k_u) \left[ i_{u+1} q_{u+1}^\Omega + \dots + i_{d-1} q_{d-1}^\Omega \right] \left[ j_{u+1} q_{u+1}^\Omega + \dots + j_{d-1} q_{d-1}^\Omega \right]$$

To simplify the notations we will write it as

$$M^\Omega \left[ b_0^{u-1} \right] (d_u^{u+s}) \left[ b_{u+s+1}^{d-1} \right] \quad b_h^{h+y-1} \in (\mathbb{Z}^*)^{2y}, d_h^{h+y-1} \in \mathbb{Z}^y,$$

where for  $s > 0$  the matrix is  $s$ -toeplitz characters.

**Proposition 6.1.**  $\forall \Omega'$ , any  $(\gamma, u, \Omega)$  toeplitz character matrix can be transformed into  $(\gamma, u', \Omega')$  toeplitz character using the walking transformation  $W_{\Omega \rightarrow \Omega'}(M)$ , and we have  $u' = \Omega'^{-1}(\Omega_u)$ .

**Theorem 6.1.** For any full rank matrix  $(\gamma, u, \Omega)$ - $s$ -toeplitz character matrix,

$$M^\Omega \left[ b_0^{u-1} \right] (t_{u_0}, t_{u_1}, \dots, t_{u_{s-1}}), \text{ with } t_{u_i} \in [-\infty, \infty], \text{ the inverse matrix } iM \text{ is equal to}$$





$$\left[ \frac{dw}{(2\pi)^d} CC^H \right]_{i,j} = \frac{1}{(2\pi)^d} \oint_w e^{jw(k_i - k_j)^T} dw = \begin{cases} 1 & \text{if } i = j \\ 0 & \text{if } i \neq j \end{cases}.$$

From which, we have  $\frac{dw}{(2\pi)^d} CC^H = \mathbf{1}$ .

In the case that  $s < d$ , then we will note  $h := q_{d-s}^\Omega$  as the non-toeplitz part matrix size. As a counter part to the multidimensional Fourier transform vector in the previous definition we will define the block multidimensional Fourier transform vector as

$$F^{w_i, t} := \begin{bmatrix} \overbrace{0 \dots 0}^t & e^{-jw_i(k_{-\infty})^T} & \overbrace{0 \dots 0}^{h-t-1} & \dots & \overbrace{0 \dots 0}^t & e^{-jw_i(k_{\infty})^T} & \overbrace{0 \dots 0}^{h-t-1} \end{bmatrix}^T,$$

$0 \leq t \leq h-1$ . By considering the Block diagonal matrix  $\lambda_s$ , which is by

definition do contain the matrix value  $\left[ \sum_{k_u} M^\Omega(t_{u_0}, t_{u_1}, \dots, t_{u_{s-1}}) e^{-jw_i(t_u)^T} \right]$ , at the

diagonal index  $w_i$ , it is simple to prove that

$$\lambda_s = \frac{dw}{(2\pi)^s} C_s^H (M^\Omega) C_s$$

where  $C_s = \begin{bmatrix} F^{w_{-\infty}, 0} & F^{w_{-\infty}, 1} & \dots & F^{w_{-\infty}, h} & \dots & F^{w_{\infty}, h-1} & F^{w_{\infty}, h} \end{bmatrix}$ . Next, by observing that  $C_s$  is full rank, we prove that  $\lambda_s$  is full rank also, and that proves the theorem.

## II Multidimensional Extension Approximation

Our approximation that we are proposing in this chapter depends strongly on the previous work done in the treatment of the generalized reflection coefficients [18], and [28]. To better explain this extension we start with the 1 dimensional case. For a positive definite toeplitz matrix  $M^N(l)$ ,  $l := -N+1, \dots, N-1$ , we define the polynomial  $p^{N-1}, q^{N-1}$ , as the solution for the linear system  $M^N(l) p^{N-1} = e_0$ ,  $M^N(l) q^{N-1} = e_{N-1}$ . These solutions in fact can be obtained recursively according to

$$p'^N = \begin{bmatrix} p'^{N-1} \\ 0 \end{bmatrix} + \sigma_N \begin{bmatrix} 0 \\ q'^{N-1} \end{bmatrix}.$$

Where  $v'$  is  $v$  normalized by the first value for  $p^N$ , and the last for  $q^N$ ,  $\sigma$  is the famous reflection coefficient. Putting the reflection coefficient to zero is equivalent to the existence of a positive definite matrix  $M^{N+1}(l)$ , which coincides with  $M^N(l)$ , so that  $M^{N+1}(l) = M^N(l), l = -N+1, \dots, N-1$ . By repeating the procedure until infinity, we obtain that

$$\left[ M^\infty(l) \right]^{-1} = \rho^{-1} P P^H \quad (6.1)$$



**PROOF.** Starting from  $x = 1$ ,  $R_0^{-1} := \left[ R \left( c \left( \left[ \gamma_0, \gamma_2, \dots, \gamma_{d-1} \right] \right) \right) \right]^{-1}$ , relation (6.3)

forwards the block-vector  $p_x$  with columns of size  $q_{d-x}^{(0,1,\dots,x-1,d-1,d-2,\dots,d-x+1,d-x)}$ , which is next applied according to the form (6.1). By accepting the proposed approximation, we assume that form (6.1) represents the inverse of ND-Toeplitz matrix  $R \left( c \left( \left[ \gamma_0, \gamma_2, \dots, \gamma_{d-x-1}, \gamma_{d-1}^\infty, \gamma_{d-2}^\infty, \dots, \gamma_{d-x}^\infty \right] \right) \right)$ , with infinite dimension according to the dimension  $d - x$ , and - by construction- coincide with the original matrix in its finite part. From that, and by **Theorem 6.1**, the inverse can be written according to the form (6.2). By Advancing  $x$ , and by **Proposition 6.1**, relation (6.4) permits us to continue the extension on the next dimension. Hence our proof is completed.

### III Sequential Multidimensional Spectral Estimation Algorithm

**Theorem 6.2** presents an analytic representation of the spectral estimation and that is by taking advantage of both the **Theorem 6.1** and the proposed approximation. From numerical point of view, we need more finite simple Algorithm. On the contrary to the 1 dimensional case, in the general case, there is no known finite time representation for the proposed estimation. On the other hand even in the 1 dimensional case the numerical representation of the estimation is obtained always as

a Fourier series of the prediction polynomial i.e.  $C(jw) = \frac{\rho}{\left| \sum_{k=0}^{\gamma-1} p_k^\gamma e^{jwk} \right|^2}$

And  $w$  is taken to a large finite number of points on the spectral circle, that is in an effort to approximate the continuous field of values.

By examining relation (6.2), and replacing by (6.3) starting from  $x = d$ , and descending in the reverse order of **Theorem 6.2**, we find that the spectral inverse of correlation signal  $c \left( \left[ \gamma_{d-1}^\infty, \gamma_{d-2}^\infty, \dots, \gamma_0^\infty \right] \right)$  can be obtained by a finite series of block exponential sum, with a diminishing Block size at each step. According to the previous discussion, the algorithm takes the following form:

1. Calculate the inverse of the correlation matrix,

$$R_0^{-1} := \left[ R^{(0,1,\dots,d-1)}(l_0, l_1, \dots, l_{d-1}) \right]^{-1},$$

set  $x = 1$

set

$$G(k) := R_0^{-1} \left[ i_0 q_0^\Omega + i_1 q_1^\Omega + \dots + i_{d-2} q_{d-2}^\Omega + k q_{d-1}^\Omega \right] \left[ j_0 q_0^\Omega + j_1 q_1^\Omega + \dots + j_{d-2} q_{d-2}^\Omega + 0 q_{d-1}^\Omega \right]$$

2. Apply relation (1)  $M(w_{d-1}, \dots, w_{d-x}) = \sum_{k=0}^{\gamma_x-1} G(k)(w_{d-1}, \dots, w_{d-x+1}) e^{jk w_{d-x}}$

3. Set  $G'(w_{d-1}, \dots, w_{d-x}) = M(w_{d-1}, \dots, w_{d-x}) \left[ G(0) \right]^{-1} M^H(w_{d-1}, \dots, w_{d-x})$

4. if  $(x = d)$  {

```

    stop
  }
  else {
    set
      
$$G(k)(w_{d-1}, \dots, w_{d-x}) := G' \left[ i_0 q_0^\Omega + \dots + k q_{d-x-1}^\Omega \right] \left[ j_0 q_0^\Omega + \dots + 0 q_{d-x-1}^\Omega \right] (w_{d-1}, \dots, w_{d-x})$$

    set  $x = x + 1$ 
    go to 2
  }

```

#### IV Numerical calculation cost

In this part we will try to shed light on the numerical efficiency of the algorithm. For that, we will measure the number of operations needed to obtain the spectral estimation over an ND spectral grid with size  $C_w := [C_{w_{d-1}}, C_{w_{d-2}}, \dots, C_{w_0}]$ , where  $C_{w_i}$  is the number of points in the  $i$  dimension. In the following discussion we will omit the *Step 1* from our Calculus Cost. This is due to the fact that  $R_0^{-1}$ , and more precisely  $G(k), x = 1$ , could be obtained in different manners, like in [4], or [5], all irrelevant to the estimation method.

From the algorithm's *Step 2* and *Step 3* we can write the number of operations needed at each  $t := d - x + 1$  as

$$\left[ \frac{3}{2}(q_{t-1})^3 + (q_{t-1}q_t) \right] \prod_{f=0}^{d-t} C_{w_{d-f-1}},$$

The total sum is equal to the sum from  $t = d$ , and down until  $t = 1$ , which can be expressed as

$$T_A := \sum_{t=1}^d \left( \left[ \frac{3}{2}(q_{t-1})^3 + (q_{t-1}q_t) \right] \prod_{f=0}^{d-t} C_{w_{d-f-1}} \right)$$

Figure 6.1 graphs the above relation in function of  $C_{w_0} = C_{w_1} = \dots = C_{w_{d-1}}$ , with values taken as  $\gamma_0 = \gamma_1 \dots = \gamma_{d-1} = 10$ , and  $d = 5$ . Also for the same values Figure 6.2 represents the number of operations needed by Capon Estimation, which is equal to

$$T_C := (q_d)^2 \prod_{f=0}^{d-1} C_{w_f}.$$

We see clearly a very good advantage to using the proposed algorithm, from a calculus cost point of view.

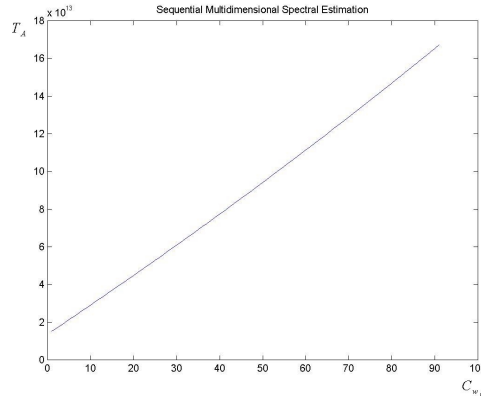


Figure 6.1

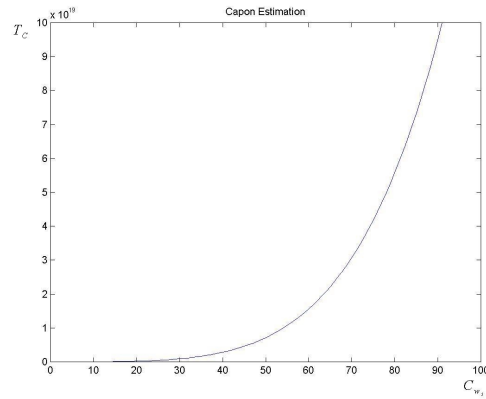


Figure 6.2

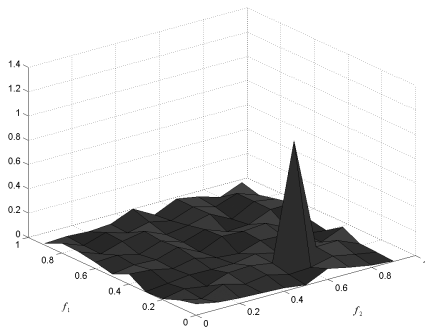
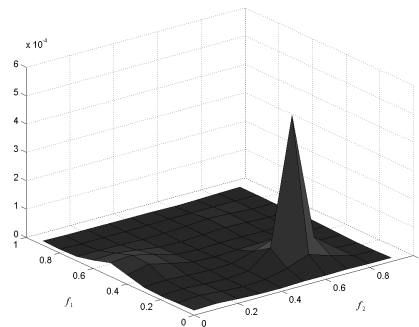
## V Numerical simulations and discussion

In an effort to evaluate the proposed estimation we will present a three-dimensional test signal  $c(f_0, f_1, f_2)$ , defined in its spectral composition as zero everywhere except for  $c(0.1, 0.3, 0.7) = 1$ ,  $c(0.1, 0.6, 0.2) = 1$ ,  $c(0.6, *, *) = 1$ . Next, the signal was plunged in a white noise of variance 0.1. In our simulation we took our estimation on a grid of equal size in all dimensions,  $C_{w_i} = 10$ , and the same for the correlation matrix order, having a uniform value of  $\gamma_i = 3$ . Figure 6.3-Figure 6.22 show a series cuts in the cube for the simulated signal, with the noised spectrum on the left and the calculated estimation on the right.

In Figure 6.23, the graph representing the correlation matching accuracy of the proposed estimation for a two dimensional signal was also presented. The value present in the graph is the relative difference between the original correlation values

$$r_{k,l}, \text{ and the estimated ones } \hat{r}_{k,l}, \text{ that is } \frac{|\hat{r}_{k,l} - r_{k,l}|}{r_{k,l}}.$$

From the presented Figures, and from other observed numerical simulations we found that the proposed algorithm provide a good estimation of the simulated signal, and contrary to the quarter-hyper plan filters proposed for the 2D case by [14][11], it enjoys a high degree of stability when the Correlation matrix order  $\gamma_i$  is increased.


 Figure 6.3 3D Test spectrum,  $f_0 = 0$ .

 Figure 6.4 3D spectral estimation,  $f_0 = 0$ .

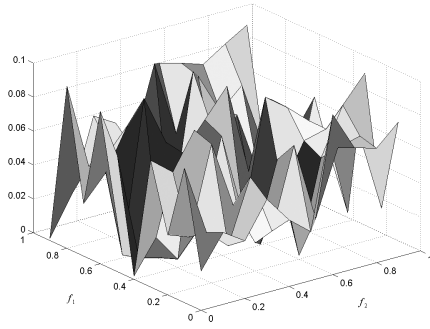


Figure 6.5 3D Test spectrum,  $f_0 = 0.1$  .

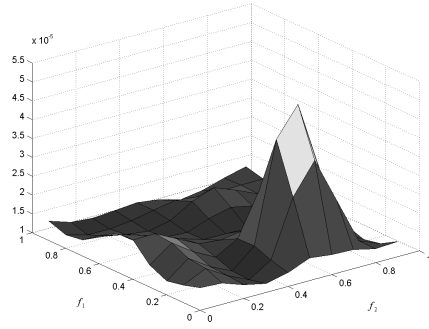


Figure 6.6 3D spectral estimation,  $f_0 = 0.1$  .

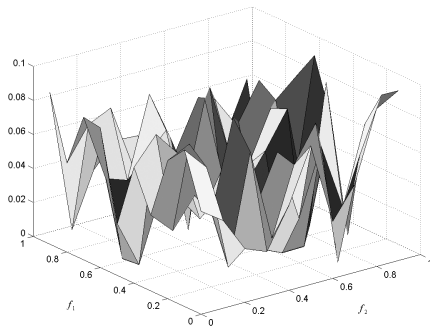


Figure 6.7 3D Test spectrum,  $f_0 = 0.2$  .

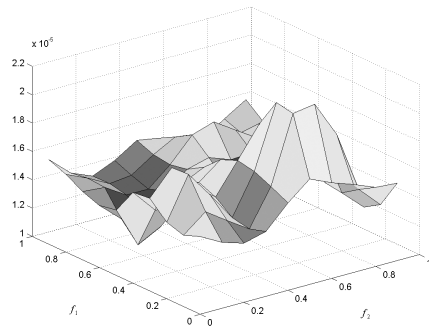


Figure 6.8 3D spectral estimation,  $f_0 = 0.2$  .

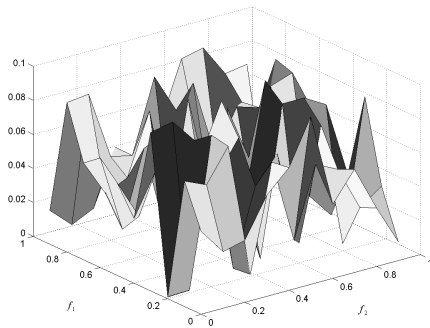


Figure 6.9 3D Test spectrum,  $f_0 = 0.3$  .

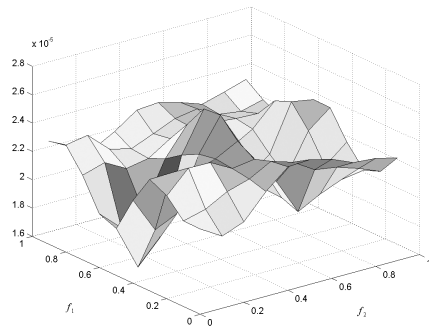


Figure 6.10 3D spectral estimation,  $f_0 = 0.3$  .

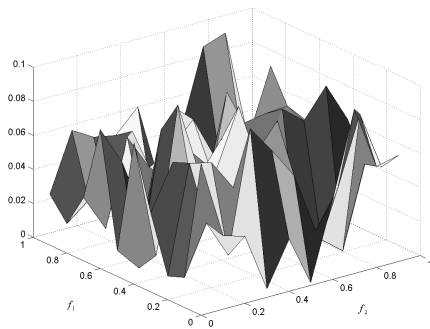


Figure 6.11 3D Test spectrum,  $f_0 = 0.4$  .

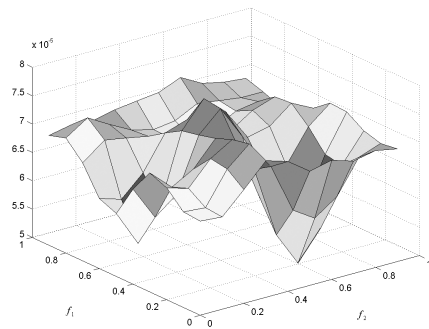


Figure 6.12 3D spectral estimation,  $f_0 = 0.4$  .

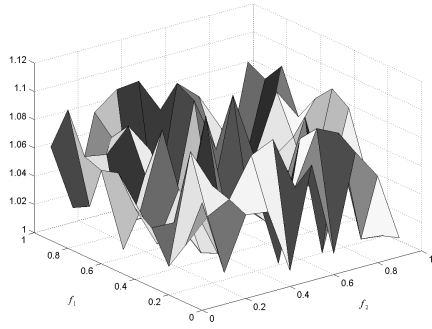


Figure 6.13 3D Test spectrum,  $f_0 = 0.5$ .

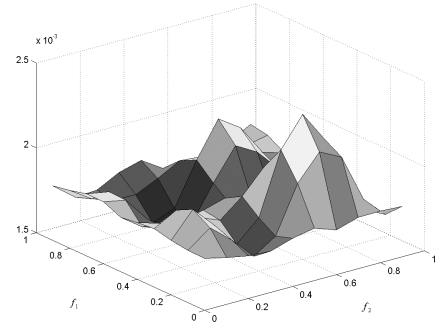


Figure 6.14 3D spectral estimation,  $f_0 = 0.5$ .

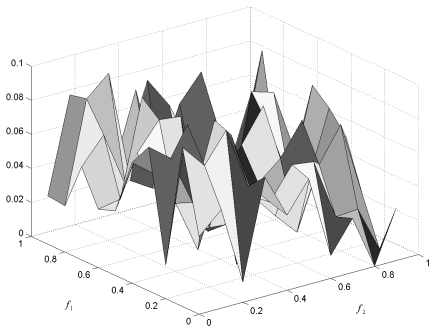


Figure 6.15 3D Test spectrum,  $f_0 = 0.6$ .

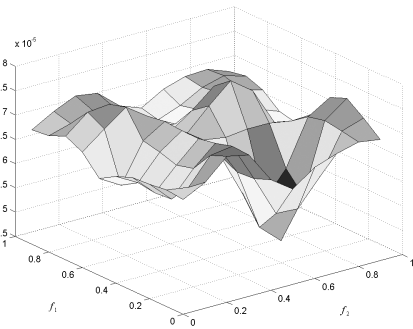


Figure 6.16 3D spectral estimation,  $f_0 = 0.6$ .

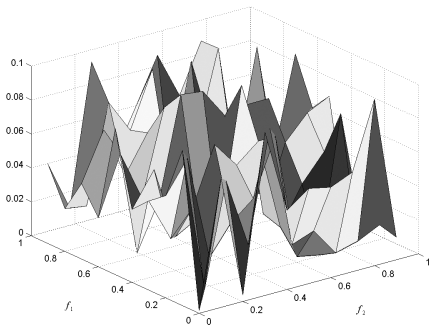


Figure 6.17 3D Test spectrum,  $f_0 = 0.7$ .

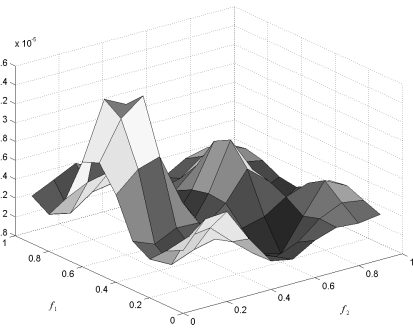


Figure 6.18 3D spectral estimation,  $f_0 = 0.7$ .

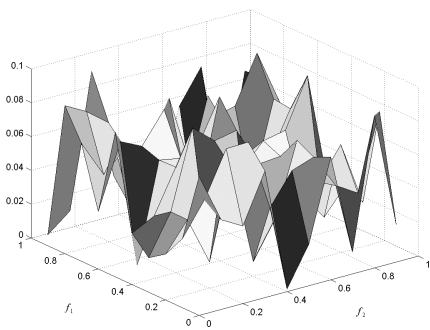


Figure 6.19 3D Test spectrum,  $f_0 = 0.8$ .

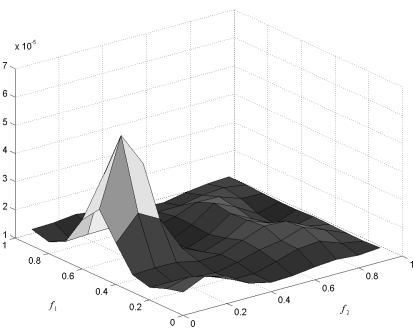


Figure 6.20 3D spectral estimation,  $f_0 = 0.8$ .



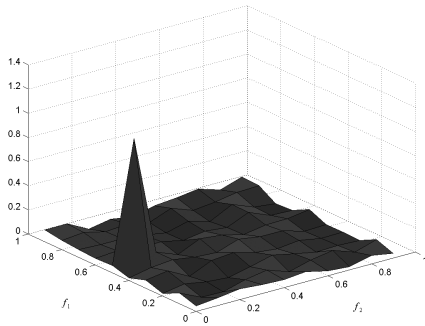


Figure 6.21 3D Test spectrum,  $f_0 = 0.9$ .

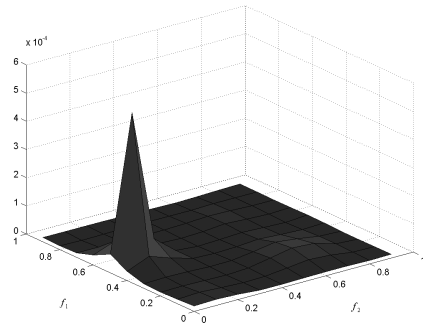


Figure 6.22 3D spectral estimation,  $f_0 = 0.9$ .

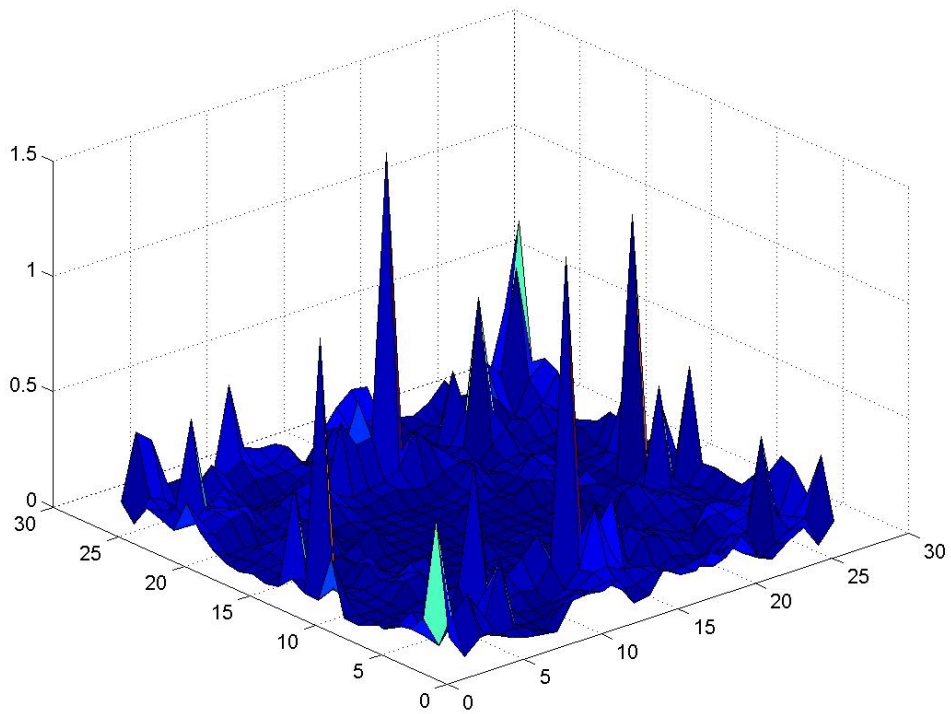


Figure 6.23 Correlation matching ratio.

---

## MULTIDIMENSIONAL CORRELATION EXTENSION USING GENERALIZED REFLECTION COEFFICIENTS WITH APPLICATION TO SPECTRAL POWER ESTIMATION

*Abstract*-We put forward an algorithm for Multidimensional Extension that generalizes the 1D case in the aspect of zero reflection coefficient replacement. The presented algorithm achieves the extension of any Hermitian, positive definite, ND-Toeplitz matrix, in a way realizing always a positive spectral measure. The Spectral Power Estimation application is invested. Numerical simulations, and comparison with Capon estimation confirm the 1D case situation, where the maximum of entropy extension realizes better SNR than minimum variance spectral power estimation.

*Résumé*- Nous présentons un algorithme d'extension multidimensionnelle généralisant le cas 1D dans l'aspect du remplacement des coefficients de réflexion par zéro. L'algorithme présenté réalise une extension de toute matrice hermitienne définie positive, ND-Toeplitz, en donnant toujours une mesure spectrale positive. L'application de l'estimation de la puissance spectrale est investie. Les simulations numériques et la comparaison avec l'estimation de Capon, confirment la situation d'un signal 1D où l'extension de maximum d'entropie réalise un rapport de SNR meilleur que celui de Capon.

### I Introduction

**P**ower Spectrum Estimation, as a mathematical problem unfolding from many physical systems, remains an unresolved problem in its multidimensional aspect. In the 1D case, the foundation of the theory were established by [25], [26], and later, a very series of important advances in the field were achieved, especially the connection to information theory [27], and the introduction of the spectral maximum of entropy principle in [6]. Also the connection to an optimized Toeplitz linear system solution was made in [22]. For the multidimensional case, and especially in the 2D case, different algorithms were put forward, as in [11] and [15]. As is shown in [33], the maximum of entropy spectral estimation is a special solution to the more general problem of correlation extension. In this chapter we will build upon this fact, to propose a stable, positive definite, multidimensional correlation extension, and eventually, a solution, to the multidimensional spectral estimation problem. While in [29] and [34], we did propose an approximate correlation extension solution(s), the solution that will be proposed here has a perfect correlation matching property. The solution provided is almost a maximum of entropy solution, in the sense of maximizing the resulting correlation matrix determinant. For the numerical simulations, we selected the Capon method [16] [30] as a basic comparative method. This selection is supported by two reasons. Firstly, the Capon method is well defined

in its multidimensional form. Secondly, there is a well-known mathematical relationship between the maximum of entropy spectral estimation and the Capon method. More precisely, the inverse of Capon spectral estimation of order  $\gamma$ , in the 1D case, is equal, to the sum of ME inverses for all orders from 1, up to  $\gamma$  [31][32]. In other words, the Capon method, in its 1D form has a reduced spectral resolution compared to the ME method.

This chapter is organized as follows. In section I, we present a brief introduction to the generalized reflection coefficient theory, and a new condition for the general positive definite matrix is put forward. In section II, we lay down the mathematical formulation for the multidimensional correlation matrices, and a new class of operators, for which they are invariants. In section III, we present a generalized extension theorem for any p.d. matrix, and present the minimum position reflection coefficients concept. In section IV, we present the sequential multidimensional extension algorithm. In Section V, we present the numerical simulations applied to the 2D case, and compared to the Capon method. Finally, in section VI, we try, numerically, to shed light on the temporal characteristics of the new produced linear prediction filters.

## II Generalized Reflection Coefficients, and Positiveness Condition for Hermitian Strongly Regular matrices

For any Hermitian, strongly regular matrix; the inverse can be factorized, into the form [18][34]

$$R^{-1} = (R^P)^* (D^P)^{-1} (R^P)^T, \quad (7.1)$$

where

$$D^P = (R^P)^T (R) (R^P)^* \quad (7.2)$$

is diagonal, and  $R^P$  is a lower triangular matrix, formed from Vectors  $\mathbf{p}_{k,l}$ ,  $k, l = 0, 1, \dots, n-1$ ,  $k \leq l$  according to

$$R^P = [\mathbf{p}_{0,n-1}, \mathbf{p}_{1,n-1}, \dots, \mathbf{p}_{n-1,n-1}]. \quad (7.3)$$

These vectors (or polynomials) are mutually orthogonal, relatively to the matrix defined cross product

$$\langle \mathbf{v}_1, \mathbf{v}_2 \rangle := \mathbf{v}_1^T R \mathbf{v}_2 \quad (7.4)$$

$$\forall 0 \leq k, 0 \leq k', k < l, k' < l, l \leq n-1$$

$$\langle \mathbf{p}_{k,l}, \mathbf{p}_{k',l} \rangle = 0 \text{ if } k \neq k'$$

$$\langle \mathbf{p}_{k,l}, \mathbf{p}_{k',l} \rangle > 0 \text{ if } k = k'$$

This also do apply for a second family of polynomials  $\mathbf{q}_{k,l}$ , which are orthogonal, according to

$$\forall 0 \leq k, k < l, k < l', l \leq n-1, l' \leq n-1$$

$$\langle \mathbf{q}_{k,l'}, \mathbf{q}_{k,l'} \rangle = 0 \text{ if } l \neq l' \quad (7.5)$$

$$\langle \mathbf{q}_{k,l'}, \mathbf{q}_{k,l'} \rangle > 0 \text{ if } l = l'$$

The two families,  $\mathbf{p}_{k,l}$ ,  $\mathbf{q}_{k,l}$ , are produced from  $R$ , in a recursive manner. The matrix  $R$ , being strongly regular, allows us to establish a recursive system in which the

famous reflection coefficients are used. The Generalized Reflection Coefficients define the relation between a group of vectors  $\mathbf{p}_{k,k+d}, \mathbf{q}_{k,k+d}$ , and the next step's group of vectors;  $\mathbf{p}_{k,k+d+1}, \mathbf{q}_{k,k+d+1}$ , according to

$$\mathbf{p}_{k,l} = \mathbf{p}_{k,l-1} - a_{k,l} \mathbf{q}_{k+1,l} \quad (7.6)$$

$$\mathbf{q}_{k,l} = \mathbf{q}_{k+1,l} - a'_{k,l} \mathbf{p}_{k,l-1},$$

And that is starting from the canonical basis vectors  $\mathbf{p}_{k,k} := \mathbf{e}_k, \mathbf{q}_{k,k} := \mathbf{e}_k$   $k = 0, 1, \dots, n-1$ .

The Generalized Reflection Coefficients are complex numbers, obtained at each step according to

$$a_{k,l} = \frac{\mathbf{p}_{k,l-1}^T R \mathbf{e}_l}{\mathbf{q}_{k+1,l}^T R \mathbf{e}_l}, \quad (7.7)$$

$$a'_{k,l} = \frac{\mathbf{q}_{k+1,l}^T R \mathbf{e}_k}{\mathbf{p}_{k,l-1}^T R \mathbf{e}_k}. \quad (7.8)$$

The definition of  $\mathbf{v}_{k,l} := \mathbf{q}_{k,l}^T R \mathbf{e}_l, \mathbf{v}'_{k,l} := \mathbf{p}_{k,l}^T R \mathbf{e}_k$  installs the following recursive system

$$\mathbf{v}_{k,l} = \mathbf{v}_{k+1,l} (1 - a_{k,l} a'_{k,l}), \quad (7.9)$$

$$\mathbf{v}'_{k,l} = \mathbf{v}'_{k,l-1} (1 - a_{k,l} a'_{k,l}). \quad (7.10)$$

This allows us to avoid applying the product in the denominator in (7.7) and (7.8) at each step, while for numerators; the following holds

$$\mathbf{p}_{k,l-1}^T R \mathbf{e}_l = \left( \mathbf{q}_{k+1,l}^T R \mathbf{e}_k \right)^*. \quad (7.11)$$

**Theorem 7.1.** For any group of reflection coefficients  $\{a_{k,l}, a'_{k,l}\}_{0 \leq k < l \leq n-1}$ ,

corresponding to a strongly regular Hermitian matrix  $R$ , each of the following is, a necessary, and a sufficient condition for  $R$  to be positive definite:

- i)  $0 \leq a_{0,l} \cdot a'_{0,l} < 1$  for  $0 < l \leq n-1$ ,
- ii)  $0 \leq a_{k,n-1} \cdot a'_{k,n-1} < 1$  for  $0 \leq k < n-1$ .

To prove **Theorem 7.1** we will need the next Lemma.

**Definition 7.1.** A Step matrix is any matrix of the form

$$\begin{bmatrix} h_0 & h_1 & h_2 & \cdots & h_{n-1} \\ h_1 & h_1 & h_2 & \ddots & h_{n-1} \\ h_2 & h_2 & h_2 & \ddots & h_{n-1} \\ \vdots & \ddots & \ddots & \ddots & h_{n-1} \\ h_{n-1} & h_{n-1} & h_{n-1} & h_{n-1} & h_{n-1} \end{bmatrix}.$$

**Lemma 7.1.** A necessary and a sufficient condition, for a step matrix  $H$ , to be positive is that  $h_0 \geq h_1 \geq h_2 \dots \geq h_{n-1} \geq 0$ .

**PROOF.** We start by considering, for any given vector  $C := [c_i]_{i=0..n-1}$ , the form  $u := C^H H C$ , which is equal to  $\sum_{i,j} c_i^* h_{ij} c_j$ . Since, for the Matrix H, we have the property of

$$h_{i,j} = \begin{cases} h_{i,i} & \text{if } i \geq j \\ h_{j,j} & \text{if } i < j \end{cases},$$

then, we can find that  $u = \sum_{i=0}^{n-1} h_{i,i} \left[ |c_{i,i}|^2 + \sum_{j=0}^{i-1} c_i^* c_j + \sum_{j=0}^{i-1} c_i c_j^* \right]$ .

By considering the definition  $u_i := |c_{i,i}|^2 + \sum_{j=0}^{i-1} c_i^* c_j + \sum_{j=0}^{i-1} c_i c_j^*$ , we observe that

$$|c_0 + c_1 \dots + c_{n-1}|^2 = u_0 + u_1 + \dots + u_{n-1} \geq 0.$$

By multiplying the previous relation, by  $h_{n-1}$ , we write

$(u_0 + u_1 + \dots + u_{n-2}) h_{n-1} + u_{n-1} h_{n-1} \geq 0$ . Since the term  $(u_0 + u_1 + \dots + u_{n-2})$ , is always positive, then  $(u_0 + u_1 + \dots + u_{n-2}) h_{n-2} + u_{n-1} h_{n-1} \geq 0$ , is always true if  $h_{n-2} \geq h_{n-1} \geq 0$ .

By repeating the same judgment we prove the sufficiency part.

To prove the necessity of the condition, we will consider, a positive matrix H, for which there is a value  $h_i < 0$ , then for the vector, of the form

$$C^T = [0 \quad \dots \quad 0 \quad c_i \quad 0 \quad \dots \quad 0], \text{ we have } C^T H C = h_i |c_i|^2 < 0, \text{ and by}$$

contradiction; the necessity of the condition  $h_i \geq 0$ , is realized. For the

necessity of the condition  $h_i \geq h_{i+1}$ , we will consider, the case of a positive matrix H, where  $u = u_0 h_0 + u_1 h_1 + \dots + u_i h_i + u_{i+1} h_{i+1} + \dots$ , and

$h_0 \geq h_1 \geq \dots \geq h_{i-1} \geq h_i < h_{i+1}$ , then for the given vector

$$C^T = [0 \quad \dots \quad 0 \quad -1 \quad c_{i+1} \quad 0 \quad \dots \quad 0], \forall h_i < h_{i+1} \geq 0, \exists c_{i+1} \in \mathbb{R}, \text{ so that}$$

$u = h_i + h_{i+1} (|c_{i+1}|^2 - 2c_{i+1}) < 0$ , more precisely, the “discriminant” of the equation

$$c_{i+1}^2 - 2c_{i+1} + \frac{h_i}{h_{i+1}} = 0 \text{ is positive only in the case when } h_i < h_{i+1}.$$

**PROOF OF Theorem 7.1.** By taking the family of polynomial;  $\{p_{0,l}\}_{l=0..n-1}$ , into a matrix  $\vec{P}$ , defined as  $\vec{P} := [p_{0,0} \quad p_{0,1} \quad \dots \quad p_{0,n-2} \quad p_{0,n-1}]$ , we observe that the multiplication  $\vec{P}^T R \vec{P}^*$ ; is a step matrix, equal to

$$\vec{P}^T R \vec{P}^* = \begin{bmatrix} v'_{0,0} & v'_{0,1} & \dots & v'_{0,n-1} \\ v'_{0,1} & v'_{0,1} & \dots & v'_{0,n-1} \\ \vdots & \vdots & \ddots & v'_{0,n-1} \\ v'_{0,n-1} & v'_{0,n-1} & v'_{0,n-1} & v'_{0,n-1} \end{bmatrix},$$

from which, a necessary, and, a sufficient condition, for the strongly regular matrix R to be positive definite, is the realization of the condition

$$v'_{0,0} \geq v'_{0,1} \geq \dots \geq v'_{0,n-1} > 0.$$

By relation (7.10) the previous condition is equivalent to (i). The proof of (ii) can be forwarded, by the same manner.

### III Multidimensional Toeplitz Matrices

For a multidimensional signal,  $x(t) \in \mathbb{C}$ ,  $t \in \mathbb{Z}^d$ , we will define the  $\gamma$  order correlation matrix as  $R := E \left( X(t) (X(t))^H \right)$ , with  $\gamma \in (\mathbb{Z}^+)^d$ , and  $X(t)$  defined as

$$X(t) := \begin{bmatrix} x(t_0, t_1, \dots, t_{d-1}) \\ x(t_0+1, t_1, \dots, t_{d-1}) \\ \vdots \\ x(t_0+\gamma_0-1, t_1, \dots, t_{d-1}) \\ x(t_0, t_1+1, \dots, t_{d-1}) \\ \vdots \\ x(t_0, t_1+\gamma_1-1, \dots, t_{d-1}) \\ \vdots \\ x(t_0, t_1, \dots, t_{d-1}+\gamma_{d-1}-1) \end{bmatrix}.$$

In the case where the correlation matrix admits a toeplitz nature in all dimensions- in other words, it is  $d$  time toeplitz- then it is adequate to represent it, as an operator of a  $d$  dimension(s) correlation signal  $c(t)$ , so that

$$c(t) \in \mathbb{C}, t \in [-\gamma, \gamma], \gamma \in (\mathbb{Z}^+)^d,$$

$$c(t) := \sum_{n \in \mathbb{Z}^d} x(n+t) x^*(n),$$

and we will write

$$R := R(c(\gamma)), \text{ which is a matrix of size } q = \prod_{i=0}^{d-1} \gamma_i.$$

It is also well known, and according to [16]'s relation, that

$$c(t) = \frac{1}{(2\pi)^d} \oint_{|\mathbb{C}^d|=1} \left| \sum_{n \in \mathbb{Z}^d} x[n] e^{jw \cdot (n^T)} \right|^2 e^{-jw \cdot (t^T)} .dw.$$

By considering  $\Omega$ ; a redistribution of the dimensions nesting

$$\Omega \in \left\{ (\Omega_0, \Omega_1, \dots, \Omega_{d-1}) : k \neq l \Rightarrow \Omega_k \neq \Omega_l, \forall \Omega_l \in \mathbb{N}, 0 \leq \Omega_l \leq d-1 \right\},$$

we can define

$$q_l^\Omega := \begin{cases} \prod_{i=0}^{l-1} \gamma_{\Omega_i} & \text{if } l \neq 0 \\ 1 & \text{if } l = 0 \end{cases}.$$

Of course,  $\Omega$ , is invertible, in the sense that  $\Omega_k = l \Rightarrow \Omega^{-1}(l) = k$ .

**Definition 7.2.** We will define the walking operator as

$$W_{\Omega \rightarrow \Omega'}(M) : [M]_{i,j} \rightarrow [M]_{X^{\Omega \rightarrow \Omega'}(i), X^{\Omega \rightarrow \Omega'}(j)},$$

$$X^{\Omega \rightarrow \Omega'}(i_0 q_0^\Omega + i_1 q_1^\Omega + \dots + i_{d-1} q_{d-1}^\Omega) = i_0 q_{\Omega^{-1}(\Omega_1(0))}^{\Omega'} + i_1 q_{\Omega^{-1}(\Omega_1(1))}^{\Omega'} + \dots + i_{d-1} q_{\Omega^{-1}(\Omega_1(d-1))}^{\Omega'},$$

where  $[i_0, i_1, \dots, i_{d-1}] \in (\mathbb{Z}^*)^d$ ,  $0 \leq i_k \leq \gamma_{\Omega(k)}$ .

From a basic point of view, the walking operator does correspond to the convention used in the relation defining the vector  $X(t)$ . As we will see later, it also represents a very important constraint, over the degree of liberty concerning the Correlation matrix, and eventually, its inverse.

**Definition 7.3.** We call a  $t$ -block matrix,  $t \in (\mathbb{Z}^+)^d$ , any matrix of size  $\prod_{i=0}^{d-1} t_i$ .

A  $d$ -block matrix  $M$  can be indexed by the virtue of some dimensions nesting  $\Omega$ , according to

$$M \left[ i_0 q_0^\Omega + i_1 q_1^\Omega + \dots + i_{d-1} q_{d-1}^\Omega \right] \left[ j_0 q_0^\Omega + j_1 q_1^\Omega + \dots + j_{d-1} q_{d-1}^\Omega \right], \quad 0 \leq i_l \leq \gamma_{\Omega(l)}, 0 \leq j_l \leq \gamma_{\Omega(l)}.$$

**Definition 7.4.** A matrix admits a  $(\gamma, u, \Omega)$ -toeplitz character, when it is  $\gamma$ -block matrix and do realize

$$M \left[ i_0 q_0^\Omega + i_1 q_1^\Omega + \dots + i_{d-1} q_{d-1}^\Omega \right] \left[ j_0 q_0^\Omega + j_1 q_1^\Omega + \dots + j_{d-1} q_{d-1}^\Omega \right] =$$

$$M \left[ i_0 q_0^\Omega + i_1 q_1^\Omega + (i_u - j_u) q_u^\Omega \dots + i_{d-1} q_{d-1}^\Omega \right] \left[ j_0 q_0^\Omega + j_1 q_1^\Omega + 0 \cdot q_u^\Omega + \dots + j_{d-1} q_{d-1}^\Omega \right] \quad \text{if } i_u - j_u \geq 0$$

$$M \left[ i_0 q_0^\Omega + i_1 q_1^\Omega + (0) q_u^\Omega \dots + i_{d-1} q_{d-1}^\Omega \right] \left[ j_0 q_0^\Omega + j_1 q_1^\Omega + (j_u - i_u) q_u^\Omega + \dots + j_{d-1} q_{d-1}^\Omega \right] \quad \text{if } i_u - j_u < 0$$

, we will call the indices

$$\left[ i_0 q_0^\Omega + i_1 q_1^\Omega + (i_u - j_u) q_u^\Omega \dots + i_{d-1} q_{d-1}^\Omega \right] \left[ j_0 q_0^\Omega + j_1 q_1^\Omega + 0 \cdot q_u^\Omega + \dots + j_{d-1} q_{d-1}^\Omega \right],$$

$$\left[ i_0 q_0^\Omega + i_1 q_1^\Omega + (0) q_u^\Omega \dots + i_{d-1} q_{d-1}^\Omega \right] \left[ j_0 q_0^\Omega + j_1 q_1^\Omega + (j_u - i_u) q_u^\Omega + \dots + j_{d-1} q_{d-1}^\Omega \right] \quad \text{as minimum position.}$$

**Definition 7.5.** In the case that a  $\gamma$ -block matrix contains more than one toeplitz character, such that, it is  $(\gamma, u_0, \Omega), (\gamma, u_1, \Omega) \dots (\gamma, u_{s-1}, \Omega)$  toeplitz character, we will call it; an  $(\gamma, u, \Omega)$ -s-toeplitz character matrix, with  $u$  equal in that case to  $[u_0, u_1, \dots, u_{s-1}]$ .

According to **Definition 7.4**, we can index the matrix elements, using the notation

$$M \left[ i_0 q_0^\Omega + \dots + i_{u-1} q_{u-1}^\Omega \right] \left[ j_0 q_0^\Omega + \dots + j_{u-1} q_{u-1}^\Omega \right] (k_u) \left[ i_{u+1} q_{u+1}^\Omega + \dots + i_{d-1} q_{d-1}^\Omega \right] \left[ j_{u+1} q_{u+1}^\Omega + \dots + j_{d-1} q_{d-1}^\Omega \right]$$

To simplify the notations, we will write it as

$$M^\Omega \left[ b_0^{u-1} \right] (d_u^{u+s}) \left[ b_{u+s+1}^{d-1} \right] \quad b_h^{h+y-1} \in (\mathbb{Z}^*)^{2y}, d_h^{h+y-1} \in \mathbb{Z}^y,$$

where, for  $s > 0$ ; the matrix is  $s$ -toeplitz characters.

**Proposition 7.1.**  $\forall \Omega'$ , any  $(\gamma, u, \Omega)$  toeplitz character matrix, can be transformed into  $(\gamma, u', \Omega')$  toeplitz character using the walking transformation  $W_{\Omega \rightarrow \Omega'}(M)$ , and we have  $u' = \Omega'^{-1}(\Omega_u)$ .

#### IV Multidimensional Correlation Matrix Extension

Before going into the details of the new proposed algorithm, which as we will see is designated for fully toeplitz matrices, the next theorem also provides a robust extension for any symmetric, positive definite matrix.

**Theorem 7.2.** For any p.d Hermitian matrix, it exist an infinite extension.

**PROOF.** Let us consider a symmetric p.d matrix  $R := [r_{i,j}]_{i,j=0,\dots,n-1}$ . According to the generalized reflection coefficients theory, for each of the submatrices  $R_{k,n-1} := [r_{k+i,k+j}]_{i,j=0,\dots,n-1-k}$ ,  $0 \leq k \leq n-1$ , there is always, a value  $r_{k,l+1}$ ; solution to each of the equation  $a_{k,n} = \langle p_{k,n-1}^T, e_n \rangle_R = 0$ , in the case of  $0 \leq k < n-1$ . And for the  $2 \times 2$  sub-matrix, which is the extension starting point, we can always define values  $r_{n-1,n}, r_{n,n}$  so that

$$\begin{bmatrix} r_{n-1,n-1} & r_{n-1,n} \\ (r_{n-1,n})^* & r_{n,n} \end{bmatrix}$$
 is positive definite. A good choice, according to **Theorem 7.1**,

would be to set  $r_{n-1,n} = r_{n,n} \leq r_{n-1,n-1} \geq 0$ . The new generated matrix

$R_{0,n} := [r_{i,j}]_{i,j=0,\dots,n}$ , is, by construction, a positive, full rank, matrix. By repeating the procedure, on each new generated matrix, we prove the existence of infinite extensibility.

The previous theorem can be of good use in an extension effort where we need to process correlation matrices not having any special structure. On the other hand, for many practical systems, the extension needs to take into consideration the preservation of the toeplitz structure.

In the 1D case, for any positive definite toeplitz matrix  $M^N(l)$ ,  $l := -N+1, \dots, N-1$ , we define the polynomials  $p^{N-1}, q^{N-1}$ , as the solution, for the linear system  $M^N(l)p^{N-1} = e_0$ ,  $M^N(l)q^{N-1} = e_{N-1}$ . These solutions, in fact, can be obtained recursively according to

$$p'^N = \begin{bmatrix} p'^{N-1} \\ 0 \end{bmatrix} + \sigma_N \begin{bmatrix} 0 \\ q'^{N-1} \end{bmatrix}.$$

Where  $p'^N$ , and  $q'^N$ , are  $p^N$ , and  $q^N$ , normalized by there first, and last element, respectively.  $\sigma$  is the famous reflection coefficient. Putting the reflection coefficient to zero is equivalent to the existence of a positive definite matrix  $M^{N+1}(l)$ , which





minimum position so that it can be obtained from the minimum reflection coefficients group.

According to the previous proposition it is even possible to explicitly formulate non-minimum reflection coefficients, as a function of minimum reflection coefficients. For example in the case of 2D  $([2,2],[1,2],[1,2])$ -2 toeplitz character matrix, and for the corresponding upper triangular reflection coefficients matrix

$$\begin{bmatrix} a_{0,1} & a_{0,2} & a_{0,3} \\ & a_{1,2} & a_{1,3} \\ & & a_{2,3} \end{bmatrix}, \text{ we have } a_{0,1}, a_{0,2}, a_{0,3}, a_{1,2} \text{ representing the minimum reflection}$$

group, while the dependent values  $a_{2,3}, a_{1,3}$ , are subject to the relations

$$a_{2,3} = a_{0,1},$$

$$a_{1,3} = \frac{|a_{1,2}|^2 a_{0,2}}{-|a_{1,2}|^2 a_{0,2} + |a_{0,1}|^2 a_{0,2} + |a_{0,1}|^2}.$$

Figure 7.1 shows minimum position localization, for a  $([3,3,3],[1,2,3],[1,2,3])$ -3-toeplitz character matrix.

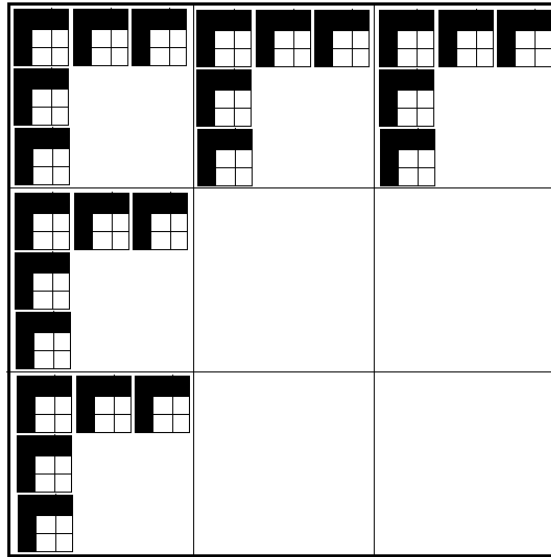


Figure 7.1

To be able to achieve adequate multidimensional correlation extension we will proceed by setting to zero all minimum position reflection coefficients, corresponding to the extended outer blocks. In the case of a simple one-dimensional toeplitz matrix case, this does collapse to the standard 1D ME extension. Next, in a sequential manner, and for each dimension, we will use a walking operator to switch dimensional nesting and to continue the extension in other directions. To better explain this let us consider the example of the  $([2,2],[1,2],[1,2])$ -2-toeplitz character matrix. We will engage the extension toward  $([k_1, k_2],[1,2],[1,2])$ -2-toeplitz character matrix. The steps are as the following:

- a) Proceed in the extension from  $([2, 2], [1, 2], [1, 2]) - 2$  toward  $([2, k_2], [1, 2], [1, 2]) - 2$ .
- b) By applying a walking operator we can inverse dimensions order and transform the matrix into  $([k_2, 2], [1, 2], [2, 1]) - 2$ .
- c) Restart the same operation as (a) to obtain an extension form  $([k_2, 2], [1, 2], [2, 1]) - 2$ , to  $([k_2, k_1], [1, 2], [2, 1]) - 2$  matrix. Again, a walking operator, can rearrange the  $([k_2, k_1], [1, 2], [2, 1]) - 2$ , into a  $([k_1, k_2], [1, 2], [1, 2]) - 2$  matrix.

In the next section; a more detailed implementation of the proposed algorithm is exposed.

## V Sequential Multidimensional Correlation Extension Algorithm

The generalized reflection coefficients algorithm can be applied directly, onto the correlation matrix, and by taking **Proposition 7.2** into consideration, we have a totally feasible extension algorithm. On the other hand, we need to optimize calculations cost, and memory usage. This can be achieved by applying the algorithm put forward in [23], or [28], which take into consideration the ND Toeplitz structure of the correlation matrix. The advantage of using the algorithm in [28], is that it takes into consideration, the skew symmetry in the reflection coefficients, and the calculated polynomials. The skew symmetry property; is a characteristic of toeplitz-block-toeplitz matrices, and does hold in the ND-Toeplitz case also.

To be able to apply the Algorithm in [28]; we will consider the input  $([\gamma_0, \dots, \gamma_{s-1}], u, \Omega) - s$ -toeplitz matrix, as a toeplitz-block-toeplitz matrix, with the toeplitz blocks being of size  $q_{s-1}^\Omega \times q_{s-1}^\Omega$ , and the blocks matrix of block-size  $\gamma_{s-1} \times \gamma_{s-1}$ . For that, and according to [28] terminology, we will set  $n_1 := q_{s-1}^\Omega$ , and  $n_2 := \gamma_{s-1}$ .

◆ *SMCE*

### Input

An  $R := ([\gamma_0, \gamma_1, \dots, \gamma_{s-1}], [0, 1, \dots, s-1], [0, 1, \dots, s-1]) - s$ -toeplitz character matrix. The vector  $\gamma' := [\gamma'_0, \gamma'_1, \dots, \gamma'_{s-1}]$ , representing the new generated extents of the matrix,  $\gamma'_i \geq \gamma_i$ .

### Start

for  $\text{dim} = s-1$  to 0 {  
 set  $R_{\text{dim}} = R$   
 set  $\Omega_1 = [0, 1, \dots, \text{dim}, \text{dim}+1, \dots, s-1]$   
 set  $\Omega_2 = [0, 1, \dots, \text{dim}-1, s-1, \text{dim}+1, \dots, \text{dim}]$   
 set  $R = W^{\Omega_1 \rightarrow \Omega_2} (R)$

set  $n_1 := q_{s-1}^{\Omega_2}$   
 set  $n'_2 := \gamma'_{s-1}$ ,  $n_2 := \gamma_{s-1}$   
 apply Subroutine 2 to extend  $R$  from a  
 $([\gamma_0, \gamma_1, \dots, \gamma_{\dim}, \gamma'_{\dim+1}, \dots, \gamma'_{s-1}], [0, 1, \dots, s-1], \Omega_2)$  -  $s$ -toeplitz character matrix into a  
 $([\gamma_0, \gamma_1, \dots, \gamma'_{\dim}, \gamma'_{\dim+1}, \dots, \gamma'_{s-1}], [0, 1, \dots, s-1], \Omega_2)$  -  $s$ -toeplitz character matrix.  
 Set  $R = W^{\Omega_2 \rightarrow \Omega_1}(R)$   
 }

### Subroutine 1

$$\begin{aligned}
 a_{k,l} &= \frac{\hat{\mathbf{p}}^T R \mathbf{e}_l}{\hat{\mathbf{v}}} & a'_{k,l} &= \frac{\hat{\mathbf{q}}^T R \mathbf{e}_k}{\hat{\mathbf{v}}'} \\
 \mathbf{p}_{k,l} &= \hat{\mathbf{p}} - a_{k,l} \hat{\mathbf{q}} & \mathbf{q}_{k,l} &= \hat{\mathbf{q}} - a'_{k,l} \hat{\mathbf{p}} \\
 \mathbf{v}_{k,l} &= \hat{\mathbf{v}}(1 - a_{k,l} a'_{k,l}) & \mathbf{v}'_{k,l} &= \hat{\mathbf{v}}'(1 - a_{k,l} a'_{k,l})
 \end{aligned}$$

### Subroutine 2

*Initialization:*

For  $k = 0$  to  $n_1 - 1$ : {

$$\mathbf{p}_{k,k} = \mathbf{q}_{k,k} = \mathbf{e}_k, \mathbf{v}_{k,k} = \mathbf{v}'_{k,k} = r_{0,0}$$

}

*Main Subroutine*

For  $d_2 = 0$  to  $n'_2 - 1$  do :

{

If  $d_2$  not equal to zero:

{

For  $d_1 = n_1 - 1$  to 0 do : (Lower triangle loop)

{

For  $u = 0$  to  $n_1 - d_1 - 1$  do :

{

$$k = u + d_1 \quad l = d_2 n_1 + u$$

if  $(k, l)$  is in minimum position and  $d_2 \geq n_2$  {

$$\text{set } a_{k,l} = a'_{k,l} = 0$$

calculate  $r_{k,l}$ , and fill in  $R$  accordingly .

}

$$k' = k \text{ sec } n_1 + n_1 - 1 - l \text{ mod } n_1$$

if  $k \leq k'$  {

$$(k^0, l^-) = (k, l - 1)$$

if  $u$  equal to 0: {

$$(k^{0'}, l^{-'}) = (k^0 \otimes l^-)$$

```

         $\hat{p} = U^{n_1-1} \left( \tilde{q}_{k^0, l^-} \right)^*, \hat{v}' = v_{k^0, l^-}$ 
    }
    else {
         $\hat{p} = p_{k^0, l^-}, \hat{v}' = v'_{k^0, l^-}$ 
    }
    if  $k$  equal to  $k'$  : {
         $\hat{q} = U \left( \tilde{p} \right)^*, \hat{v} = \hat{v}'$ 
    }
    else {
         $(k^+, l^0) = (k + 1, l)$ 
         $\hat{q} = q_{k^+, l^0}, \hat{v} = v_{k^+, l^0}$ 
    }
    Apply Subroutine 1
    }
}
}
}
For  $d_1 = 1$  to  $n_1 - 1$  do : (Exclusively Upper triangle loop)
{
    For  $u = 0$  to  $n_1 - d_1 - 1$  do :
    {
         $k = u \quad l = d_2 n_1 + u + d_1$ 
        if  $(k, l)$  is in minimum position and  $d_2 \geq n_2$  {
            set  $a_{k, l} = a'_{k, l} = 0$ 
            calculate  $r_{k, l}$  and fill in  $R$  accordingly
        }
         $k' = k \text{ sec } n_1 + n_1 - 1 - l \text{ mod } n_1$ 
        if  $k \leq k'$  {
             $(k^0, l^-) = (k, l - 1)$ 
             $\hat{p} = p_{k^0, l^-}, \hat{v}' = v'_{k^0, l^-}$ 
            if  $k$  equal to  $k'$  : {
                 $\hat{q} = U \left( \tilde{p} \right)^*, \hat{v} = \hat{v}'$ 
            }
            else {
                 $(k^+, l^0) = (k + 1, l)$ 
                 $\hat{q} = q_{k^+, l^0}, \hat{v} = v_{k^+, l^0}$ 
            }
        }
        Apply Subroutine 1
    }
}
}

```

}  
}

## VI Numerical simulations and application to Spectral Power Estimation

Spectral Power Estimation is the main application domain for correlation extension methods. The new proposed Algorithm proceeds in the same way as the ME method, in the aspect of zero reflection coefficient filling. Therefore it should be expected that it would realize good quality in estimation precision. In the 1D case, compared to minimum variance technique the maximum of entropy method is more accurate in Spectral Estimation. For that, we will consider the Capon method, as the comparison method in evaluating the performance of the newly presented method.

The application of the SMCE to Spectral Estimation follows these steps:

- a) For a multidimensional signal of size  $[T_0, T_1, \dots, T_{s-1}]$ , we calculate the correlation matrix  $([\gamma_0, \gamma_1, \dots, \gamma_{s-1}], [0, 1, \dots, s-1], [0, 1, \dots, s-1]) - s$ , with  $\gamma_i \ll T_i$ .
- b) Next, we apply SMCE algorithm to obtain a  $([\gamma'_0, \gamma'_1, \dots, \gamma'_{s-1}], [0, 1, \dots, s-1], [0, 1, \dots, s-1]) - s$  - toeplitz character matrix  $R = R(c(\gamma))$  with  $\gamma'_i \gg \gamma_i$ ,  
 $c(t) \in \mathbb{C}, t := [t_0, t_1, \dots, t_{s-1}], t_i \in [-\gamma_i, \dots, \gamma_i]$ .
- c) The SMCE spectral power Estimation is defined as the Fourier series of the new generated correlation signal

$$|\hat{X}(j\omega)|_{\text{SMCE}}^2 := \sum_{t \in \{(t_0, t_1, \dots, t_{s-1}) : -\gamma_i \leq t_i \leq \gamma_i\}} c(t) e^{-j\omega^T t}, \omega \in 2\pi \times [0, 1]^s.$$

To realize the numerical simulations, we followed a uniform framework. That is, for multiple types of signals, and different parameters, we will follow these steps:

- a) For a spectral image, of size  $T_i \times T_i$ , we added noise, in an amount corresponding to a given SNR value  $SNR_i$ .
- b) Next, using *IFFT*, we obtain the time representation, from which Spectral Power Estimation, on a grid of size  $T_i \times T_i$ , is calculated. And that is starting from a correlation signal of size (support)

$$[-\gamma_i, \gamma_i]^2, \text{ with } \gamma_i < \frac{T_i}{2}.$$

Accordingly, our framework is dependant on the variables;  $i$  the sample image,  $T_i$  its size,  $SNR_i$  the spectral noise, and  $\gamma_i$ , the correlation order in use.

For our simulations, and in a statistical validation effort, we applied the algorithm on 4 different images, each resized down to sizes;  $15 \times 15$ , and  $21 \times 21$ . The images are displayed in Appendix 7.1. For all eight images,  $SNR_i$  was varied according to the values, -5, 0, 5 db. Also,  $\gamma_i$ , was varied to take the values, 2, 3, and 4. Finally, for each combination of  $(i, T_i, SNR_i, \gamma_i)$ , the test was repeated 3 times. At each run, SMCE Estimation, and Capon Estimation were compared to the noise-free original spectral image, and an Estimation SNR value was calculated. Figure 7.2 shows the mean resulting Estimation SNR, for the different  $SNR_i$  values. SMCE Estimation, and

Capon Estimation, are displayed in solid line, and in dashed line, respectively. The results confirm the enhancement provided by the new proposed method over Capon Estimation. This enhancement, is due to the fact that the new method has a great degree of frequency precision in localizing spectral peaks.

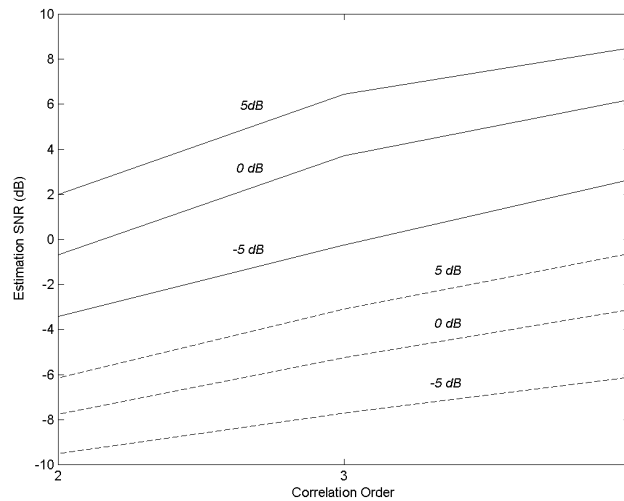


Figure 7.2

We show, in Figure 7.3, Figure 7.4, Figure 7.5 and Figure 7.6, Original, and corresponding Noised, SMCE Estimated, and Capon Estimated Spectral Power, respectively. The parameters used are  $\gamma_i = 4$ , and  $SNR_i = 5 \text{ dB}$ . The extension was not limited to input signal size –equal to  $21 \times 21$ , but instead, continued until  $\gamma'_i = 20$ . We observe that SMCE method has a spectral energy concentration precision more accurate than the Capon method. Also, for the same example, Figure 7.7 shows the absolute value of the new extended correlation signal.

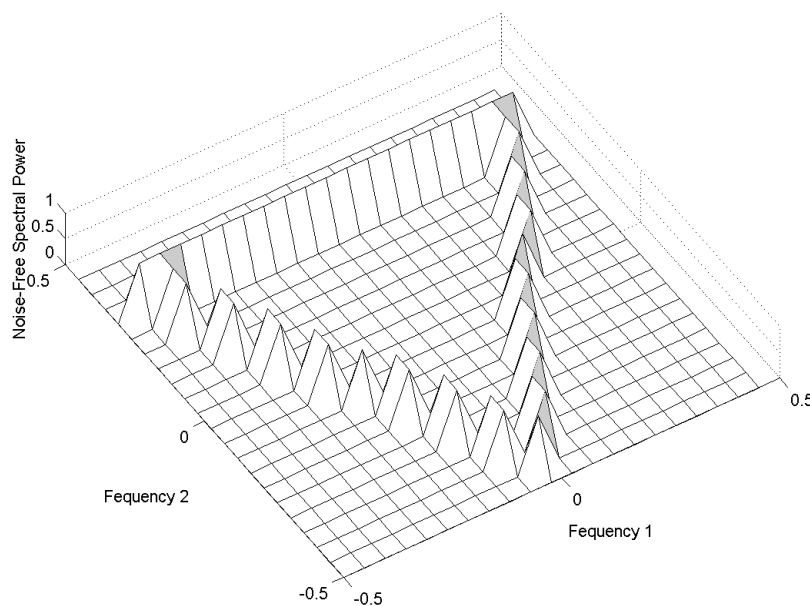


Figure 7.3

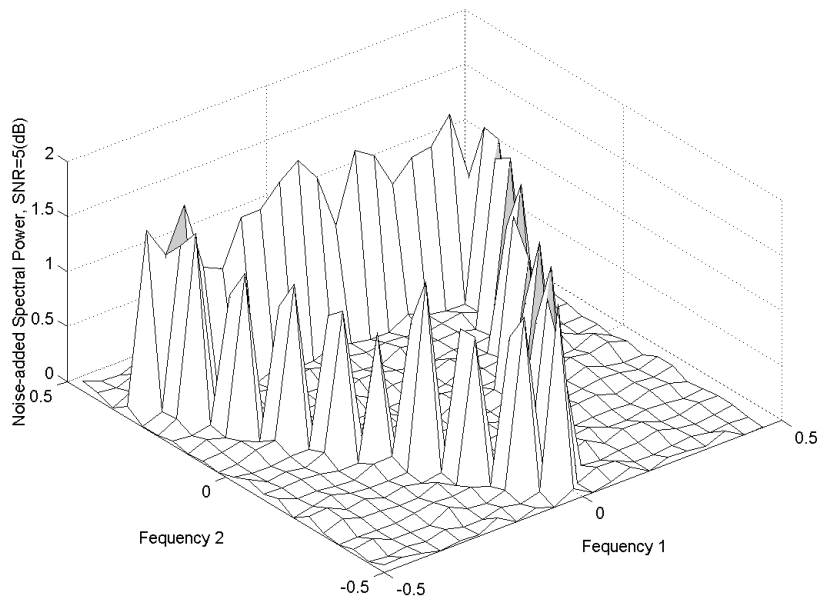


Figure 7.4

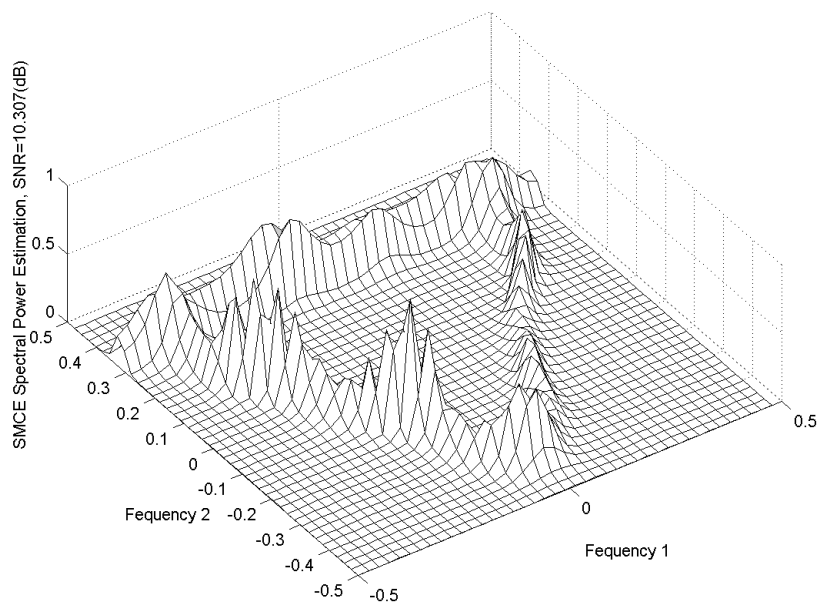


Figure 7.5



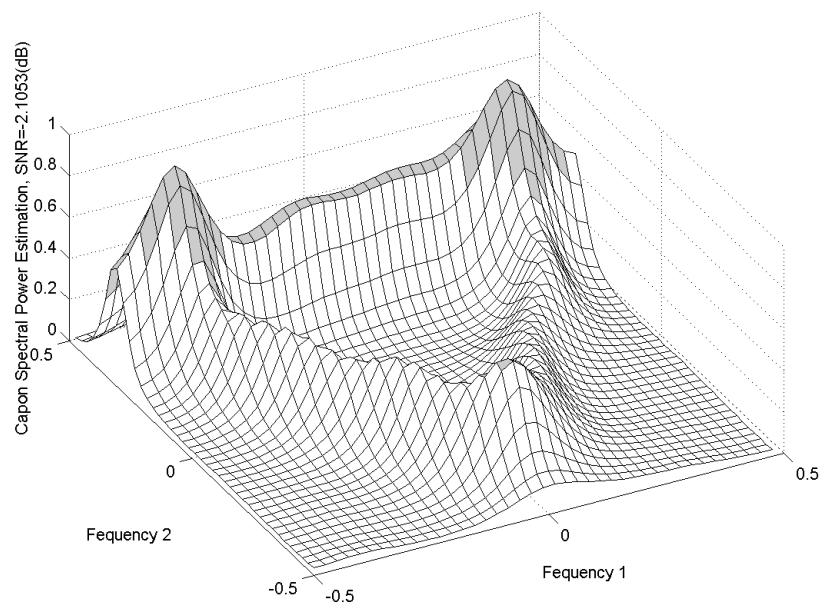


Figure 7.6

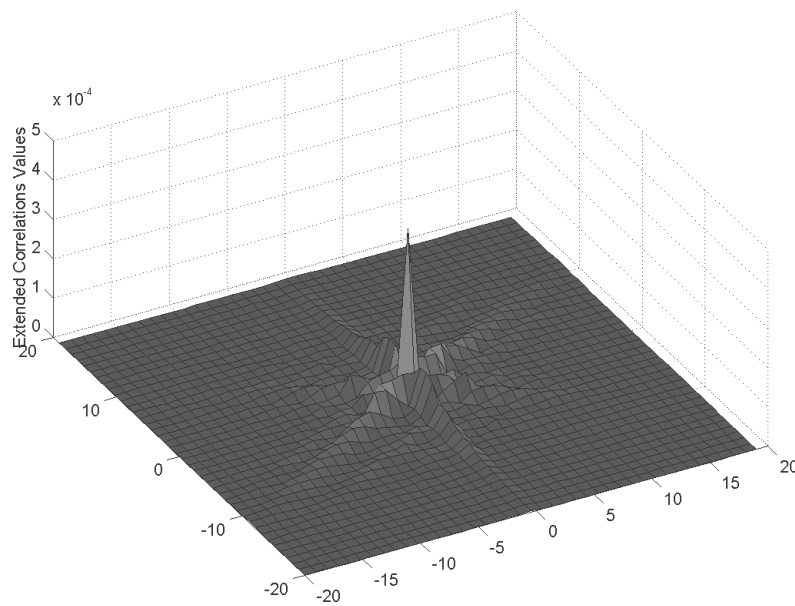


Figure 7.7

In Figure 7.8, Figure 7.9 and Figure 7.10, we show Spectral Power Estimation, for a simulated signal<sup>3</sup>, using direct FFT, Capon method and SMCE, respectively. The input time signal is of size  $64 \times 64$ , for which  $\gamma = 20$  correlation values were calculated. Starting from the calculated correlation values; Capon Spectral Estimation was estimated for a spectral grid of size  $T_i = 2\gamma' + 1$ , with  $\gamma' = 40$ . Also, for the same correlation values, SMCE was engaged for an extension from  $\gamma = 20$  to  $\gamma'$ . This produced the same image size for both of Capon and SMCE,  $T_i = 81$ .

<sup>3</sup> File Mig25.mat downloadable at <http://airborne.nrl.navy.mil/~vchen/data/>

In Figure 7.11, Figure 7.12 and Figure 7.13, we show the same results for direct FFT, Capon and SMCE, respectively, each resampled for clarity -using bicubic resampling, to the size of  $243 \times 243$ .



Figure 7.8



Figure 7.9



Figure 7.10



Figure 7.11



Figure 7.12



Figure 7.13

## VII Time domain extension characteristic

In this section, we will try to provide an insight, concerning the fallbacks of the extension on the time domain. In the general multidimensional case, and contrary to the 1D Case, the linear prediction filter connected to the inverse of the correlation matrix; takes a new value at each extension step. For the 2D Case, let us consider the linear prediction model of a stationary process

$$\mathbf{x}(t) = -\sum_{k=1}^{N_1} A_k^{N_1} \mathbf{x}(t-k) + \mathbf{e}_f^{N_1}(t), \quad (7.12)$$

where  $\mathbf{x}(t)$  is a vector of length  $N_2$ . The filter  $A_k^{N_1}$ , that minimizes the trace of the error power  $E(\mathbf{e}_{N_1}^f \mathbf{e}_{N_1}^{Hf})$  matrix, is the solution to the linear system

$$\begin{bmatrix} A_1^{N_1} & A_2^{N_1} & \dots & A_{N_1}^{N_1} \end{bmatrix} R = -\begin{bmatrix} R_1 & R_2 & \dots & R_{N_1} \end{bmatrix},$$

where  $R_i := E(\mathbf{x}(t+i) \mathbf{x}^H(t))$ , and the correlation matrix  $R$ , is defined as

$$R := \begin{bmatrix} R_0 & R_1 & \dots & R_{N_1-1} \\ R_{-1} & R_0 & \ddots & \vdots \\ \vdots & \ddots & \ddots & R_1 \\ R_{1-N_1} & \dots & R_{-1} & R_0 \end{bmatrix}.$$

The fact that we can use SMCE to extend the involved  $([N_2, N_1+1], [0,1], [0,1]) - 2$  toeplitz character matrix, defines a new 2D Filter, with a new extended time characteristics.

One of the time characteristics that we will examine here is the super resolution aspect. More precisely, we will try to investigate the effect of signal resolution augmentation, and that is, using the known autoregressive representation of the signal; as “Filter+Error”. We will proceed according to these steps:

- a) For a given Signal of size  $(s_1 \times s_2)$ , we will obtain the corresponding filter of size  $(N_1 \times N_2)$ .
- b) The filter will be applied and the error signal will be isolated, according to (7.12).
- c) The error signal resolution is doubled, using bicubic resampling.
- d) Each of the original filter, of size  $(N_1 \times N_2)$ , and the new extended filter of size  $(2N_1 \times 2N_2)$  are used to obtain a double-sized signal, using the isolated double-sized error signal.

The previous steps represent a super-resolution technique. In this context, we are more interested in this technique usage of the new extended filter, than its actual performance. In Figure 7.14, we see the resulting double-sized image, using the original  $(2 \times 2)$  filter, and Figure 7.15 shows the image built by the same manner, using an extended filter of size  $(4 \times 4)$ . We notice that the new extended filter is “error-synchronized” with the original image (signal). While, on the other hand, the original filter was not compatible with the resampled error signal, and thus the image in Figure 7.14 is distorted. The original image is shown in Figure 7.16.



Figure 7.14

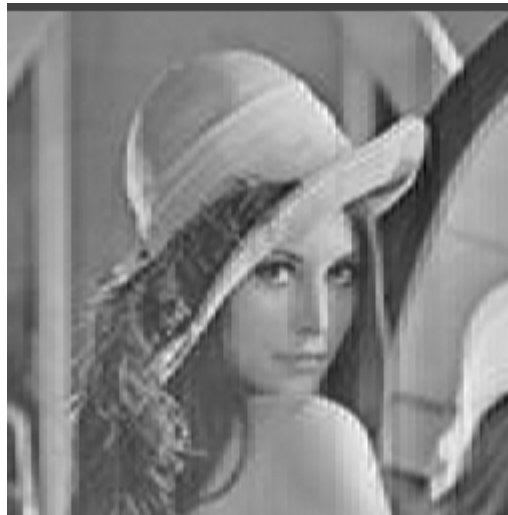


Figure 7.15



Figure 7.16


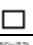

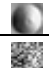



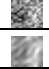

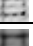
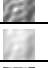
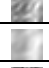




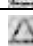

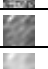
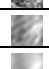






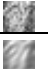




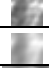





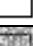






























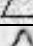







## VIII Conclusion

We found that SMCE represents a stable and accurate correlation extension technique. While we did not provide an infinite extension existence proof, all the simulation shown, and other simulations that we applied, converged to their target extension distances with no singularity. On the other hand **Theorem 7.1** guarantees the

positiveness of the solution. Therefore, while applying SMCE Algorithm we would face only situations in which the target extension limits were attained successfully, or singularity detected and extension stopped before, with always a positive solution. For Spectral Power Estimation application, numerical simulations showed the advantage of using SMCE over the Capon method. The presented Spectral Power Estimation is a Maximum of Entropy Estimation because the produced extension preserves the starting correlation matrix's determinant value.

**APPENDIX 7.1**

We show here Original Test Images, with Estimation results for  $\gamma_i = 4$ .

Size						
15×15	$SNR_i = -5 \text{ dB}$	Noise-added				
		SMCE				
		Capon				
	$SNR_i = 0 \text{ dB}$	Noise-added				
		SMCE				
		Capon				
	$SNR_i = 5 \text{ dB}$	Noise-added				
		SMCE				
		Capon				
21×21	$SNR_i = -5 \text{ dB}$	Noise-added				
		SMCE				
		Capon				
	$SNR_i = 0 \text{ dB}$	Noise-added				
		SMCE				
		Capon				
	$SNR_i = 5 \text{ dB}$	Noise-added				
		SMCE				
		Capon				



---

## NUMERICAL COMPARATIVE STUDY OF 2D SPECTRAL POWER ESTIMATION TECHNIQUES

**Abstract-**In this chapter we present a comparative study concerning a multiple of Spectral Power Estimation techniques. The examined techniques are the Approximative Sequential Multidimensional Spectral Estimation method, the Sequential Multidimensional Correlation Extension method, the Capon method, the Autoregressive Quarter plan Filter method, 2-D Spectrum Estimate using Multichannel AR Approach of 2-D Fast RLS Algorithms and the Correlogram method. The study was run over artificially generated data and over data obtained from different sources according to the domain of the application. The result of applying each technique is displayed with its counter parts, and for the artificially generated data a performance measure was calculated.

**Abstrait-** On présente une étude comparative concernant plusieurs techniques pour l'estimation de la Puissance Spectrale. Les techniques expérimentées sont la méthode ASMSE, la méthode SMCE, la méthode de Capon, la méthode du filtre autoregressif de quart plan, la méthode de l'estimation spectrale 2D utilisant une approche multichannel AR, et la méthode de corrélograme. L'étude a été effectuée sur des données générées artificiellement et des autres appartenant à différents domaines d'application. Pour les données réelles on montre les résultats de l'application de chaque méthode et pour les données artificielles on calcule aussi une mesure de performance.

### I Introduction

It is a hard task to give an equitable global point of view of all the techniques used for Spectral Power Estimation in modern day. This is due to the fact that an enormous amount of work has been done previously in this domain. The main motivation of this study is the evaluation of two new methods for Spectral Power Estimation presented in [29] and in [58]. We believe that the newly presented methods present a considerable advancement in the field of Spectral Power Estimation. The theoretical virtues of the newly presented methods can be summarized in the following:

- The method presented in [29] have an infinite spectral support, and an approximative correlation matching property. The method has an infinite spectral support because the stability of the method is proven by the positiveness of the extended auto-correlation matrix.
- The method presented in [58] have an exact correlation matching properties which is optimum for spectral restoration since the low frequencies constructing the spectrum are not effected at all. Also the produced Spectral Power Estimation is a Maximum of Entropy Solution because the method follows a process that preserves the Determinant of the original Auto-Correlation matrix.



- Both of the methods depend on no presumption of the Auto-Correlation matrix being circular.

In an effort to show the practical meaning of the discussion above, only a comparative numerical simulation could help us to better evaluate the quality of each Spectral Estimation method.

In this chapter we will present a comparative study between the following techniques:

- Approximative Sequential Multidimensional Spectral Estimation (ASMSE) [29].
- Sequential Multidimensional Correlation Extension (SMCE) [58].
- Minimum Variance (Capon) [15],[30].
- Autoregressive Quarter Plan Filter (QP) [60].
- 2-D Spectrum Estimate using Multichannel AR Approach of 2-D Fast RLS Algorithms (HMHV)[59].
- Correlogram (CORR).
- Fast Fourier Transformation. (FFT).

In all the previously mentioned methods –except for FFT- we calculate the Auto-Correlation matrix, and at a second step, the Spectral Estimation method is applied as a function of that matrix.

The method used for the estimation of the Auto-Correlation matrix is important in all situations to provide a good and stable estimate. In this study, which deals with the 2D signal, we used the TBT estimate. The TBT estimate is defined for a given signal  $x(t_1, t_2)$ ,  $t_1 \in [0, \dots, N_1 - 1]$ ,  $t_2 \in [0, \dots, N_2 - 1]$  as:

$$r(k, l) := \begin{cases} \frac{1}{N_1 N_2} \sum_{t_1=0}^{N_1-k-1} \sum_{t_2=0}^{N_2-l-1} x(t_1+k, t_2+l) (x(t_1, t_2))^* & \text{if } k \geq 0, l \geq 0 \\ \frac{1}{N_1 N_2} \sum_{t_1=-k}^{N_1-1} \sum_{t_2=0}^{N_2-l-1} x(t_1+k, t_2+l) (x(t_1, t_2))^* & \text{if } k < 0, l \geq 0 \\ (r(-k, -l))^* & \text{if } l < 0 \end{cases}$$

with  $k \in [-\gamma_1, \dots, 0, \dots, \gamma_1]$ ,  $l \in [-\gamma_2, \dots, 0, \dots, \gamma_2]$ , where  $\gamma_1 \times \gamma_2$  is the correlation signal size, which is known also as the system order. Calculating the estimate according to this manner, produce a positive Auto-Correlation matrix, which is essential to produce a correct Spectral Estimation.

The Correlogram method is just a Fast Fourier Transformation of the provided auto-correlation signal  $r(k, l)$ :

$$P_{Corr}(j\omega_1, j\omega_2) := \sum_{k=-\gamma_1}^{\gamma_1} \sum_{l=-\gamma_2}^{\gamma_2} r(k, l) e^{-j\omega_1 k} e^{-j\omega_2 l}$$

The FFT method in (g) is the expression of the Spectral Power of a given signal of size  $N_1 \times N_2$  as

$$P_{FFT}(j\omega_1, j\omega_2) := \left| \sum_{t_1=0}^{N_1-1} \sum_{t_2=0}^{N_2-1} x(t_1, t_2) e^{-j\omega_1 t_1} e^{-j\omega_2 t_2} \right|^2.$$

In fact, the Correlogram method is totally equivalent to the FFT method in the case of a circular Auto-Correlation signal calculus -which is not the case in here. Circular calculus of the Auto-Correlation signal lowers significantly the condition of the Auto-Correlation matrix, and with it the extension limits

Also, being able to compare at once the performance of the previously presented techniques is a very good hint to the performance capabilities of other methods not taken in consideration in this study. The reason for that is that many of the other methods for Spectral Power Estimation are derived from the ones presented above.

## II Controlled Performance measure

In this experimentation we advance a test signal  $X(f_1, f_2)$  having spectral support of  $121 \times 121$  points. The spectral peaks of the signal are located at frequencies  $a := -\frac{31}{121}, b := \frac{29}{121}$  according to the following:

$$X(a, a) = 1$$

$$X(a, b) = 0.75 e^{j2\pi 0.75}$$

$$X(b, b) = 0.5 e^{j2\pi 0.5}$$

$$X(b, a) = 0.25 e^{j2\pi 0.25}$$

With zero filled elsewhere. In Figure 8.1 we see a representation of this signal.

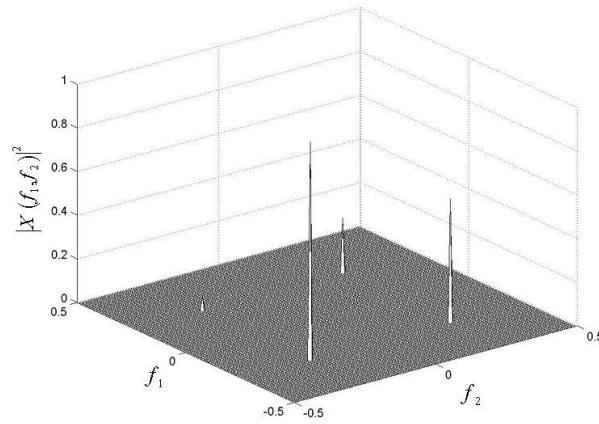


Figure 8.1

The experimentation are engaged for each Spectral Estimation method as the following:

- a) Natural distribution Noise signal  $N(jw_1, jw_2)$  is added to the test signal  $X(jw_1, jw_2)$  according to a given  $SNR_{noise}$  defined as

$$SNR_{noise} := 10 \log_{10} \frac{\sum_{w_1, w_2} |X(jw_1, jw_2)|^2}{\sum_{w_1, w_2} |N(jw_1, jw_2)|^2}.$$

- b) Time signal  $x(t_1, t_2)$  is obtained using IFFT.

- c) From the  $121 \times 121$  points present in the time signal only the first  $30 \times 30$  points were considered as the input signal for Spectral Power Estimation.
- d) Each Spectral Power Estimation method is applied to reconstruct the original spectral image with the original resolution  $121 \times 121$ .
- e) A Performance measure is calculated between the original spectrum  $|X(j\omega_1, j\omega_2)|^2$  and the estimated one  $\tilde{P}(j\omega_1, j\omega_2)$ , according to:

$$SNR_{est} := 10 \log_{10} \frac{\sum_{\omega_1, \omega_2} \left| |X(j\omega_1, j\omega_2)|^2 \right|^2}{\sum_{\omega_1, \omega_2} \left| |X(j\omega_1, j\omega_2)|^2 - \tilde{P}(j\omega_1, j\omega_2) \right|^2}$$

- f) For estimation methods depending on the value of the correlation order; the operations in (d) and (e) are repeated for correlation lags increasing from  $\gamma_1 = \gamma_2 = 10$ , for both dimensions, to the value 20.

For the application of SMCE the extension was engaged always from the used input signal's correlation order  $\gamma_1 = \gamma_2$  to the order value 50.

In Figure 8.2, Figure 8.3 and Figure 8.4 we show the result of the application of the previously explained framework, and that is for  $SNR_{noise}$  values which are equal to  $-5$  dB,  $0$  dB and  $5$  dB respectively. We observe that ASMSE and SMCE got a relatively equal performance; which over powered the other methods in the cases of low  $SNR_{noise}$  and low Correlation Order. The performance of other methods was considerably enhanced when the noise level was reduced and when the correlation order was increased. For the method HMHV a good results were observed for low noise level  $-$ high  $SNR_{noise}$ . The artificially generated signal permits us to perform a statistical evaluation; meanwhile, real world application remains the real area for a final and accurate evaluation of any Spectral Power Estimation method.

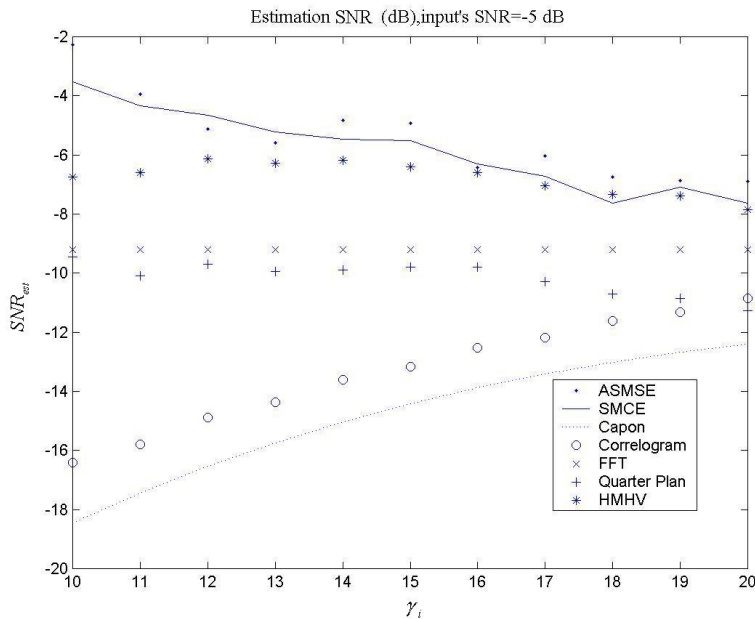


Figure 8.2

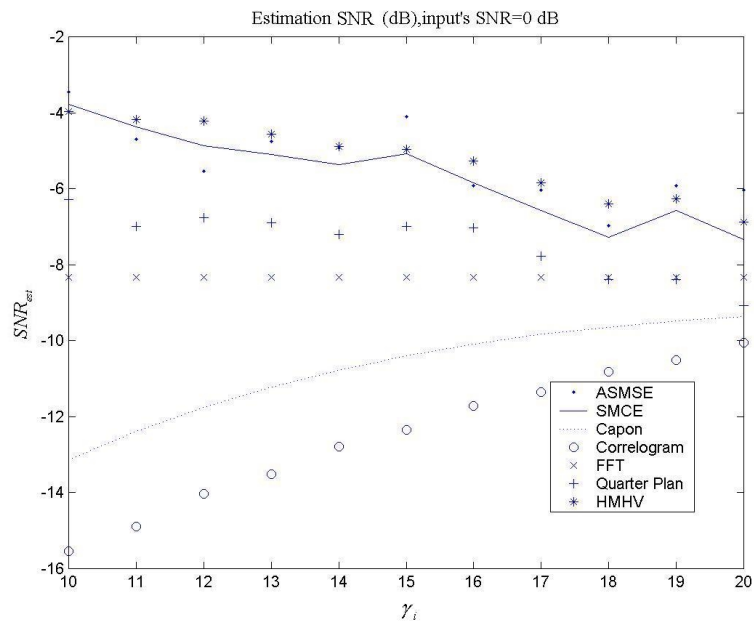


Figure 8.3

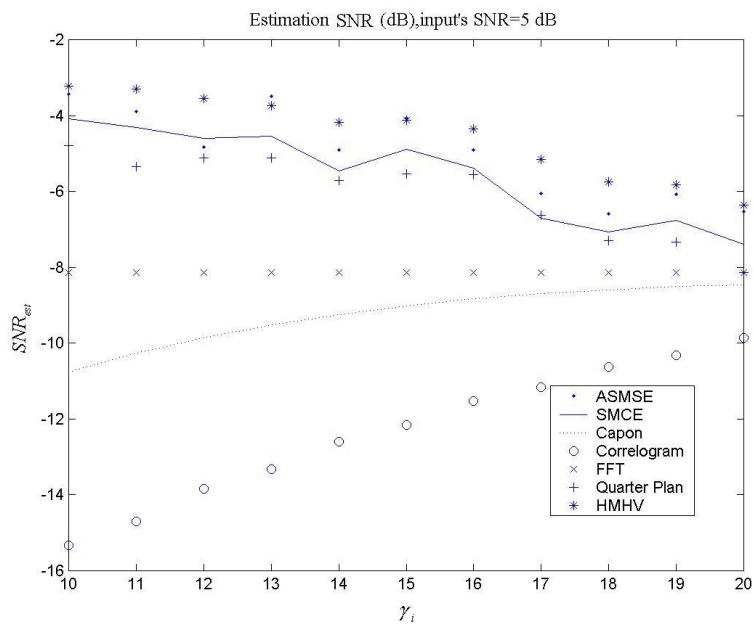


Figure 8.4

### III Application to Synthetic Aperture Radar (SAR)

Synthetic Aperture Radar (SAR) is one of the main application domains for Spectral Power Estimation. After the development of SLAR (Side Looking Aperture Radar), the development of SAR (Synthetic Aperture Radar) was motivated by the need of more practical and accurate radar imaging system. Having an array of radiating

elements, and depending on the Doppler effect SAR was capable of realizing more range and cross range precision.

SAR is still an active domain of research, with multiple types of configurations and increasing complexity.

The need for high precision Spectral Estimation techniques was reported by different sources. The text in [2] is recommended for providing a good insight about this subject.

◆ *Naval Research Laboratory Database*

We applied the examined methods on the file Mig25.mat<sup>4</sup> published by the Naval Research Laboratory. The file is a simulated SAR signal for a combat air plan. The signal size is 64×64 from which we produced the estimations in two resolutions; the first is 81×81- Figure 8.5-Figure8.11, and the second is 264×264- Figure 8.12-Figure8.18. The used correlation order was 19×19. For the SMCE method the extension limits were 40×40.



Figure 8.5, ASMSE



Figure 8.6, SMCE



Figure8.7, FFT



Figure8.8, Capon



Figure8.9, Correlogram



Figure8.10, QP



Figure8.11, HMMV



Figure 8.12, ASMSE



Figure8.13, SMCE

<sup>4</sup> File Mig25.mat downloadable at <http://airborne.nrl.navy.mil/~vchen/data/>



Figure8.14, FFT



Figure8.15, Capon



Figure8.16, Correlogram



Figure8.17, QP



Figure8.18, HMMV

◆ *Application to MSTAR Database*

We did apply the studied methods on the file HB03793 acquired from the MSTAR Database [68]. The file is a synthesized SAR signal of a ground vehicle.

The file is of size  $128 \times 128$  and already has suffered from a Fast Fourier Transformation. To be able to apply Spectral Estimation we did reproduce the original signal data using IFFT. Next we applied each method using the correlation order  $30 \times 30$  to obtain a spectrum with the resolution  $264 \times 264$ . The results are displayed in Figure 8.19-Figure 8.25.



Figure 8.19, ASMSE



Figure 8.20, SMCE



Figure 8.21, FFT



Figure 8.22, Capon



Figure 8.23, Correlogram



Figure 8.24, QP



Figure 8.25, HMMV

◆ *Sandia National Laboratory SAR Complex Data*

The examples in here show the application of spectral estimation methods for the data file *MiniSAR20050519p0001image008.gff*, published by the Sandia National Laboratory [67]. The signal present in the file was produced following an actual acquisition of a real SAR signal. Since time domain data are not provided; we proceeded using an IFFT in both dimensions to obtain the quasi-time domain values for the data present in this file.

In Figure 8.26 we display the image present in the file as it was processed by the program provided by Sandia laboratory. The data contains a considerable amount of additive and multiplicative noise, and for that, a threshold was used to produce the spectral image displayed in Figure 8.26,  $|X(jw_1, jw_2)|$ . For all the other results present in this section we have used the logarithmic scale to display the Spectral Power Estimation  $|X(jw_1, jw_2)|^2$ .

The signal has the size  $2510 \times 1638$ , which demands a considerable calculus time. To be able to apply each Spectral Estimation method on the present example, we



proceeded into block processing. Spectral Estimation by block is a well-known method and was proposed by different authors as in [2] and [15]. The following steps compose block-processing Spectral Estimation:

- a) For the signal  $x(t_1, t_2)$ , we calculate  $X(jw_1, jw_2)$  using FFT.
- b) The image  $X(jw_1, jw_2)$  is segmented into blocks of equal size  $\{X_i(jw_1, jw_2)\}_i$ .
- c) The time domain representation  $x_i(t_1, t_2)$  for each spectral block  $X_i(jw_1, jw_2)$  is obtained independently using *IFFT*.
- d) Starting from each block's time values we apply the Spectral Power Estimation method to obtain the block's Spectral Power Estimation.

In our experimentation we have used the block size  $200 \times 200$ , and that is for all the tested methods. Also the correlation Order used for all the tested methods was  $\gamma_1 = \gamma_2 = 30$ , which corresponds to a correlation signal of size  $(2\gamma_1 + 1) \times (2\gamma_2 + 1)$ . In what concerns SMCE method application the extension limits were set to  $\gamma'_1 = \gamma'_2 = 50$ .

In Figure 8.27-Figure 8.33 we display the results of the block-processing Spectral Power Estimation according to each of the considered methods.

To have more detailed observations we are showing also a “zoom in” image for these results in Figure 8.34-Figure 8.40, the “zoom in” image have a block size  $2 \times 4$ , and its top left block is located at the block coordinates  $(7, 4)$ .

In Figure 8.29 the black regions corresponds to a non-convergent SMCE situations in which the target correlation value 50 was not attained, meaning that the correlation matrix has fallen into a singular region before that the correlation order was attained. By comparing these regions with the Correlogram image in Figure 8.31, we observe that these regions correspond to the spectral locations with a high noise peaks. Also we observe that the SMCE method was relatively successful in adding valuable details in comparison to the non-extended Correlation image. This could be clearly observed also by comparing Figure 8.36 and Figure 8.38.

The QP method as SMCE and ASMSE methods was successful in removing a considerable amount of noise in the image but suffered from inconsistency across blocks and lower image quality. This could be observed in Figure 8.32 and Figure 8.39. The fact that the QP method suffers from this inconsistency across blocks is a revealing proof of the inherent ambiguity of the relation connecting the Autoregressive 2D modeling in time domain to the spectral domain. This ambiguity is due to the fact that contrary to the 1D case the 2D autoregressive model have no theoretical connection in the spectral sense to the original signal. More precisely, in

the 1D case, the autoregressive model in its spectral expression  $\tilde{P}(jw) := \frac{c}{\left| \sum_{k=0}^{\gamma} a_k e^{-jwk} \right|^2}$

do produce the same correlation coefficients as the original input signal when taken back to the time domain (signal correlation) according to

$$\hat{r}(n) = \int_w \frac{c}{\left| \sum_{k=0}^{\gamma} a_k e^{-jwk} \right|^2} e^{jwn} dw .$$

This is known as the matching property [33], in which  $\hat{r}(k) = r(k)$ ,  $k := 0 \dots \gamma$ . On the other hand in the 2D case (the QP method) this is not realized, more to that, there is no known proof for the filter stability. The ASMSE, and SMCE methods was constructed to remedy both of the disadvantages that we have come to explain by providing the following points:

- a) Stability through proven positiveness.
- b) Approximative correlation matching in ASMSE and an exact matching in SMCE.

The previous discussion explains why ASMSE and SMCE methods provide a more accurate Spectral Power Estimation than the other methods, Figure 8.28, Figure 8.29. It is important to mention also that increasing the extension limit could further enhance the results of the SMCE method.

From Figure 8.30 and Figure 8.37 we observe that the result provided by Capon method had a good consistency across blocks, with a good image quality. The details level provided by Capon method is inferior to the one provided by the ASMSE. The later fact is a numerical confirmation of the known relation between the 1D autoregressive estimation (or the maximum of entropy) and the 1D Capon method, where the Capon Spectral Power Estimation could be described roughly as a “blurring” of the maximum of entropy Spectral Power Estimation result.



Figure 8.26, image as produced by the program provided by Sandia (by thresholding).



Figure 8.27, FFT (logarithmic).



Figure 8.28, ASMSE (logarithmic).



Figure 8.29, SMCE (logarithmic).



Figure 8.30, Capon (logarithmic).



Figure 8.31, Correlogram (logarithmic).



Figure 8.32, QP (logarithmic).



Figure 8.33, HMHV (logarithmic).



Figure 8.34, FFT (logarithmic).





Figure 8.35, ASMSE (logarithmic).

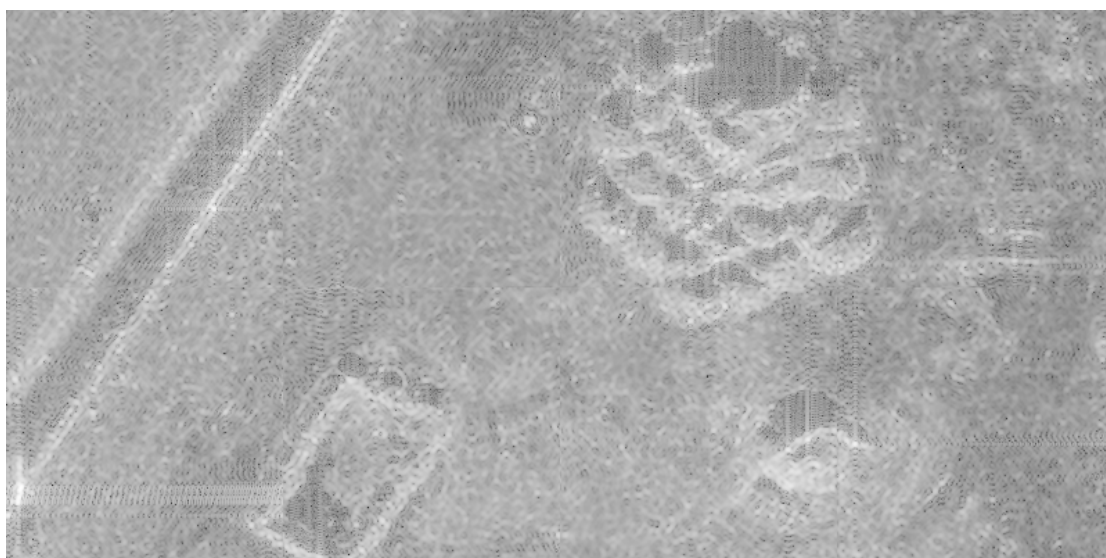


Figure 8.36, SMCE (logarithmic).

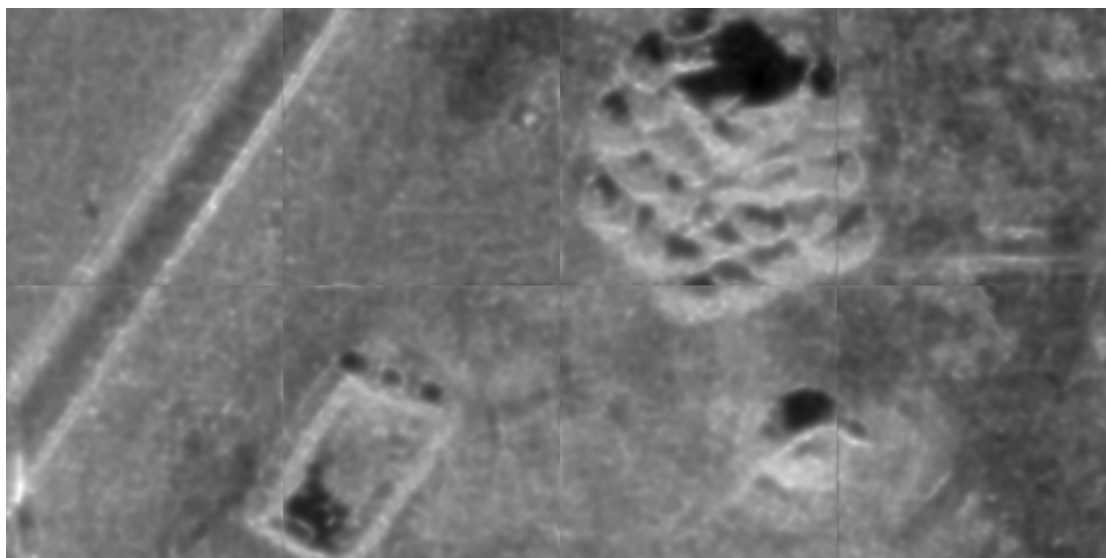


Figure 8.37, Capon (logarithmic).

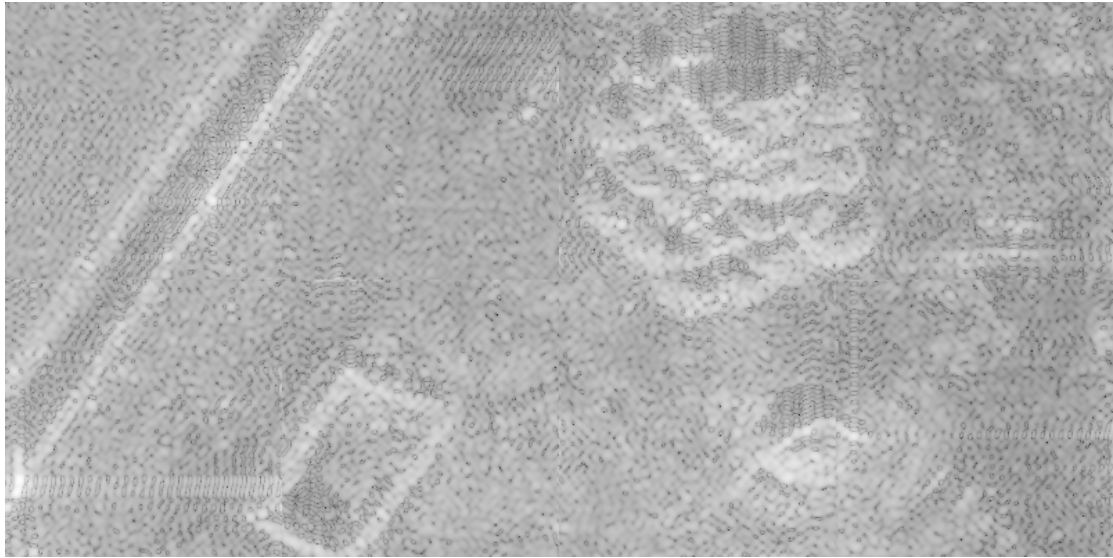


Figure 8.38, Correlogram (logarithmic).

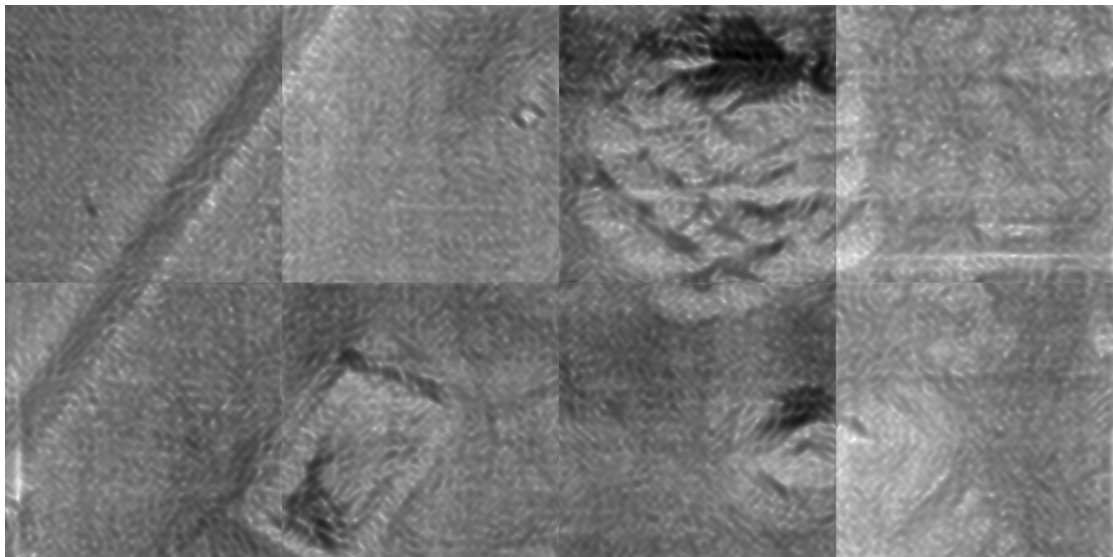


Figure 8.39, QP (logarithmic).

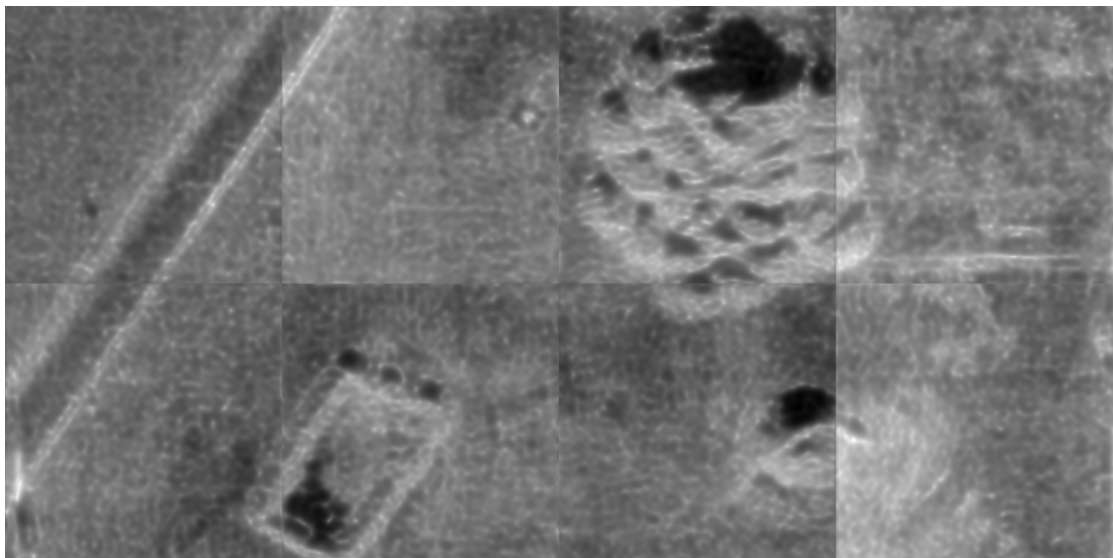


Figure 8.40, HMHV (logarithmic).



## IV Conclusion

In this chapter, we have seen the application of multiple methods for Spectral Power Estimation for a multiple of examples. From the examples shown we observed the importance of providing a good Spectral Power Estimation when the input signal is badly defined and there is a need to have a better estimation of the spectral power. The following could express the points according to which we can evaluate the quality for a given Spectral Power Estimation method:

- 1- Noise Removal Criteria: in the application where a high degree of additive and multiplicative noise, Spectral Estimation method should have the property of providing a relatively noise-free image that is acceptable to the human eye.
- 2- Spectral Interpolation Criteria: from a given number of samples in the 2D plan, Spectral Interpolation Criteria is the capability of the method to provide an increased resolution in the spectral domain. More precisely, the resolution support should goes beyond the limited size of the input signal.
- 3- Details Restoration Criteria: this is the ability of the methods to produce an estimation that preserves signal information, so that noise removal would not produce details lost.

According to the previous Criteria and from the examples shown previously, we find that the QP method produce a better quality than the Capon method, but it is rarely stable and statistically could not be considered as a better method. The ASMSE methods and SMCE performed well across all the presented simulations. The ASMSE method showed also an advanced capability according to the Spectral Interpolation Criteria. This is most obvious in the examples shown in Figure 8.12 and Figure 8.28. The SMCE method showed an advanced capability according to the Details Restoration Criteria. This is due, of course, to its exact correlation matching property. In general ASMSE and SMCE method could be considered a good advancement over the QP and the Capon methods. The HMMV method was successful in enhancing the results of QP method, but as the QP method suffered in some examples from instability. For block-processing scenario the Capon method, ASMSE, and SMCE showed an acceptable across blocks consistency.

In what concerns SAR application we have seen that for real signal a great amount of multiplicative noise still exist even after that the Spectral Estimation method is applied. This invites us to consider the development of Spectral Estimation methods that take this into account, and goes beyond the simple assumption of the independence of the noise signal from the correct signal. The development of such a model could impose also that main components of the Radar theory are taken into consideration.

---

## CONCLUSION AND FUTURE WORK

### I Main contribution of this thesis

**F**or Multidimensional Spectral Power Estimation, we had the opportunity to examine, in details, the structure of the ND-Toeplitz matrices using the Generalized reflection Coefficients. Different algorithms were presented; each is of different estimation quality and demanding a greater or lesser number of calculations. Concerning the Generalized Reflection Coefficients, we studied its behaviour in the ND-Toeplitz case and found its usage for matrix inversion. The effort we invested using the Generalized Reflection Coefficients instead of other known algorithms for Toeplitz Systems inversion was rewarded in Chapter 7, where it permitted realization of a Maximum of Entropy Multidimensional Correlation Extension with an exact matching property.

Here we will mention the main points representing the theoretical and practical contributions of this thesis:

- Clarifying the relation between Burg Algorithm and Levinson Algorithm toward a stable 1D and 2D, Spectral Power Estimation and Linear Prediction.
- The study of the Generalized Reflection Coefficients in the case of ND-Toeplitz matrix.
- New Multidimensional Spectral Power Estimation method, which is approximative in its matching property, with good quality and guaranteed stability, and a structure adapted for implementation using Fast Fourier Transformation.
- New Multidimensional Spectral Power Estimation and Correlation Extension method, which is exact in its matching property, with a maximum of entropy quality, and a guaranteed stability.

### II Theoretical horizon and future work

Behind this text, as any thesis of course, there is a lot of unfinished work, or lines of thinking. The main ideas that motivated this work still need to be better understood. For Spectral Power Estimation, while we presented an algorithm for a Maximum of

Entropy solution, we still had no analytical representation of the general multidimensional case. Also, almost all of the presented algorithms, in the multidimensional case, still contain a strong degree of redundancy. Hence we do not know how to exploit totally the ND-Toeplitz structure. For example, in the 1D case, for a toeplitz matrix of size  $(n \times n)$ , we need  $n \log n$  operations to obtain the first column of the inverse; meanwhile, for the 2D case we do not have the same logarithmic reduction. The same type of controversy between the 1D case and the 2D case exist also for the bezoutian form of the inverse. While in 1D case, the same 1D prediction filter coefficients do construct the bezoutian form for correlation matrix's inverse, in the 2D case there is no known 2D plan filter coefficients capable of constructing the correlation matrix inverse. We hope that these "missing puzzles" can be solved in the future, which would represent a strong advancement in the domain of Multidimensional Signal Processing.

*The End*

## BIBLIOGRAPHY

- [1] S. Haykin, *"Adaptive Filter Theory"*. PRENTICE-HALL, UPPER SADDLE RIVER, NEW JERSEY, THIRD EDITION, 1996.
- [2] S. R. DeGraaf, *"SAR Imaging via Modern 2-D Spectral Estimation Methods"*, IEEE TRANS. ON IMAGE PROCESSING, VOL. 7, NO. 5, PP. 729-761, MAY 1998.
- [3] R. E. Hoffman, A. Kumar, K. D. Bishop, P. N. Borer, G. C. Levy, *"Application of the Maximum Likelihood Method to a Large 2D NMR Spectrum Using a Parallel Computer"*, JOURNAL OF MAGNETIC RESONANCE, NO. 83, PP. 586-594, 1989.
- [4] I. C. Gohberg, G. Heining, *"Inversion of finite Toeplitz matrices made of elements of a non-commutative algebra"*, REV. ROUMAINE MATH. PURES APPL., XIX(5):623-663, 1974, (IN RUSSIAN).
- [5] I. C. Gohberg, A. Semencul, *"on the inversion of finite Toeplitz matrices and their continuous analogs"*, MAT. ISSLED., 2(201:-233), 1972, (IN RUSSIAN).
- [6] J. P. Burg, *"Maximum Entropy Spectrum Analysis"*, PH. D. DISSERTATION, STANFORD UNIV., 1975.
- [7] N. Levinson, *"The wiener RMS (root-mean-square) error criterion in Filter design and prediction"*, J. MATH. PHYS., VOL. 25, PP. 261-278, 1947.
- [8] P. Whittle, *"On the Fitting of Multivariate Autoregressions, and the Approximative Canonical Factorization of a Spectral Density Matrix"*, BIOMETRICA, NO. 50, PP. 129-134, 1963.
- [9] R. A. Wiggins, E. A. Robinson, *"Recursive Solution of the Multichannel Filtering Problem"*, J. GEOPHYS. RES., VOL. 70, PP. 1885-1891, APRIL 1965.
- [10] B. McGuffin, B. Liu, *"An Efficient Algorithm for Two-Dimensional Autoregressive Spectrum Estimation"*, IEEE TRANS. ACOUST. SPEECH SIGNAL PROCESS., VOL. 37, NO. 1, PP. 106-117, 1989.
- [11] C. W. Therrien, H. T. El-Shaer, *"A direct algorithm for computing 2-D AR power spectrum estimates"*, IEEE TRANS. ASSP, VOL. 37, NO. 11, PP. 1795-1798, NOV. 1989.

- [12] O. N. Strand, "*Multichannel Complex Maximum Entropy (Autoregressive) Spectral Analysis*", IEEE TRANS. AUTOMATIC CONTROL, VOL. 22, NO. 4, PP. 634-640, AUGUST 1977.
- [13] G. R. Kuduvali, R. M. Rangayyan, "*An Algorithm for Direct Computation of 2-D Linear Prediction Coefficients*", IEEE TRANS. ON SIGNAL PROCESSING, VOL. 41, NO. 2, PP. 996-1000, FEB. 1993.
- [14] C. W. Therrien, "*Relation Between 2-D and Multichannel Linear Prediction*", IEEE TRANS. ASSP, VOL. ASSP-29, NO. 3, PP. 454-457, JUNE 1981.
- [15] A. Jakobsson, S. L. Marple, P. Stoica, "*Computationally Efficient Two-Dimensional Capon Spectrum Analysis*", IEEE TRANS. ON SIGNAL PROCESSING, VOL. 48, NO. 9, SEPTEMBER 2000.
- [16] S.L Marple Jr., "*Digital Spectral Analysis With Application*", PRENTICE-HALL, ENGLEWOOD CLIFFS, N.J., 1987.
- [17] P.F. Fougere, E. J. Zawalick, H. R. Radoski, "*Spontaneous line splitting in maximum entropy power spectrum analysis*", PHYS. EARTH PLANET. INTERIORS, NO. 12, 201-207, 1976.
- [18] G. Castro, "*Coefficients de Réflexion Généralisée. Extension de Covariance Multidimensionnelles et Autres Applications*", PH.D. THESIS, UNIVERSITE DE PARIS-SUD CENTRE.
- [19] S. Dégerine, "*Sample partial autocorrelation function of a multivariate time series*", J. MULTIVARIATE ANAL., NO. 50, PP. 294-313, 1994.
- [20] PH. Delsarte, Y. Genin, Y. Kamp, "*Schur parameterization of positive definite block-Toeplitz systems*", SIAM J. APPL. MATH., VOL. 36, NO. 1, PP 34-45, 1979.
- [21] J. Durbin, "*The fitting of times-series models*", REV. INST. STATIST., VOL. 28 PP 233-244, 1960.
- [22] N. Levinson, "*The Wiener RMS (root-mean-square) error Criterion in filter design and prediction*", J. MATH. ANAL. PHYS., VOL. 25, PP 261-278, 1947.
- [23] R. Kanhouche, "*Generalized Reflection Coefficients and Inverse Factorization of Hermitian Block Toeplitz Matrix*", <http://hal.ccsd.cnrs.fr/ccsd-00003892>, JANUARY 2005.
- [24] R. Kanhouche, "*A Modified Burg Algorithm Equivalent In Results to Levinson Algorithm*", <http://hal.ccsd.cnrs.fr/ccsd-00000624>, SEPTEMBER 2003.

- [25] N. Wiener, “*Extrapolation, interpolation, and smoothing of stationary time series with engineering applications*”, JOHN WILEY AND SONS, INC., NEW YORK, 1950.
- [26] A. Kolmogoroff, “*Sur l'interpolation et extrapolation des suites stationnaires*”, C.R. ACAD. SCI. PARIS, VOL. 208, PP. 2043-2045, 1939.
- [27] Claude E. Shannon, Warren Weaver, “*The Mathematical Theory of Communication*”, THE UNIVERSITY OF ILLINOIS PRESS. URBANA. 1959.
- [28] R. Kanhouche, “*Generalized Reflection Coefficients in Toeplitz-Block-Toeplitz Matrix Case and Fast Inverse 2D Levinson Algorithm*”, <http://hal.ccsd.cnrs.fr/ccsd-00001420>, APRIL 2004.
- [29] R. Kanhouche, “*Sequential Multidimensional Spectral Estimation*”, <http://hal.ccsd.cnrs.fr/ccsd-00005351>, JUNE 2005.
- [30] J. Capon, “*High-resolution frequency-wavenumber spectrum analysis*”, PROC. IEEE, VOL. 57, NO. 8, PP. 1408-1418, AUGUST 1969.
- [31] R. T. Lacoss, “*Data Adaptive Spectral Analysis Methods*”, GEOPHYSICS, VOL. 36, PP. 661-675, AUGUST 1971.
- [32] B. Musicus, “*Fast MLM power spectrum estimation from uniformly spaced correlations*”, IEEE TRANS. ACOUST. SPEECH SIGNAL PROCESS., VOL. ASSP-33, NO. 5, PP. 1333-1335, OCTOBER 1985.
- [33] H. J. Landau, “*Maximum Entropy And The Moment Problem*”, BULL. AMERIC. MATH. SOC., VOL. 16, NO. 1, PP. 47-77, JANUARY 1987.
- [34] G. Castro, A. Seghier, “*Schur-Szeg coefficients for definite positive Hermitian forms and orthogonal polynomial*”, UNIV. PARIS SUD, PREPUB. NO. 95.79.
- [35] N. Akrouf, R. Prost, R. Goutte, “*Image compression by vector Quantization: a review focused on codebook generation*”, IMAGE AND VISION COMPUTING, VOL. 12, NO. 10, PP. 627-637, DECEMBER 1994.
- [36] Allen Gersho, Robert M. Gray, “*Vector quantization and signal compression*”, KLUWER ACADEMIC PUBLISHERS, 1992.
- [37] Qun Gu, Scott E. Budge, “*Rate-distortion adaptive vector quantization for wavelet image coding*”, IEEE INTERNATIONAL CONFERENCE ON ACOUSTICS, SPEECH AND SIGNAL PROCESSING, VOL. 6, PP. 1903 – 1906, 5-9 JUNE 2000.

- [38] Syed A. Rizvi, Nasser M. Nasrabadi, "*Residual vector quantization using a multilayer competitive neural network*", IEEE JOURNAL ON SELECTED AREAS IN COMMUNICATIONS, VOL. 12, NO. 9, PP. 1452-1459, DECEMBER 1994.
- [39] Syed A. Rizvi, Ling-Cheng Wang, Nasser M. Nasrabadi, "*Neural network architectures for vector prediction*", PROCEEDINGS OF THE IEEE, VOL. 84, NO. 10, PP. 1513-1528, 1996.
- [40] H. Sun, M. Goldberg, "*Radiographic image sequence coding using two-stage adaptive vector quantization*", IEEE TRANSACTIONS ON MEDICAL IMAGING, VOL. 7, NO. 2, PP. 118-126, 1988.
- [41] Peter L. Venetianer, Tam. Roska, "*Image compression by CNN*", NEURAL NETWORKS, 1996, IEEE INTERNATIONAL CONFERENCE ON, VOL. 3, PP. 1510 – 1515, 3-6 JUNE 1996.
- [42] Jianhua Xuan, T. ulay Adali, "*Learning Tree-Structured Vector Quantization for Image Compression*", WORLD CONGRESS ON NEURAL NETWORK, VOL. 1, PP. 756-759, 1995.
- [43] Marco Balsi, Stefano David, "*Cellular neural network for image compression by adaptive morphological subband coding*", 13 EUROPEAN CONFERENCE ON CIRCUIT THEORY AND DESIGN, (ECCTD'97), VOL. 2, PP. 634-638, 1997.
- [44] Oscar Moreira-Tamayo, Jose Pineda de Gyvez, "*Preprocessing operators for image compression using cellular neural networks*", IEEE INTERNATIONAL CONFERENCE ON NEURAL NETWORKS, VOL. 3, PP. 1500-1505, JUIN 1996.
- [45] Christophe Foucher, thèse, "*Analyse et amélioration d'algorithmes neuronaux et non neuronaux de quantification vectorielle pour la compression d'images*", UNIVERSITE DE RENNES 1, DECEMBRE 2002.
- [46] Susan S. Young, Peter D. Scott, Nasser M. Nasrabadi, "*Object recognition using multilayer Hopfield neural network*", IEEE TRANSACTION ON IMAGE PROCESSING, VOL. 6, NO. 3, PP. 357-372, MARCH 1997.
- [47] Kamgar-Parsi, B. Jain, A.K.Dayhoff, J.E., "*Aircraft detection: a case study in using human similarity measure*", IEEE TRANSACTIONS ON PATTERN ANALYSIS AND MACHINE INTELLIGENCE, VOL.23, NO. 12, PP.1404-1414, DEC. 2001.
- [48] S.C. Zhu, "*Embedding Gestalt laws in Markov random fields*", IEEE TRANSACTIONS ON PATTERN ANALYSIS AND MACHINE INTELLIGENCE, VOL. 21, NO. 11, PP. 1170-1187, NOV. 1999.

- [49] Jinhai Cai, Zhi-Qiang Liu, “*Hidden Markov models with spectral features for 2D shape recognition*”, IEEE TRANSACTIONS ON PATTERN ANALYSIS AND MACHINE INTELLIGENCE, VOL. 23, NO. 12, PP. 1454-1458, DECEMBER 2001.
- [50] Shih-Ping Liou, H. Chiu, Ramesh C.Jain, “*A parallel technique for signal-level perceptual organization*”, IEEE TRANSACTIONS ON PATTERN ANALYSIS AND MACHINE INTELLIGENCE, VOL. 13, NO. 4, PP. 317-325, APRIL 1991.
- [51] P. P. Raghu, R. Poongodi, B. Yegnanarayana, “*Unsupervised texture classification using vector quantization and deterministic relaxation neural network*”, IEEE TRANSACTION ON IMAGE PROCESSING, VOL. 6, NO. 10, PP. 1376-1387, OCTOBER 1997.
- [52] Pablo MUSÉ, Frédéric SUR, Frédéric CAO, Yann GOUSSEAU, Jean-Michel MOREL, “*An a contrario decision method for shape element recognition*”. [http://www.loria.fr/~sur/download/IJCV\\_final.pdf](http://www.loria.fr/~sur/download/IJCV_final.pdf).
- [53] Lin-Cheng Wang, Sandor Z. Der, Nasser M. Nasrabadi, “*Automatic target recognition using a feature-decomposition and data-decomposition modular neural network*”, IEEE TRANSACTION ON IMAGE PROCESSING, VOL. 7, NO. 8, PP. 1113-1121, AUGUST 1998.
- [54] Paul Kiernan, “*High resolution two-dimensional minimum free energy AR spectral estimation*”, J. MULTIDIMENSIONAL SYST. SIGNAL PROCESS., VOL. 6, NO. 3, PP. 237-249, 1995.
- [55] S. W. Lang, James H. McClellan, “*Multidimensional MEM spectral estimation*”, J. IEEE TRANS. ACOUST. SPEECH SIGNAL PROCESS., VOL. 30, NO. 6, PP. 880-887, DEC. 1982.
- [56] Y. Meyer, “*Perception et compression des images fixes*”, <http://www.cmla.ens-cachan.fr/Cmla/Publications/2005/CMLA2005-23.pdf>, 2005.
- [57] J.P. Guillois, “*Techniques de compression des images*”, HERMES, PARIS, 1996.
- [58] R. Kanhouche, “*Multidimensional Correlation Extension using The Generalized Reflection Coefficients with Application to Spectral Power Estimation*”, TO BE PUBLISHED.
- [59] O. Alata, P. Baylou, M. Najim, “*A new 2-D spectrum estimate using multichannel AR approach of 2-D fast RLS algorithms*”, PROC. OF ICIP, VOL. 2, PP. 442-445, OCTOBRE 1997.
- [60] L. B. Jackson, H.C. Chein, “*Frequency and Bearing Estimation by Two-Dimensional Linear Prediction*”, DPROC. OF ICASSP, PP. 665-668, APRIL 1979.



- [61] L. E. Kinsler, A. R. Frey, A. B. Coppens, J. V. Sanders, “*Fundamentals of Acoustics*”, JOHN WILEY & SONS, NEW YORK, THIRD EDITION, 1982.
- [62] P. M. Morse, K. U. Ingard, “*Theoretical Acoustics*”, MCGRAW-HILL, NEW YORK, 1968.
- [63] J.A. Jensen, “*Field: A Program for Simulating Ultrasound Systems*”, [http://www.es.oersted.dtu.dk/ftp/bme/conferences/1996/jaj\\_nbc\\_1996.pdf](http://www.es.oersted.dtu.dk/ftp/bme/conferences/1996/jaj_nbc_1996.pdf), PAPER PRESENTED AT THE 10TH NORDIC-BALTIC CONFERENCE ON BIOMEDICAL IMAGING PUBLISHED IN MEDICAL & BIOLOGICAL ENGINEERING & COMPUTING, PP. 351-353, VOLUME 34, SUPPLEMENT 1, PART 1, 1996.
- [64] Marzban R. Palsetia, Jian Li, “*Using APES for interferometric SAR imaging*”, IEEE TRANSACTIONS ON IMAGE PROCESSING, VOL. 7, NO. 9, PP. 1340-1353, SEPTEMBER 1998.
- [65] Kiyoo Tomiyasu, “*Tutorial review of synthetic-aperture radar (SAR) with applications to imaging of the ocean surface*”, PROCEEDINGS OF THE IEEE, VOL. 66, NO. 5, PP. 563-583, MAY 1978.
- [66] Stuart R. DeGraaf, “*SAR Imaging via Modern 2-D Spectral Estimation Methods*”, IEEE TRANSACTIONS ON IMAGE PROCESSING, VOL. 7, NO. 5, MAY 1998.
- [67] “*Sandia Complex Image Data*”, <http://www.sandia.gov/RADAR/sar-data.html>, Sandia Corporation.
- [68] “*Sensor Data Management System Page*”, <http://www.mbvlab.wpafb.af.mil/public/MBVDATA>.
- [69] Arnaud E. Jacquin, “*Image coding based on a fractal theory of iterated contractive image transformations*”, IEEE TRANSACTIONS ON IMAGE PROCESSING, VOL. 1, NO. 1, PP. 18-30, JANUARY 1992.
- [70] R. Kanhouche, “*Combinatorial Approach to Object Analysis*”, <http://arxiv.org/ftp/nlin/papers/0511/0511015.pdf>.
- [71] O. ALATA, M. Najjim, C. Ramananjarasoa, F. Turcu, “*Extension of the Schur-Cohn stability test for 2-D AR quarter-plane model*”, IEEE TRANS. ON INFORMATION THEORY, VOL. 49, NO. 11, PP. 3099-3106, NOVEMBERE 2003.
- [72] Clarisse Ramananjarasoa, “*Modélisation paramétrique de processus stochastiques bidimensionnels : étude de la stabilité des processus autorégressifs bidimensionnels et des modèles fondés sur la décomposition de Wold*”, ECOLE NATIONALE SUPERIEURE D'ELECTRONIQUE, D'INFORMATIQUE ET DE RADIOCOMMUNICATIONS DE BORDEAUX, THESE SOUTENUE LE 16 OCTOBRE 2002.
- [73] A. Seghier, “*Extension of positive definite functions and associated entropy. The multidimensional case*”, ANN. INST. HENRI POINCARÉ, ANALYSE NON-LINÉAIRE, VOL. 8, NO. 6, PP. 651-675, 1991.

[74] A. Calderón, R. Pepinsky, "*on the phases of Fourier Coefficients for positive Real Periodic Function, in Computing Methods and the Phase Problem in X-Ray Crystal Analysis*", PP. 339-346, RAY PEPINSKY EDITOR, 1950.

[75] W. Rudin, "*The extension problem for positive-definite functions*", ILLINOIS J. MATH., VOL. 7, PP. 532-539, 1963.



## TABLE OF FIGURES

FIGURE 1.1 .....	16
FIGURE 1.2 .....	16
FIGURE 1.3 .....	17
FIGURE 1.4 .....	17
FIGURE 2.1 .....	20
FIGURE 2.2 .....	21
FIGURE 2.3 .....	23
FIGURE 3.1, THE COLUMNS OF $X(k)$ ARE GENERATED BY A SLIDING VECTOR OF SIZE $n_2 + 1$ IN THE SIGNAL LINE $k$ .....	31
FIGURE 3.2 .....	38
FIGURE 3.3 .....	38
FIGURE 3.4 .....	38
FIGURE 3.5 .....	39
FIGURE 3.6 .....	39
FIGURE 3.7 .....	39
FIGURE 3.8 .....	40
FIGURE 3.9 .....	40
FIGURE 5.1 .....	63
FIGURE 5.2 .....	64
FIGURE 6.1 .....	72
FIGURE 6.2 .....	73
FIGURE 6.3 3D TEST SPECTRUM, $f_0 = 0$ .....	73
FIGURE 6.4 3D SPECTRAL ESTIMATION, $f_0 = 0$ .....	73
FIGURE 6.5 3D TEST SPECTRUM, $f_0 = 0.1$ .....	74
FIGURE 6.6 3D SPECTRAL ESTIMATION, $f_0 = 0.1$ .....	74
FIGURE 6.7 3D TEST SPECTRUM, $f_0 = 0.2$ .....	74
FIGURE 6.8 3D SPECTRAL ESTIMATION, $f_0 = 0.2$ .....	74
FIGURE 6.9 3D TEST SPECTRUM, $f_0 = 0.3$ .....	74
FIGURE 6.10 3D SPECTRAL ESTIMATION, $f_0 = 0.3$ .....	74
FIGURE 6.11 3D TEST SPECTRUM, $f_0 = 0.4$ .....	74
FIGURE 6.12 3D SPECTRAL ESTIMATION, $f_0 = 0.4$ .....	74
FIGURE 6.13 3D TEST SPECTRUM, $f_0 = 0.5$ .....	75
FIGURE 6.14 3D SPECTRAL ESTIMATION, $f_0 = 0.5$ .....	75
FIGURE 6.15 3D TEST SPECTRUM, $f_0 = 0.6$ .....	75
FIGURE 6.16 3D SPECTRAL ESTIMATION, $f_0 = 0.6$ .....	75
FIGURE 6.17 3D TEST SPECTRUM, $f_0 = 0.7$ .....	75
FIGURE 6.18 3D SPECTRAL ESTIMATION, $f_0 = 0.7$ .....	75
FIGURE 6.19 3D TEST SPECTRUM, $f_0 = 0.8$ .....	75
FIGURE 6.20 3D SPECTRAL ESTIMATION, $f_0 = 0.8$ .....	75
FIGURE 6.21 3D TEST SPECTRUM, $f_0 = 0.9$ .....	76

FIGURE 6.22 3D SPECTRAL ESTIMATION, $f_0 = 0.9$ .....	76
FIGURE 6.23 CORRELATION MATCHING RATIO. ....	76
FIGURE 7.1 .....	85
FIGURE 7.2 .....	90
FIGURE 7.3 .....	90
FIGURE 7.4 .....	91
FIGURE 7.5 .....	91
FIGURE 7.6 .....	92
FIGURE 7.7 .....	92
FIGURE 7.8 .....	93
FIGURE 7.9 .....	93
FIGURE 7.10 .....	93
FIGURE 7.11 .....	93
FIGURE 7.12 .....	93
FIGURE 7.13 .....	93
FIGURE 7.14 .....	95
FIGURE 7.15 .....	95
FIGURE 7.16 .....	95
FIGURE 8.1 .....	101
FIGURE 8.2 .....	102
FIGURE 8.3 .....	103
FIGURE 8.4 .....	103
FIGURE 8.5, ASMSE .....	104
FIGURE 8.6, SMCE .....	104
FIGURE 8.7, FFT .....	104
FIGURE 8.8, CAPON .....	104
FIGURE 8.9, CORRELOGRAM .....	104
FIGURE 8.10, QP .....	104
FIGURE 8.11, HMHV .....	104
FIGURE 8.12, ASMSE .....	104
FIGURE 8.13, SMCE .....	104
FIGURE 8.14, FFT .....	105
FIGURE 8.15, CAPON .....	105
FIGURE 8.16, CORRELOGRAM .....	105
FIGURE 8.17, QP .....	105
FIGURE 8.18, HMHV .....	105
FIGURE 8.19, ASMSE .....	106
FIGURE 8.20, SMCE .....	106
FIGURE 8.21, FFT .....	106
FIGURE 8.22, CAPON .....	106
FIGURE 8.23, CORRELOGRAM .....	107
FIGURE 8.24, QP .....	107
FIGURE 8.25, HMHV .....	107
FIGURE 8.26, IMAGE AS PRODUCED BY THE PROGRAM PROVIDED BY SANDIA (BY THRESHOLDING) .....	109
FIGURE 8.27, FFT (LOGARITHMIC) .....	110
FIGURE 8.28, ASMSE (LOGARITHMIC) .....	110
FIGURE 8.29, SMCE (LOGARITHMIC) .....	111
FIGURE 8.30, CAPON (LOGARITHMIC) .....	111
FIGURE 8.31, CORRELOGRAM (LOGARITHMIC) .....	112

FIGURE 8.32, QP (LOGARITHMIC) .....	112
FIGURE 8.33, HMHV (LOGARITHMIC).....	113
FIGURE 8.34, FFT (LOGARITHMIC) .....	113
FIGURE 8.35, ASMSE (LOGARITHMIC).....	114
FIGURE 8.36, SMCE (LOGARITHMIC).....	114
FIGURE 8.37, CAPON (LOGARITHMIC).....	114
FIGURE 8.38, CORRELOGRAM (LOGARITHMIC).....	115
FIGURE 8.39, QP (LOGARITHMIC) .....	115
FIGURE 8.40, HMHV (LOGARITHMIC).....	115



## Méthodes Mathématiques En Traitement Du Signal Pour L'Estimation Spectrale

### Abstract

We study the theory and the application for a multiple of methods in the domain of spectral power estimation. In the 1D case, the Levinson and Burg approach are exposed into the same theoretical and numerical context. In the 2D case, and the general ND case new methods are proposed for spectral power estimation following the criteria of an associated positive definite ND correlation matrix extension, and the Maximum of Entropy spectral power measure. Also, ND-Toeplitz correlation systems are exposed in the context of the generalized reflection coefficients for the block-Toeplitz case and the Toeplitz-block-Toeplitz case. In both cases, corresponding algorithms are proposed for the solution of the autoregressive ND linear system. The ND-Toeplitz correlation matrix structure is studied under two conditions. The first is the infinite positive extension support with an approximate matching property. The second is a positive extension with a Maximum of Entropy property. Following the second condition, we formalize a fundamental positiveness theory establishing the correspondence between a minimum group of reflection coefficients and the ND-Toeplitz correlation matrix, with the same degree of liberty.

### Résumé

On étudie la théorie et l'application pour plusieurs méthodes dans le domaine de l'estimation de la puissance spectrale. Dans le cas 1D, les deux approches de Levinson et Burg sont exposées dans le même contexte théorique et numérique. Dans le cas 2D, et plus généralement le cas ND, de nouvelles méthodes sont proposées pour l'estimation de la puissance spectrale. Ces méthodes conduisent à des extensions répondant à un critère de positivité et d'une maximisation d'une entropie adaptée à la puissance spectrale : la matrice de corrélation ND doit être définie positive et doit vérifier un critère de maximum d'entropie. Aussi, les systèmes de corrélation ND-Toeplitz sont exposés dans le contexte des coefficients de réflexion généralisés pour le cas bloc-Toeplitz, et le cas Toeplitz-bloc-Toeplitz. Dans les deux cas, on propose des nouveaux algorithmes pour la solution du système linéaire autorégressif. La structure ND-Toeplitz de la matrice de corrélation est étudiée sous deux conditions. La première est le support d'extension positive est infini avec une propriété de « matching » approximative. La deuxième est l'extension positive avec une propriété de maximum d'entropie. Suivant la deuxième condition, on formalise une théorie de positivité fondamentale établissant la correspondance entre un group minimal des coefficients de réflexion généralisés et la matrice de corrélation ND avec le même degré de liberté.



